STRUCTURE-FUNCTION STUDIES OF FLAVIVIRUS NON-STRUCTURAL PROTEIN 1

A Dissertation

Submitted to the Faculty

of

Purdue University

by

Thu M. Cao

In Partial Fulfillment of the

Requirements for the Degree

of

Doctor of Philosophy

May 2020

Purdue University

West Lafayette, Indiana

THE PURDUE UNIVERSITY GRADUATE SCHOOL
STATEMENT OF DISSERTATION APPROVAL

Dr. Richard J. Kuhn, Chair

Department of Biological Sciences

Dr. R. Claudio Aguilar

Department of Biological Sciences

Dr. Andrew D. Mesecar

Department of Biochemistry

Dr. Douglas J. LaCount

Department of Medicinal Chemistry and Molecular Pharmacology

Approved by:

Dr. Janice Evans

Head of the School Graduate Program

Dedicated to my beloved family

ACKNOWLEDGMENTS

I would like to express my great appreciation to my advisor, Dr. Richard J. Kuhn. PhD is a long journey and I have been learning a tremendous amount of knowledge in virology, experiment management, and collaborations. None of that could have been done without my advisor. I am grateful for his support, guidance and encouragement. His hard work and success are the inspiration. It is my honor to work with him and learn from him. Right at the end of this dissertation journey, Coronavirus disease (COVID-19) has been spreading all over the world and we are as human beings are fighting in this battle. The calmness and expertise of my advisor are truly helpful for myself as well as our lab and the community. I am always grateful for all of that.

I am also thankful to my committee members for providing feedback and suggestions for my study. I would like to thank Dr. Aguilar Claudio for his creativity and wonderful suggestions for all my studies. I would like to thank Dr. Douglas LaCount for his keen of details, experiment controls, and experiment designs. Lastly, I would like to thank Dr. Andrew Mesecar for his passion and critique of science. All of those have help to shape my science.

I would like to thank all the former and current lab mates for their support. I am fortunate to have labmates as my friends. In particular, Dr. Joyce Jose have been a great scientist who brought me to NS1 studies and showed me new virology techniques. Without her initial help, I would not have enjoy this project this much. I would like to thank Anita Robinson for all the paper works, meeting arrangement, cookies, cakes and a lot of caring. I would like to thank Andy Miller for maintaining the lab facilities, reagent order, technical support and understanding. To Mike, Matt, Shishir, and Adriano, your friendship is beyond my wish. I will miss you and our coffee break.

Lastly, I would like to thank my parents, Cuc and Dung for the understanding and full support. I am geographically far away and focusing on my study while you are always looking after me no matter how far away I am. I would like to thank my brother, Dung, my sister in-law, Tram and their beautiful daughters, Chloe and Lucie. Thanks for understanding and being here with me during my long PhD journal. For Chloe and Lucie, thanks to you, I no longer want to look at the world as whatever it is but I want to do my best to make it a better place for you. Thanks to the COVID-19, you have more time with our big family, but the next pandemic may not be kind to us. I will continue working on virology so that day may postpone as long as possible or even better, it will be under control when it comes.

TABLE OF CONTENTS

Page

Page

Page

LIST OF FIGURES

Figure Page

LIST OF TABLES

ABBREVIATIONS

BHK	baby hamster kidney cells
HEK	human embryonic kidney cells
C	capsid protein
CPE	cytopathic effect
ER	endoplasmic reticulum
kb	kilobasepair
kDa	kilodalton
nm	nanometer
NS	nonstructural protein
MOI	multiplicity of infection
ORF	open reading frame
PBS	phosphate buffered saline
PBST	phosphate buffered saline and Tween 20
PCR	polymerase chain reaction
PEG	polyethylene glycol
pfu/ml	plaque forming units per milliliter
RenLuc	Renilla luciferase
SDS-PAGE	sodium dodecyl sulphate polyacrylamide
SINV	Sindbis virus
μl	microlitre
μm	micrometre
Å	Angstron
Aq	Aqueous phase
Det	Detergent phase

UTR	untranslated region
YFV	Yellow Fever virus
DENV	Dengue virus
WNV	West Nile virus
ZIKV	Zika virus
Ab	antibody
HS	Heperan Sulfate
GAGs	glycosoaminoglycans
hpe	hours post electroporation
dpe	days post electroporation
hrs	hours
PE	phosphatidylethanolamine
PS	phosphatidylserine
PG	phosphatidylglycerol
PC	phosphatidylcholines
PI	phosphatidylinositol
Cer	ceramide
SM	sphingomyelin
Ch-E	cholesteryl ester
TAG	triacylglyceride
$\triangle$B	deletion of the β-roll domain
$\triangle$F	deletion of the flexible loop
$\triangle$G	deletion of the greasy finger
WT	wild-type

ABSTRACT

Cao, Thu M. Ph.D., Purdue University, May 2020. Structure-Function Studies of Flavivirus Non-Structural Protein 1. Major Professor: Richard J. Kuhn.

Flaviviruses is a genus within the family Flaviviridae. The genus consists of more than 70 viruses, including important threatening human pathogens such as dengue virus (DENV), West Nile virus (WNV), and Zika virus (ZIKV). These viruses are causative agents for a range of mild to lethal diseases and there are currently no US-licensed therapeutic treatments for infection. The virus genome is a positive-sense, single-stranded RNA, encoding ten viral proteins. Of the ten flavivirus proteins, Non-Structural protein 1 (NS1) remains the most elusive in terms of its functions. To date NS1 has been linked to disease pathology and progression and plays roles in virus replication and assembly. However, little is understood how NS1 orchestrates these functions and how NS1 from different viruses function distinctively from one another. Moreover, flavivirus NS1 has a peculiar ability to associate with lipid membranes. During the life cycle of NS1, the protein travels through the classical secretory pathway, similar to infectious virus particles, and is secreted into the extracellular space as mostly hexameric oligomers containing a lipid core. How the protein binds to lipids and whether such lipid binding is important for NS1 functions and overall flavivirus pathology remain unknown. Using structure-based mutagenesis, we found a group of mutants on WNV NS1, which particularly altered the viral specific infectivity but maintained wild-type level of virus replication. Purified mutated virus particles revealed that the specific infectivity alteration was not because of the particle but interaction of the virus particles and NS1 mutated proteins. Here we demonstrated that specific residues on NS1 were responsible for distinctly roles in NS1 functions and the virus specific infectivity was regulated by NS1 protein. In other structure-based

study, we focused on the membrane association ability of NS1. All structure-predicted regions on NS1 were examined for its contribution for the membrane/lipid binding function. This interaction was required for NS1 biology activities including intracellular trafficking, oligomerization, and endocytosis. The lipidomes from deletion of each membrane association region revealed differences in lipid classes binding to each region and the composition flexiblity of the lipid cargo of NS1 hexamer.

1. FLAVIVIRUS NON-STRUCTURAL PROTEIN 1

1.1 Flaviviruses

1.1.1 Flaviviruses and epidemics

Flavivirus is a genus within family *Flaviviridae*. The genus consists of more than 70 viruses, including important threatening human pathogens such as dengue virus (DENV), West Nile virus (WNV), Zika virus (ZIKV), yellow fever virus (YFV), and Japanese encephalitis virus (JEV). Three current re-emerging viruses, DENV, WNV, and ZIKV, will be discussed in more detail in this dissertation. DENV can cause symptoms ranging from self-limiting febrile to severe diseases such as dengue fever (DF), dengue hemorrhagic fever (DHF), and dengue shock syndrome (DSS). An estimated about 390 million cases are infected annually, resulting in 25,000 deaths [1]. DENV is a global threat and can be found in 128 countries spanning all continents except Antarctica [1]. WNV is also globally distributed but infects significantly less than DENV (507 cases in America and less than 300 in Europe)(CDC,2019; ECDC, 2019). The virus can cause encephalitis or meningitis when it infects the human brain [2]. The emerging flavivirus, ZIKV, has been suggested as a causative agent for microcephaly and Guillain Barre syndrome (GBS) [3,4]. A major ZIKV outbreak happened in 2015 and 2016, and was declared by the World Health Organization as an international public health emergency.

Flaviviruses are transmitted via an arthopod vector to humans. Infection can occur following a bite from infected mosquitoes such as *Aedes aegypti* and *Aedes albopictus* (transmit DENV and ZIKV) or *Culex pipiens* (transmit WNV) [5,6]. ZIKV is the only flavivirus able to be transmitted from an infected mother to her fetus or through sexual contact [7, 8]. Flaviviruses can infect a wide range of vertebrate

hosts [9]. DENV reservoirs include monkeys and domestic dogs [10]. In nature, WNV is maintained in avian species (house sparrows, crows, American robins), raccoons, horses, and camels [11]. ZIKV can be detected in a wide array of hosts from monkeys and apes to goats, sheep, horses, cows, ducks, bats, etc. [12].

1.1.2 Flavivirus tropism

When infecting a host, flaviviruses travel to different susceptible tissues and organs which allow its replication. In mosquitoes, flaviviruses enter via a blood meal and travel to the midgut lumen. It infects midgut epithelial cells and replicates to generate new viruses. The virus then travels and amplifies in hemocytes, fat body, visceral muscles and neural tissue (depending on virus) before spreading to the salivary gland [13, 14]. During blood feeding of the infected mosquitoes, viruses are transmitted via mosquito saliva to the next host. In humans, different flaviviruses travel to different organs. DENV can infect and grow in the liver and peripheral blood mononuclear cells. It was also reported to be present in the spleen, kidney, bone marrow,thymus and brain [15]. WNV organ tropism is the brain (peripheral and central nervous system tissues), spleen, lymph node, lung, skin, pancreas, and duodenum [16]. Zika organ tropism includes the eyes, brain, placenta, and male and female reproductive tracts (uterus, vagina, and testis) [17].

1.1.3 Flavivirus life cycle

Flaviviruses are small enveloped viruses of approximately 500Å in diameter. DENV, WNV, and ZIKV all share similar icosahedral structure [18–20]. The viral genome is a positive sense, single-stranded RNA, which is about 11 kb in length with a 5' cap and untranslated regions (UTR) at both 5' and 3' ends. It encodes for three structural proteins (capsid-C, precursor membrane-prM and envelope-E) and seven nonstructural proteins (NS1, NS2A, NS2B, NS3, NS4A, NS4B, and NS5). A virion

is composed of prM and E on the host-derived membrane, whereas capsid proteins forms nucleocapsid with the vRNA at the core [21].

When flaviviruses infect a cell, they first bind to the cell surface via attachment and entry factors and/or receptors such as mannose receptors, heparan sulfate proteoglycans (HSPG), heat shock proteins (HSP70), DC-SIGN, TIM/TAM family, [23–26]. The interactions with the cell receptors mediate virus endocytosis through the clathrin-dependent pathway, which is regulated by the size of the virion [27–29]. The virus is delivered to early endosomes then late endosomes within 5 minutes post-entry [30]. The viral membrane rearranges and goes through membrane fusion which requires two conditions including acidic pH and the presence of late-endosome specific lipids, bis(monoacylglycero)phosphate and phosphatidylserine [31]. As the result of fusion, the nucleocapsid is released into the host cytoplasm and disassembled. The capsid protein is degraded and vRNA is used for translation to produce viral proteins. The viral genome is translated into a polyprotein at the ER membrane and also translocated into the ER lumen. Viral proteins are cleaved into individual proteins by host signal peptidase and viral protease (NS2B-NS3). The (+) sense vRNA serves as a template for both the translation and synthesis of (-) sense RNA for new vRNA. Viral proteins modify ER membrane to generate replication complexes (RCs), specific viral membrane structures formed by invagination into the ER lumen [32]. A single RC is 80-100 nm in diameter and has an open neck towards the cytoplasm [33]. This structure provides a platform with high concentration of viral proteins for generating new vRNA (mostly double-strand RNA) and hide the newly-synthesized vRNA from host innate immune response [32]. New (+) sense RNA is capped, methylated and encapsidated with capsid protein. The nucleocapsid is transported to the assembly site which has prM and E on the ER membrane and forms a new virion by budding into the ER lumen. The replication and assembly processes are suggested to be tightly coupled [34]. The virions go through the conventional secretory pathway from ER to Golgi, transitioning from immature to mature by furin (a Golgi-resident

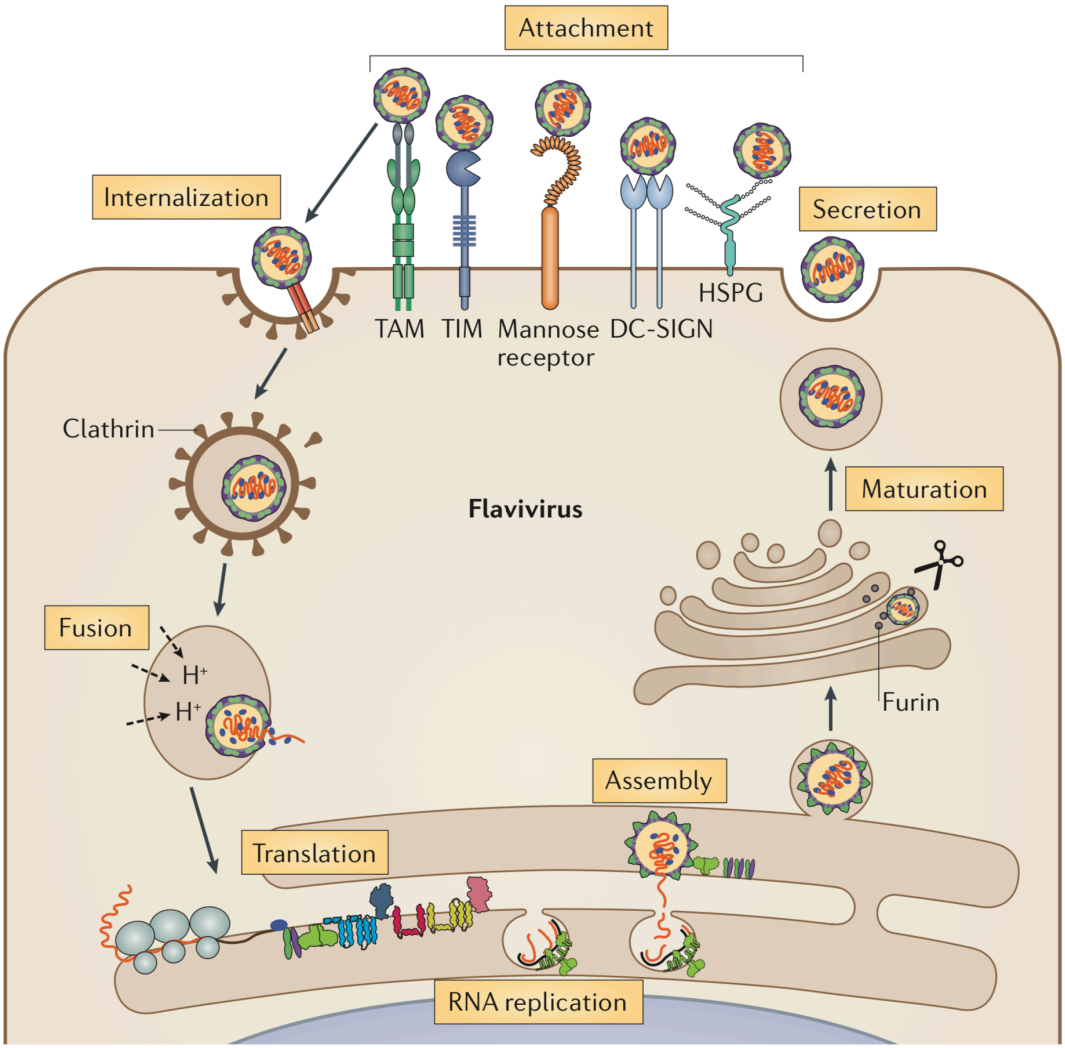

Fig. 1.1. Flavivirus life cycle. Virus first attaches to cellular attachment factors and receptors. It is endocytosed via clathrin-dependent pathway. Upon getting to the late endosome, virus fuses its membrane and releases the genome into the cytosol. The genome uncoats and translates into viral proteins in the ER. ER membrane is modified to form replication complexes where new vRNA are actively synthesized. The new vRNA is encapsidated, moving to the assembly site, budding into the ER lumen and forming new immature virions. The virions travel along the secretory pathway, maturing after cleavage via furin in the Golgi and get secreted to the extracellular environment. Image is adapted from Neufeldt et al., 2018 [22]. https://doi.org/10.1038/nrmicro.2017.170

protein) cleavage of prM. Infectious virions are then secreted to the extracellular environment [35] (Fig 1.1).

1.2 NS1 biology

1.2.1 NS1 shares the same virus trafficking pathway

NS1 is the only non-structural protein sharing the same intracellular trafficking pathway as the virion. It is also the only nonstructural protein that gets secreted and is able to attach and enter new cells via similar attachment factors (HSPG) as the virus particles [36]. Figure 1.2 highlights the similarity of the trafficking pathway of NS1 and the virus particle. In the infected cells, NS1 travels to three destinations including replication complexes, the secretory pathway and cellular plasma membrane (Muller and Young, 2013). The protein is synthesized in the ER and stays in the ER lumen, which is on the other side of the replication complex compared to all other non-structural proteins which remain on the cytosolic side. Both newly-formed virions and NS1 are present in the ER lumen before traveling from the ER to Golgi. However, there are no reports of co-trafficking or if the virion and NS1 are in the same transport vesicle from ER to Golgi. In the secretory pathway, the virus particle matures via furin cleavage and glycosylation while NS1 matures via only glycosylation. When the protein is secreted, it is able to attach to new cells, get endocytosed and is found to accumulate and stay stable in the late endosome for up to 48 hours after endocytosis [37]. In clinical samples, secreted NS1 can accumulate to a high concentration (up to 50μg/ ml) [38]. NS1 has a special intracellular pathway that it does not share with the particle, involving direct trafficing from the ER lumen to the plasma membrane [39]. There is exceedingly little information about this pathway or how NS1 regulates its population to travel to different cellular destinations. However, there is a report showing different levels of NS1 on the plasma membrane between flaviviruses. This report reveals WNV NS1 travels to the plasma membrane more

than DENV NS1 and DENV NS1 is secreted more than the WNV NS1. Residues 10 and 11 on each protein are suggested to influence the destination of the proteins [39].

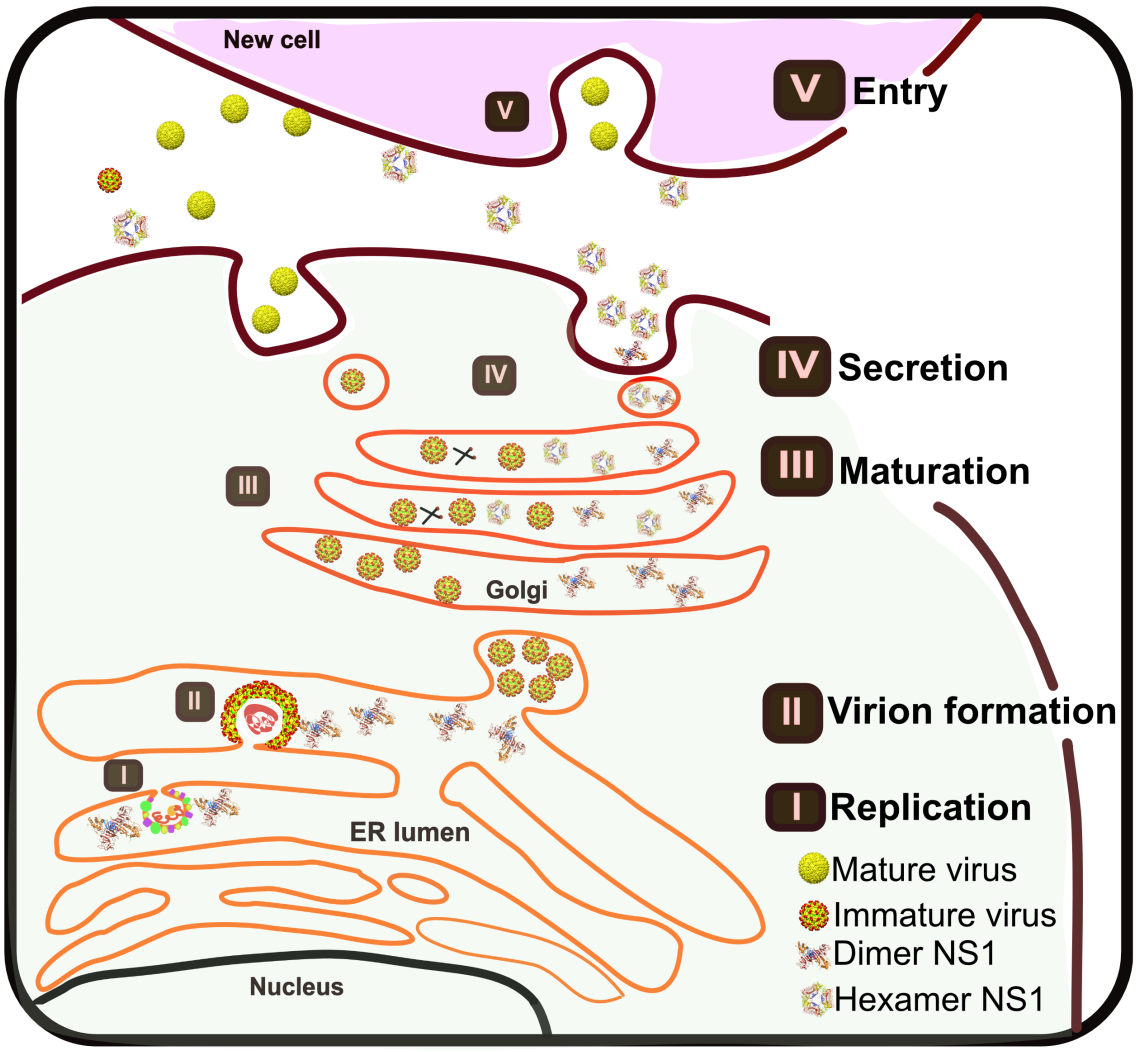

Fig. 1.2. NS1 trafficking shares the same pathway as virus particles. New virion and NS1 are present in the ER lumen and get transported to the Golgi. In the Golgi, virus particles get cleaved of prM to mature and NS1 matures via glycosylation to complex sugar. Both virus particles and NS1 are secreted into the extracellular matrix. The particle and NS1 can bind to new cells via GAG and get endocytosed and stay in late endosome vesicles.

1.2.2 NS1 tropism

Secreted NS1 attaches to a variety of cell lines. DENV NS1 is reported to bind to epithelial and fibroblast cell lines such as BHK, Vero, HEK 293T, HepG2, CHO-K1, HepB3 and primary cells such as human dermal and lung microvascular endothelial cells (HMEC) and HMEC-lung blood (HEMC-LB) [36]. In a recent study, NS1 proteins from different flavivruses are suggested to bind to specific tissues reflecting the tropism of the corresponding diseases. DENV NS1 was shown to bind to human endothelial cells of the lung, dermis, umbilical vein, brain, and liver and cause hyperpermeability and vascular leakage *in vivo* at the corresponding organs. WNV NS1 demonstrated the best binding to only brain endothelial cells and induced vascular leakage in the same organ *in vivo*. ZIKV NS1 differentially bound to placenta and brain endothelial cells and caused vascular leakage in the brain but not lung or liver *in vivo* [40].

1.2.3 NS1 maturation

The NS1 protein contains 352 amino acids, with 6 conserved disulfide bonds, and two (DENV and ZIKV) or three (WNV) N-glycosylation sites. The molecular weight, depending on the glycosylation status of the protein, is between 46-55 kDa. NS1 is highly conserved among flaviviruses and has 40-60% sequence identity. The last 24 amino acids at the C-terminusinus of E protein function as the signal sequence for NS1 to translocate into the ER lumen [41]. NS1/NS2A cleavage occurs in the ER lumen by an unknown host protease and requires 8 C-terminusinal residues of NS1 and most of NS2A for recognition and cleavage activity [42].

NS1 traffics through different cellular compartments and changes its glycosylation and oligomeric forms along the way. NS1 converts from a monomer to a dimer shortly after its synthesis in the ER lumen, then forms a hexamer in the secretory pathway [43, 44] (Fig 1.3). In the extracellular matrix, NS1 remains a hexamer with a lipid cargo similar to high-density lipoprotein (HDL). The NS1 hexamer can trans-

port about 70 lipid molecules, which are mostly cholesteryl esters, phospholipids, triacylglyceridelycerides, cholesteryl, and sphingomyelin. This content was similar for DENV1 and DENV2 [44]. Although there are reports of hexameric WNV and ZIKV NS1, the lipid secretion profile of these proteins remains unknown.

1.3 NS1 structures

The structure of flavivirus NS1 revealed three distinct domains including the β-roll (residues 1-29), wing (residues 31-180), and β-ladder (residues 181-352) [45] (Fig 1.3). NS1 proteins of flaviviruses are conserved in size and shape [45–47]. The dimer size is 90Å from wing tip to wing tip, the length of the two β-ladder is 90Å, and 40Å in the third dimension. The hexamer is 110Å in diameter with a 20Å central lipid core [45]. Within the NS1 dimer, the β-roll domain is hydrophobic, containing two intertwined β-rolls from each monomer, and is stabilized by disulfide linkages at residues 4 and 15. The wing domain forms a complex structure with the connector, α/β subdomains (2 alpha helices and 4 stranded beta sheets), flexible loop (residues 108-128), and greasy finger (residue 159-163). The wing domain also contains internal disulfide linkages at residues 55 and 143, glycosylation sites at residues 130 (for DENV, WNV and ZKV) and 175 (for WNV only) [45]. Brown et al. provided the structure of ZIKV NS1, which revealed the structure of the previously missing hydrophobic flexible loop on the wing domain. This loop is suggested to bend toward the membrane and, together with the β-roll and greasy finger, form a membrane association region on NS1 [46, 48]. The β-ladder has 18 beta strands (9 from each monomer) with a long, ordered spaghetti loop (residue 219 -272) containing 57 hydrogen bonds. There is a glycosylation site on the beta ladder at residue 207 and three disulfide bonds at the tip of the C-terminusinus of the β-ladder [45].

Based on its structure, NS1 contains as inner and outer face (Fig 1.3). The inner face includes the β-roll, flexible loop and greasy finger; which are hydrophobic and proposed as membrane association regions. In addition to potential lipid interactions

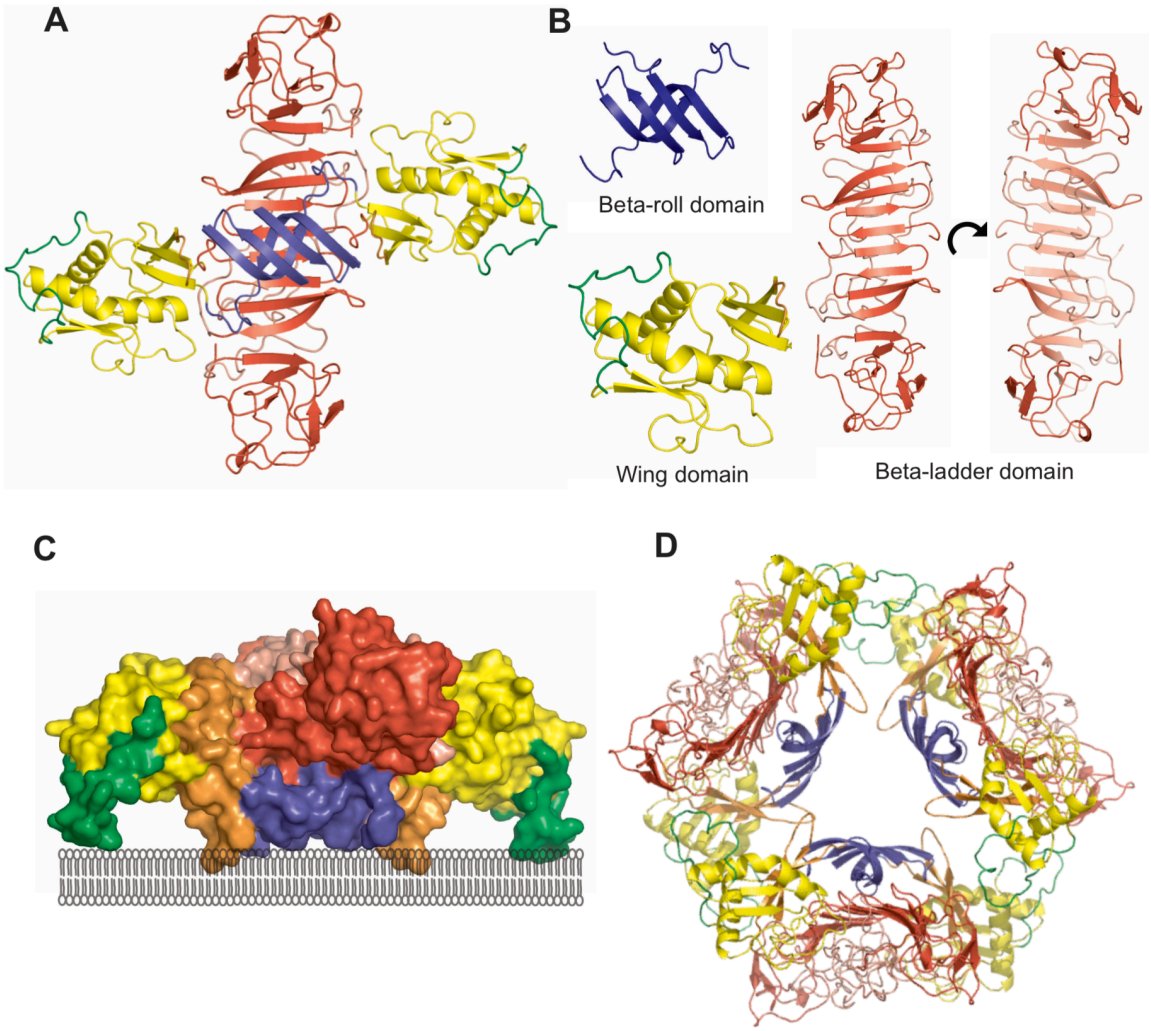

Fig. 1.3. NS1 structure and oligomer forms. **A**. Dimeric NS1 (PDB ID 5K6K) with arranged domains color coded as blue- β-roll, yellow-wing (green- flexible loop) and red- β-ladder.**B**. Individual domains of each monomer in same color code.**C**. Inner face and outer face of NS1. The inner face faces toward the membrane, including β-roll domain, flexible loop and greasy finger on wing domain. The outer face is the rest of NS1 facing against the membrane. **D**. Hexamer NS1. A hexamer has 6 monomers, arranged into 3 dimers facing each other at the inner face, forming a lipid core.

at this site, mutagenesis studies also suggest the interaction of WNV NS1 inner face with viral and host proteins [49,50]. The outer face, including the rest of the wing and β-ladder, is hydrophilic, exposed and therefore available for protein interactions [50].

Although the overall structures of flaviviruses are similar, the surface charge distribution of the inner and outer faces revealed diverse patterns among flaviviruses [46, 47, 51]. On the inner surface, both DENV NS1 and WNV NS1 display a neutral charge while ZIKV NS1 is negative. On the outer face, the electrostatic surface of DENV1, and DENV2 are positive at both the wing and β-ladder domains, while WNV is neutral [47]. ZIKV NS1, however, is positive at the center of the β-ladder but negatively charged on the wing domain. The surface charge of the β-ladder domain of JEV is similar to WNV and ZIKV NS1 [51].

1.4 NS1 functions

1.4.1 Viral RNA synthesis and replication complex formation

NS1 is an essential component for virus replication. The protein colocalizes with double stranded RNA, which is actively synthesized in the replication complex [52]. The deletion of the YFV or WNV NS1 gene led to no viral replication and could be rescued by trans-complementation with other flavivirus NS1 proteins [53,54]. Absence of NS1 causes replication complex formation defect and affects the recruitment of non-structural proteins to the replication complex [54, 55]. NS1 is suggested to play roles in viral replication at early events such as negative-strand RNA synthesis [49, 53, 54]. Genetic studies presented sites on NS1 responsible for vRNA synthesis, including residues for NS1 glycosylation [56]. Other single mutations on NS1 domains lead to lethal effect on virus replication [55, 57]. It is unclear how NS1 biology contributes to its functions in virus replication. However, being that single mutations on different domains of NS1 can inHiBiT viral RNA synthesis, do these mutations affect different aspects of replication and do individual domains serve different roles?

The function of NS1 in virus replication is suggested via direct interaction of NS1 with other viral nonstructural proteins such as NS4A, NS4B [49, 55, 58]. NS4B also interacts with NS3 and NS4A [59], suggesting that viral nonstructural proteins interact with each other to provide a scaffold for the replication complex. WNV NS1 binds to NS4B through the β-roll (residues 10 and 11) on NS1 and residue 86 on NS4B (ER lumen side) [39]. In other studies, this interaction was disrupted by ubiquitination of NS1 protein at lysine residues 182 and 189 [60] . These two residues are on the β-ladder, with their side chains pointing toward the β-roll. Since the β-roll is hydrophobic and is a putative membrane association region, the ubiquitinated K182/189 may disrupt the protrusion of the region into the cellular membranes, suggesting a role of the inner face in NS1 function and viral RNA synthesis. In addition, NS1 interacts with NS4A-2K-NS4B (precursor form of mature NS4A and NS4B) through greasy finger, another putative membrane association region. However this interaction was independent from the function of NS1 in replication complex formation [55].

NS1 function in virus replication relates to the NS1 interactome in mammalian cells. DENV NS1 is suggested to play roles in viral protein translation and the RNA synthesis process through binding to human heterogenous nuclear ribonucleoprotein (hnRNP) C1/C2 and ribosomal protein RPL18, which is involved in DENV RNA synthesis and protein translation, respectively [61, 62]. DENV NS1 protein has also been shown to interact with glyceraldehyde-3-phosphate dehydrogenase (GAPDH), an enzyme involved in glycolysis [63]. GAPDH was also found to play a role in flavivirus replication by binding to JEV RNA, and indirectly binding to NS5 in the cytoplasm [64]. NS1 increases the activity of GAPDH in transfected cells, suggesting NS1 may contribute to virus replication and infection via increasing energy available for the process [63]. Allonso et al. found that mutation of residues on the inner face of NS1 (residues 10, 11, 161, and 162) interfered with this interaction, but this needs to be further investigated. In both reports, the localization of GAPDH and (hnRNP) C1/C2 is in the cytoplasm while NS1 resides in the ER lumen. In a global

interactome study of NS1 and host proteins, a set of host proteins were classified into host restriction factors and host dependent factors. Host restriction factors (HRF) were host proteins inHiBiTing viral activities, while host dependent factors (HDF) increased virus titer [65]. The interaction of NS1 with both HRFs and HDFs suggests a regulatory function of NS1 in viral replication.

1.4.2 Virus assembly

NS1 was recently reported to be involved in virus assembly by interacting with structural proteins. In a comprehensive alanine-scanning mutagenesis study, a group of single mutations on DENV NS1 was found to either enhance or diminish intra- and/or extracellular virus titer without altering virus replication [57]. It was suggested that NS1 functions in two steps of virus assembly, including the production of infectious particles and virus trafficking. NS1 was shown to colocalize with virus particles at assembly sites using correlative light-electron microscopy (CLEM) [57]. NS1 was found to interact with envelope, precursor membrane (prM) protein and capsid. Mutations on the flexible loop of the wing domain (S114A and W115A) disrupted the interaction of NS1 and the structural proteins while the mutations in the β-ladder domain (D180A and T310A) maintained E and prM interactions but disassociated NS1 from capsid [57]. In ZIKV NS1, another mutation on the β-ladder, K265E, increased the formation of new infectious particles by enhancing the interaction of NS1 and NS2A, another nonstructural protein participating in the virus assembly process. The interaction of ZIKV NS1 and structural proteins, prM and E, was also detected in this study [66].

The role of NS1 in assembly extends to other genera of the *Flaviviridae* family. It was reported that flavivirus NS1 can behave as cofactor during the assembly of hepatitis C virus (HCV) and classical swine fever virus (CSFV). HCV and CSFV are from the genera hepacivirus and pestivirus, respectively. HCV normally utilizes a host protein, apolipoprotein E (ApoE) for the production of infectious particles while

CSFV requires its envelope protein for assembly. DENV NS1 (from all four serotypes of dengue virus) are able to substitute for both ApoE and the envelope protein of CSFV in the virus assembly process for infectious particle formation [67].

1.4.3 Virus transmission

In infected mammalian cells, NS1 traffics to three locations: the replication complex, directly to the plasma membrane and through the secretory pathway to the extracellular environment [68, 69]. In infected mosquito cells, NS1 can be found in two locations: replication complex and the extracellular environment but through an unconventional pathway. The protein bypasses the secretory pathway and interacts with the cytoplasmic cholesterol transporter chaperone caveolin complex, including caveolin-1, FKBP52, cy40, and CyA for its secretion [70, 71]. When secreted, both mammalian- and insect-derived NS1 are able to bind back to the cell surface via glycosaminoglycans (GAG) [69]. The timing of NS1 secretion varies among cell types, as DENV NS1 (serotypes 2 and 4) is secreted earlier from infected mosquito cells (6 hpi) than from infected Vero cells (12 hpi) [70]. However, the amount of NS1 secreted from mosquito cells was about two times less than that from BHK cells at 48 hpi [69]. NS1 released from insect cells was characterized as a soluble hexamer of 100Å in diameter, which is slightly smaller than the size of the mammalian hexamer. The molecular weight is also smaller than the mammalian NS1 because of its glycosylation status [44, 69, 70]. Being that NS1 glycosylation is important for NS1 stability, and mosquito-secreted DENV NS1 is decorated with high mannose glycans at both glycosylation sites (residues 130 and 207), the extracellular NS1 population was shown to be less stable and more heterogeneous in size [56, 69].

Secreted NS1 was suggested to play an important role in the transmission cycle of vertebrates and arthropods. NS1 was found in the salivary gland of infected mosquitoes, and when transferred into mammals, it binds to the human complement proteins C1s, C4, C4 binding proteins, and mannose-binding lectin (MBL). Similar

to mammalian NS1 species, insect-derived NS1 attenuated immune complement activation for DENV, WNV, and YFV infection [69, 72]. Moreover, MBL can inHiBiT DENV attachment onto mammalian cells and binding of NS1 to MBL prevents it from interfering with virus entry [69]. On the other hand, the presence of DENV or JEV NS1 in the blood meal enhances the virus infection of mosquitoes by suppressing the immune response in the mosquito midgut. Mosquitoes use primarily reactive oxygen species (ROS) production and the Janus kinase-signal transducer and activator of transcription (JAK-STAT) signaling pathway to limit virus spread. Expression of the genes for these immune responses was suppressed by purified NS1 or NS1 in blood meal, and facilitated the susceptibility for virus infection [73]. In addition, a correlation of NS1 secretion and virus infectivity in mosquitoes was reported for ZIKV NS1 [74]. A single mutation of A188V on NS1 was suggested as an evolutionary factor for the ZIKV outbreak by augmenting the efficiency of the transmission cycle. This mutation resulted in higher levels of secreted NS1, enhancing virus transmission from mice to mosquito [74]. This substitution was only found in isolates after the Zika outbreak, suggesting the change in NS1 possibly contributed to the change in Zika infectivity and virus transmission, leading to the outbreak.

1.4.4 Vascular leakage

Secreted NS1 has been suggested as the causative agent of DENV hemorrhagic fever via vascular leakage and plasminogen activation [75–77]. Vascular leakage occurs when there is damage to the endothelial cell barrier, including endothelial glycocalyx layer (EGL) and/or cell-cell junctions, leading to a loss in cell permeability control and blood vessel leakage. *In vitro* and *in vivo* assays revealed that purified DENV-NS1 causes hyperpermeability of membranes and results in vascular leakage and morbidity in mice within 3 days [75]. This function is specific for DENV NS1, since WNV NS1 does not cause the same outcome. NS1-vaccinated mice were highly protected against DENV challenge (for mice immunized with DENV2-NS1: 100% protection for

DENV2, 70% for DENV1, 60% for DENV3 and DENV4. Moreover, vascular leakage is inHiBiTed *in vivo* and *in vitro* by either NS1 monoclonal antibodies or NS1 immune serum [75]. NS1 proteins trigger cell hyperpermeability and vascular leakage in two mechanisms: cytokine release and disruption of the endothelial barriers as described below.

Purified DENV NS1 alone activates human peripheral blood mononuclear cells (PBMCs) and mouse macrophages through Toll-like receptor 4 (TLR4), subsequently inducing the secretion of pro-inflammatory cytokines and chemokines, contributing to the cytokine storm in severe DENV infection. Cytokines relating to vascular leakage such as IL-6, IL-1β and TNF-α are elevated in a dose-dependent manner in the presence of NS1. The inHiBiTion of TLR4 by a TLR4 antagonist can block cell membrane hyperpermeability *in vitro* and vascular leakage *in vivo* caused by purified NS1 or DENV2 infection [76]

NS1 can also cause vascular leakage by disrupting intercellular junctions and EGL. Those barriers maintain cellular integrity and homeostasis. TLR4 activation via NS1 also induces the secretion of macrophage migration inHiBiTor factor (MIF) which leads to the disarray of tight junction protein, ZO-1, formation of autophagy, and enhancement of cellular permeability [77, 78]. Although intercellular junctions are suggested to be regulated by autophagy, specific mechanisms for NS1 induced autophagy to disrupt the cell-cell junctions is yet to be investigated. The EGL, a layer of glycoproteins and proteoglycans which protect the vascular integrity and maintain fluid homeostasis, also get disrupted by purified NS1 protein [79]. The key components of EGL including sialic acid, heparan sulfate, and syndecan-1, were degraded and shed in the presence of NS1 while the activity and level of cathepsin L, the enzyme involved in protein degradation, increased in both *in vitro* and *in vivo* assays [79, 80].

The cytokine release and disruption of vascular barrier mechanisms are suggested to be two independent pathways that lead to the same result of vascular leakage [80]. The effect of purified NS1 on EGL can be found in HMCE-1 or mice without TLR4 activation or cytokine release; indicating NS1 protein playing multiple roles in the

pathogenesis through complex mechanisms. The mouse model for vascular leakage in these systems provides a reasonable tool for studying the pathogenesis of NS1, however, the vascular leakage effect of NS1 on the mouse model occurs in earlier time points than in clinical samples. Moreover, in clinical samples, vascular leakage is reported when NS1 reaches a peak level while the mouse system provided a dose-dependent relationship of NS1 on vascular leakage [81]. Therefore, the data should be interpreted with caution due to the differences in models studied.

Another manifestation of DENV hemorrhagic fever is the bleeding, which is associated with an increase in fibrinolysis and a decrease in thrombin formation [82]. DENV NS1 was demonstrated as an antigen inducing the production of plasminogen cross-reactive antibodies, which were found in both DENV patient and NS1-immunized-mouse sera. The antibodies enhance plasminogen activation, thus interfering with the hemostasis of coagulation and bleeding by molecular mimicry of NS1 at residues 305-311 (β-ladder domain) and plasminogen residues 590-597; or NS1 at residues 114-119 (flexible loop on wing domain) and human endothelial cell antigen (lysine-rich CEACAM1 co-isolated- LYRIC protein) at residues 334-337 [83, 84]. These auto-antibodies produced by NS1 cross-reaction are able to lead to the severe stage of dengue infection [85, 86]. Vaccine design with NS1 targets need to be approached with caution. Further studies on NS1 structure and residues will be helpful to prevent cross-reaction.

1.5 Thesis synopsis

Following first reports of the protein in dengue patients about 50 years ago [87], many aspects of NS1 have been extensively studied. The protein was demonstrated to be a viral pathogenicity factor that contributes to virus replication and assembly, evading immune response, and inducing hemorrhage. The structure of NS1 has provided a major tool for in depth functional studies. All flavivirus NS1 proteins share very similar structures. However, the NS1 tropism and their functions are specific

for each virus. Therefore, the focus of this study is to understand how NS1 can behave and function differently and how different regions on NS1 contribute to these functions. In this thesis, differences in DENV and WNV NS1 functions in the virus life cycle were examined and the mystery of the membrane association ability of NS1 were investigated.

In chapter 2, structure-function studies were performed to investigate the importance of amino acid differences between DENV and WNV NS1 proteins. A subset of mutations that have assembly defects in DENV were chosen for further characterization in the WNV system. The data showed a single substitution from WNV amino acid to DENV amino acid on WNV NS1 protein significantly altered WNV specific infectivity. Each step in the virus life cycle was examined to determine the effect of the substitution. Secretion of NS1 in different systems showed reduction of NS1 in cases of both higher and lower infectivity. Purified virus of WT and both mutants showed comparable infectivity. Purified viruses supplemented with similar amount of purified NS1 slightly changed the titer and entry rate. Chapter two revealed the two residues with opposite effects on the specific infectivity of WNV, while causing distinctive effects on DENV, contributed to the functional differences between DENV NS1 and WNV NS1 based on specific residues.

In chapter 3, the membrane association ability of DENV NS1 was examined at the molecular level of the hydrophobic regions, β-roll domain, flexible loop and greasy finger on the wing domain, which are predicted in NS1 structures. Using molecular biology, biochemistry, and biophysical approaches, each region was suggested to be important in different activities of NS1. Using both virus and expression systems, each region was investigated for its function in protein biosynthesis, cellular colocalization, trafficking, oligomerization, and membrane association. Overall, the study confirms the contribution of these regions in membrane association capability and provides insight on the importance of these regions in NS1 trafficking and oligomerization, suggesting the minimum requirements for NS1 membrane association.

In chapter 4, lipidomics of DENV NS1 proteins and truncated NS1, as described in chapter 3, were characterized and compared in order to identify the lipid class each membrane association region targets. The lipid profile of truncated DENV NS1 revealed the crucial lipid group for protein-lipid interaction and differences in concentration and level of the surface and core lipid groups of the lipid cargo. These findings all indicate the composition flexibility within the central lipid channel of NS1. The chapter provided in depth lipid information of DENV NS1 proteins and differentiated lipid classes amongst different dimeric and hexameric forms of DENV NS1.

In chapter 5, all information garnered from NS1 studies involving mutagenesis, membrane association, oligomerization, and lipidomics are synthesized in order to provide context for NS1 functions. The application of these findings for future directions in NS1 pathogenesis and vaccine development, gaps in the current literature, other questions which are answered in the study, and further questions based on these data are also discussed.

2. WNV NS1 FUNCTIONS IN VIRUS INFECTIVITY AND ENTRY

2.1 Chapter summary

West Nile virus (WNV) and Dengue virus (DENV) are arthropod-borne human pathogens within the *Flaviviridae* family. These viruses are causative agents for a range of mild to lethal diseases and there are currently no US-licensed therapeutic treatments for infection. Of the ten flavivirus viral proteins, NS1 remains the most elusive in terms of its function. To date NS1 has been linked to disease pathology and progression and plays a role in virus replication and assembly. However, little is understood how NS1 orchestrates these functions and how NS1 proteins from different viruses function distinctively from one another. In this study, a molecular genetic analysis was conducted on WNV NS1 residues 101, 218, and 343. These residues were previously identified in DENV NS1, to cause assembly defect phenotypes. In this study, reciprocal mutations on WNV revealed differences in functions of WNV and DENV NS1. Substitution at residue 343 (K343E) from WNV to DENV showed an increase in virus titer and specific infectivity while substitution at residue 218 (G218I) resulted in no change compared to WT. Mutation P101K in WNV showed a similar phenotype as the reciprocal mutation in DENV NS1, which was a reduction in titer. Further investigation on infectious virus formation, trafficking and protein secretion suggested the change in specific infectivity was affecting entry. Purified mutant viruses were trans-complemented with purified NS1 to examine the change in virus infectivity and entry. The results suggested a role of NS1 in WNV particle infectivity via an interaction of the virus particle, NS1 protein, and extracellular factor(s). Together, our data identified specific residues on NS1 important for virus assembly and entry and also highlighted differences between WNV and DENV NS1.

2.2 Introduction

West Nile virus (WNV) and Dengue virus (DENV) are members of the flavivirus genus. These viruses cause a range of illness from mild fever to severe fatal syndromes such as dengue hemorrhagic fever, dengue shock syndrome, encephalitis, and meningitis. In addition to a public health challenge, these viruses also impose a severe economic impact. Particularly for dengue illness, the annual worldwide cost was about $8.9 billion in 2013 [88]. No effective treatment is available for either virus while DENV vaccine produced by Sanofi is still controversial [89].

Flaviviruses have a single positive strand RNA, which encodes ten viral proteins including three structural proteins (envelope, membrane and capsid proteins), and seven non-structural proteins (NS1, NS2A, NS2B, NS3, NS4A, NS4B, and NS5). Among them, NS1 is a secreted protein and is widely used as a biomarker for the detection of DENV infection. The 352 amino acid protein with a molecular weight of 46-55 kDa is highly conserved in flaviviruses. The protein is known to play a key role in viral replication and recently was reported to function in viral assembly [57, 68]. Unlike other nonstructural proteins, NS1 can traffic to three destinations, including the replication complex, the plasma membrane, and the extracellular milieu. When secreted, it is found at high concentrations (up to 50 g/mL) in the sera of infected patients [90]. Secreted NS1 contributes to viral pathogenesis by antagonizing host complement by binding to complement regulator protein factor H, protein C1s, C4, and C4bP [72,91,92]. Moreover, NS1 can increase the permeability of human epithelial cells and induce vascular leakage and inflammatory cytokine production, which leads to lethal vascular leak syndrome [75, 76].

The crystal structures of the DENV and WNV NS1 proteins were solved in 2014 and revealed three distinct domains including the β-roll (amino acids 1-29), wing (amino acids 30-180), and β-ladder (amino acids 181-352) (Fig 2.1A) [45]. The dimer NS1 structure was reported to be similar between DENV and WNV although the proteins share only 55% sequence identity (Fig 1B). In addition, the NS1 proteins

from WNV and DENV differ in three aspects: i) outer surface electrostatics, which is more positive for DENV and neutral for WNV [46]; ii) localization (surface expression pattern) in which DENV NS1 is mostly secreted while WNV NS1 remains mostly at the plasma membrane [39]; and iii) vascular leakage, which is triggered by secreted DENV NS1 but not WNV NS1 [75]. It is interesting how similar the flavivirus NS1 structures are to each other, despite having such divergence in their amino acid composition. This unique attribute of NS1 allowed us to ask if the specificity of host factors or viral proteins that interact with NS1 varies from DENV to WNV. It is possible that the amino acids which act together to form similar structures might form different interactions with lipids and/or host and viral proteins, which could contribute to the pathological differences observed between DENV or WNV.

In previous studies from our laboratory, extensive mutagenesis on the wing and β-ladder domains of DENV NS1 revealed a group of mutations causing assembly defects. The substitutions were from DENV to WNV amino acids in the DENV infectious clones. Those mutations were at residues 101, 218, and 343. In this study, we introduced amino acid substitutions at the same residues from the WNV sequence to the DENV sequence in order to maintain the structure of the protein and investigate the NS1 change in its functions and behaviors. We found that substitutions of WNV to DENV influenced NS1 secretion and virus infectivity. Here we demonstrate important amino acids in WNV NS1 and begin to elucidate the role of NS1 in virus infectivity and virus entry as well as possible residues contributing to differences in DENV and WNV NS1 pathogenesis.

2.3 Materials and methods

2.3.1 Cell lines

Baby hamster kidney (BHK) cells were maintained in Minimal Essential Medium (MEM) with 10% FBS and incubated at 37°C with 5% CO_2. Vero cells were main-

tained in Dulbelcco's modified Eagle medium (DMEM) containing 2-10% FBS at 37°C with 5% CO_2.

2.3.2 Plasmids

The WNV strain NY99 infectious cDNA clone was constructed using two plasmids pWN-AB and pWN-CG as described previously [93]. Plasmid pWN-AB contained WNV nucleotides 1-2495 (encoding the 5' region, C, prM, E and the first 41 amino acids of NS1) and a T7 promoter while plasmid pWN-CG contained WNV nucleotides 2496-11029 (encoding the rest of the virus genome) and engineered XbaI restriction site for linearization in virus *in vitro* transcription.

The WNV replicon contained the WNV non-structural genes (from amino acid 43 on NS1 to NS5 and the 3' region) based on the WNV NY99 strain and encoding the *Renilla* luciferease reporter gene.

A purification system for WNV-NS1(referred as SINV-NS1-His), derived from Sindbis virus (SINV) pToto64 plasmid without the SINV structural proteins, was engineered with BssHII and XbaI restriction sites to insert a E protein signal sequence (the last 72 nucleotides) and the NS1 gene with an 6x-His tag at the end of NS1.

2.3.3 Site-directed mutagenesis

Direct complementary primers corresponding to the nucleotide changes were designed using PrimerX and synthesized by IDT. The forward and reverse primers for mutation P101K were 5'GGGAATGTACAAGTCAGCAAAGAAACGCCTCACCGCCACCAC3' and 5'GTGGTGGCGGTGAGGCGTTTCTTTGCTGACTTGTACATTCCC3'. The forward and reverse primers for mutation G218I were 5'CAAAACCAGGGCCCATGGGACCTGGGCCGGGTAGAGATTGACTTC3' and 5'GAAGTCAATCTCTACCCGGCCCAGGTCCCATGGGCCCTGGTTTT3'. The forward and reverse primers for mutation K343E were 5'GACCACAGAGACATGATGAAGAAACCCT CGTGCAGTCACAAG3' and 5'CTTGTGACTGCACGAGGGTTTCTTCA TCAT-

GTCTCTGTGGTC3'. Mutations were made using a PCR protocol for Phusion high fidelity DNA polymerase (NEB) and PCR products were digested with DpnI at 37°C for 1 hr before being transformed into DH5α cells. Colonies were selected for plasmid purification and sent for sequencing to determine if the clones had the correct mutation in NS1. Two independent correct clones were chosen for each mutation for further characterization.

2.3.4 *In vitro* transcription and viral RNA electroporation

For WNV NY99 infectious cDNA clones, three microgram of each plasmid pWN-AB and pWN-CG was digested by XbaI and NgoMIV restriction enzymes. After digestion, plasmid was extracted by gel extraction kit (Qiagen) and a total of 1 microgram product of the two plasmids was used for ligation at a molar ratio 1:1 at 16°C overnight. Ligated product was directly linearized by XbaI at 37°C for 1 hour. *In vitro* transcription was carried out using T7 RNA polymerase with cap A at 37°C for 1 hour. RNA product was confirmed by agarose gel electrophoresis.

For WNV replicon, five hundred nanogram of WT or mutated NS1 plasmids were used for *in vitro* transcription using XbaI linerization and T7 RNA polymerase with capA as described above. RNA products were also confirmed by agarose gel electrophoresis.

For SINV-NS1-His, WT and mutated plasmids were linearized by SacI and transcribed via SP6 RNA polymerase with capA. RNA was checked on an agarose gel.

For transfection into BHK cells, RNA of WT and mutants were electroporated into BHK cells using the following settings: 1.5kV, 25F, 200 Ohms and 2 pulses for 3 seconds each. Electroporated cells were incubated at 37°C with 5% CO_2 in incubator at Biosafety level 3. Supernatants and lysates were harvested at 72hpe and stored at -80°C until use.

2.3.5 Plaque assay

BHK cells were seeded into 6-well plates one day prior to plaque assay to achieve a monolayer. Serial ten-fold dilutions of virus samples was made in PBS and virus dilutions were added to each well. The plates were rocked at room temperature for 1 hour. A mixture of 1% agarose, MEM and 5% FBS was added to each well. The plates were incubated at 37^oC with 5% CO_2 for 72 hours. Plaques were stained with neutral red solutions (Sigma-Aldrich) on day 2 post infection and plaque number were visualized and reported on day 3.

2.3.6 Luciferease assay

WNV replicon expressed Renila Luciferase as a reporter for virus replication. BHK cells were electroporated with WT and mutant RNA and plated onto 24 well plates. At 16-, 24-, and 36- hpt, cell lysates were collected using lysis buffer (Promega) and 20μl of the lysed samples were incubated with Renilla substrate (Promega) in 96-well plate SpectraMax L luminometer and measured with a Softmax Pro Software (Molecular Devices). Delta DD (DDD), a lethal mutation in NS5, was used as a negative control for virus replication and background luciferase signal from the input RNA.

2.3.7 Quantitative PCR for viral RNA

BHK cells were electroporated with full-length WNV RNAs and plated into 6-well-plates. Supernatant (100 μl) and lysate (10^6 cells) from one well of the plate were used for RNA extraction using RNeasy mini kit (Qiagen). Mock well (mock electroporated cell) was used as negative control for RNA extraction. Quantative PCR was performed using SYBR Green One-step qRT kit with ROX (Invitrogen) and WNV specific primers.

2.3.8 western blot

Transfected cells were collected for supernatant and lysate. Cell lysates were washed with PBS three times before being lysed by RIPA buffer with protease inHiBiTor cocktail (Abcam). Proteins from supernatants and lysates of WT and mutants were separated by SDS-PAGE and transferred to nitrocellulose membranes. The membranes were blocked with 5% skim milk in PBST for 1 hr, followed by three PBST (PBS with 1% Tween20) washes, then incubated with either mouse monoclonal antibodies E16 for E protein (gift from Dr. Ted Pierson), Rabbit NS1 (Kuhn lab), or β-actin for actin (Abcam) for 1 hr and washed three times with PBST. Secondary anti-Rabbit or mouse antibodies (Li-COR) were incubated with the membrane for 1 hr and visualized with an Odyssey CLx Imager (Li-COR) and software Image Studio Lite 5.0.

2.3.9 ELISA

Supernatants from full-length WNV transfected cells were collected at 72 hpt and used for direct ELISA. Four ten-fold dilutions of the samples were prepared in coating buffer (Na_2CO_2, $NaHCO_3$ at pH 9.5) in 96-well microtiter plate and incubated at 4^oC overnight. The plate was washed 3 times with PBST to remove all the antigens, followed by incubation with either E16 for E protein or NS1-WN9 for NS1 (gift from Dr. Michael Diamond) at 5 μg/ml for 2 hrs at room temperature on a rocker. Washing 3x with PBST was performed again prior to addition of anti-mouse HRP (Sigma). The plate was incubated for 2 hrs at room temperature in dark. After being washed with PBST, the plate was incubated with 3,3',5,5'-tetramethylbenzidine (Abcam) in the dark for 15-20 minutes to develop color. The reaction was stopped with 1M H_2SO_4 and the absorbance was measured at 450 nm.

2.3.10 Virus purification

Vero cells were seeded into 10 T150 flasks one day before use for WNV infection ata MOI 0.01. The flasks were incubated at 37^{o}C with 5% CO_2 for 72 hpi . Supernatants were collected and filtered through a 0.22 μm filter. Virus particles were precipitated with 8% polyethylene glycol (PEG) 8000 overnight at 4^{o}C, and pelleted at 8000 x g for 50 minutes at 4^{o}C. Particles were resuspended in NTE buffer (20mM Tris pH 8.0, 120mM NaCl, 1mM EDTA). Re-suspended particles were pelleted through a 24% sucrose cushion, re-suspended in 0.5 ml NTE buffer and purified with a discontinuous gradient in 5% intervals from 35% to 10% potassium tartrate in 20mM Tris pH 8.0 and 1mM EDTA. The gradient tubes were spun at 30,000 rpm for 2 hrs at 4^{o}C in an SW-41 rotor (Beckman). Mature virus was extracted from the gradient, concentrated and buffer exchanged into NTE buffer using an 100 kDa cut-off Amicon concentrator (Sigma Aldrich).

2.3.11 His-tagged protein purification

BHK cells were seeded one day prior to electroporation with SINV-NS1-His RNA. Electroporated cells were incubated for 72 hpe and supernatants were collected, centrifuged at 3000 rpm for 5 mins at 4^{o}C. The clarified supernatants were added 50 mM Tris and 150 mM NaCl for binding to Ni-NTA beads, and 5 mM imidazole to avoid unspecific binding at the incubation stage. Supernatants with beads were incubated overnight at 4^{o}C on a rotator and purified using a gravity column purification method. The beads were washed with 40 bead volumes wash buffer (50 mM Tris, 150 mM NaCl and 30 mM Imidazole). WT and mutant proteins were eluted with elution buffer (50 mM Tris, 150 mM NaCl and 150 mM Imidazole). Eluates were concentrated and buffer exchanged into PBS buffer using an 10 kDa cut-off Amicon concentrator (Sigma Aldrich).

2.3.12 Entry assay

BHK cells were seeded into 6 well plates one day before the assay. Purified viruses at a set concentration were incubated on NS1-bound cells for 1hr at 4^oC. then washed with PBS twice. The plates were placed at 37^oC for 1 hr to allow endocytosis then washed with a cold high salt solution (1M NaCl and 50mM sodium bicarbonate, pH 9.5) for 3 minutes to remove cell surface associated virus prior to lysis and vRNA purification following manufacturers specifications (RNeasy Kit, Qiagen). After vRNA was extracted the amount of virus particles was quantified by qRT-PCR as described above.

2.3.13 Statistical analysis

All analyses and graphs were generated using GraphPad Prism 8 software. Comparison between mutants and mock with WT were analyzed using a one-way ANOVA or t-test if the comparison between a mutant and WT. Differences between groups were considered significant when p value was lower than 0.05.

2.4 Results

2.4.1 Mutations in WNV NS1 cause no effect on virus RNA synthesis but alter virus titer

Based on the high structural similarity but divergence in amino acid composition between WNV and DENV NS1, we hypothesized that substitution of non-conserved amino acids between WNV and DENV might elucidate the amino acids that determine virus-specific NS1 roles. The structures of NS1 proteins from WNV and DENV were inspected to select surface-exposed residues that were conserved among four DENV serotypes but different from WNV (Fig 2.1). Amongst 36 amino acid substitutions in DENV, a group of assembly defect mutations were selected. The group, including mutations at residues 101, 218, and 343, was characterized in DENV by

Michael J. White. Based on the characterization, mutations at residues 101, 218, and 343 in the DENV NS1 protein did not affect the NS1 function in viral RNA synthesis but caused reduced or no infectious titer.

To determine the effect of these NS1 mutations on WNV, the reciprocal mutations were generated in the WNV replicon and infectious virus systems. The WNV replicon contained only viral non-structural proteins with the reporter gene for Renilla luciferase. A negative control contained a lethal mutation in NS5 (DDD) and represented the base signal of electroporated RNA. The viral RNA synthesis of mutants and WT were monitored via Renilla luciferase assay at 0-, 6-, 12-, 16-, 18-, 24-, 36-, 42-, and 48 hours post electroporation (hpe). Mutations P101K, G218I, and K343E showed replication at WT levels (which differences within one log) at all time points (Fig 2.2A). The results showed similar effects of these mutations on WNV replication as in DENV replication, suggesting that mutations at these residues did not involve NS1 function in viral RNA replication in both flaviviruses.

The infectious WNV system contained all viral proteins and was able to produce infectious virus. The mutations were introduced into the system and *in vitro* transcribed to RNA before being electroporated into BHK cells. Supernatants and lysates of the transfected cells were collected at 72 hours when cytopathic effects was observed. In contrast to virus replication, virus titers showed dramatic changes caused by the mutations. Mutant P101K yielded lower titer (3 logs)than WT, while mutant K343E yielded higher titer (2 logs) than WT. Mutant G218I titer was within 1 log from the WT titer (Fig 2.2B). Unlike DENV, the reciprocal mutations in WNV produced not only assembly defects but also enhanced assembly, suggesting the chosen residues may play a regulatory role in virus assembly or infection and may be independent of NS1 functions in viral RNA synthesis.

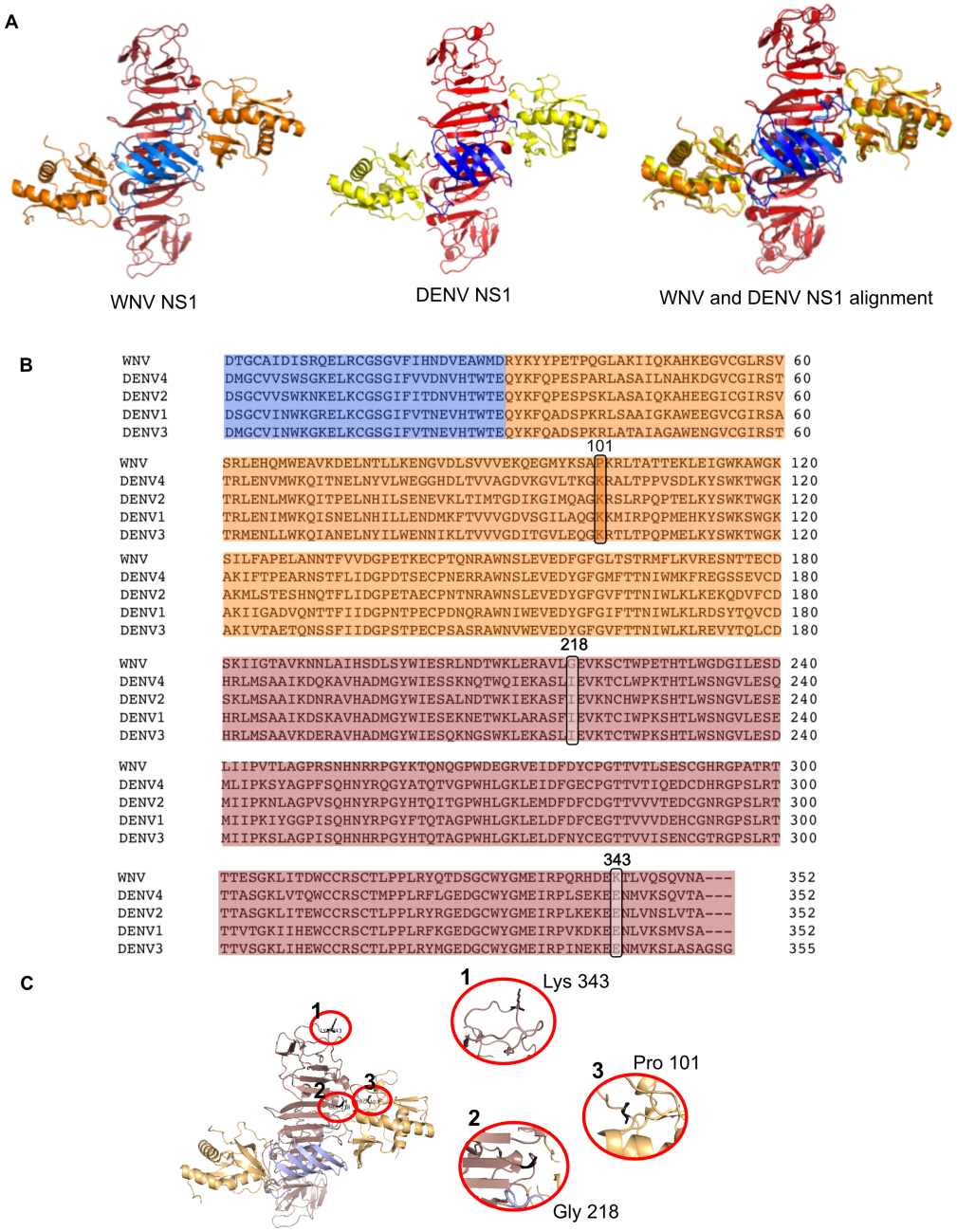

Fig. 2.1. Alignment of WNV and DENV NS1 structures and sequences. **(A)**. Structure of WNV NS1 (PDB ID 4O6C) and DENV NS1 (PDB ID 4O6B) and the alignment of the two proteins. Each domain was color coded**(B)**. Sequence alignment of four serotypes of DENV NS1 and WNV NS1 (NY99) with the same domain color code as in the WNV NS1 structure. Sequence alignment of the WNV and DENV serotypes 1, 2, 3 and 4. West Nile strain NY99 (WNV), ABA62343; Dengue 1 strain 16007 (DEN1), AAF59976; Dengue 2 strain Thailand/16681/84 (DEN2), AAB58782; Dengue 3 strain BR/D3LIMHO/2006 (DEN3), AEV42062; Dengue 4 strain 814669 (DEN4). The chosen mutations were highlighted on the sequences. **(C)**. Location of chosen mutations on WNV NS1 structure. Each mutation were enlarged in the circles at the right of the structure.

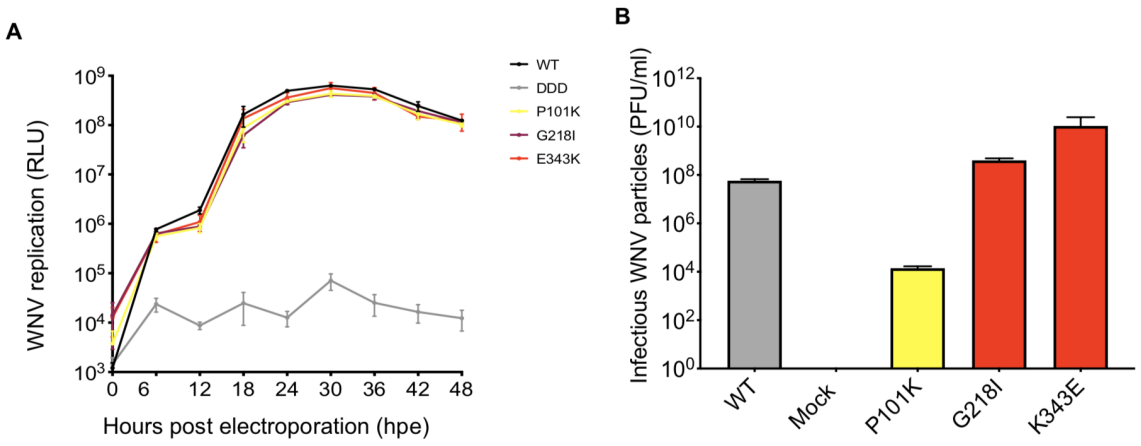

Fig. 2.2. Mutations alter virus titer but not virus replication. **(A)** Kinetics of virus replication with chosen mutations. WNV reporter replicon was used to determine the effect of NS1 mutations on virus replication in the absence of virus assembly. Cells transfected with WT and mutated NS1 were monitored for luciferease activity for every 6 hrs post electroporation. Luciferase values represented the average of three independent experiments. **(B)** Virus titer of chosen mutants. Mutations at residues 101, 218, and 343 were engineered into the infectious WNV system. Supernatants of WT and mutants were collected at 72hpe for plaque assay. Virus titer was recorded from two independent experiments.

2.4.2 Changes in infectious virus formation and release

The change in virus titer can be explained by at least one of the following possibilities: 1) virus forming more or less intracellular infectious particle leading to changes in the number of extracellular infectious particles; 2) the same amount of intracellular infectious particles were formed but the mutation caused a change in virus trafficking leading to change in the amount of extracellular infectious particles; 3) the same amount of infectious particles but mutation caused changes in virus entry efficiency. To determine the reason for the change in mutant titer, intracellular infectious particles of the mutants were analyzed and compared with WT virus. BHK cells were transfected with RNA of mutants or WT and lysates were collected at 72 hpe. Lysates were treated with three times freeze-thaw cycles to gently break the cells before being used for plaque assay. The intracellular infectious particles of both P101K and K343E showed the same titer change as the extracellular particles from the corresponding mutations (Fig 2.3A). The data showed that the P101K mutation in NS1 led to less infectious virus intracellularly and extracellularly, and the E343K mutant produced more infectious particles intracellularly and extracellularly. The ratio of intra/extra infectious particles of both mutants equal to that of WT, suggesting particle trafficking was not the reason for changes in virus titer. Thus, the two mutants fit into category 1 with either a reduction or increase in the formation of internal and thus external virus. However, the G218I mutant produced more internal infectious virus but released infectious virus at WT levels (Fig 2.2A) , which suggested the mutant fit category 2 with a partial block in virus release). Since there was no change in the level of RNA replication, it would seem that either these mutations result in more efficient packaging of vRNA into viral particles and thus an increase in total particle formation, or the changes to NS1 are altering virus entry.

To determine the total number of secreted particles (both infectious and non-infectious particles), extracellular virus RNAs were measured by qRT. For all mutants, near equal amounts of vRNAs were released for 218 and 343, and within 1 log

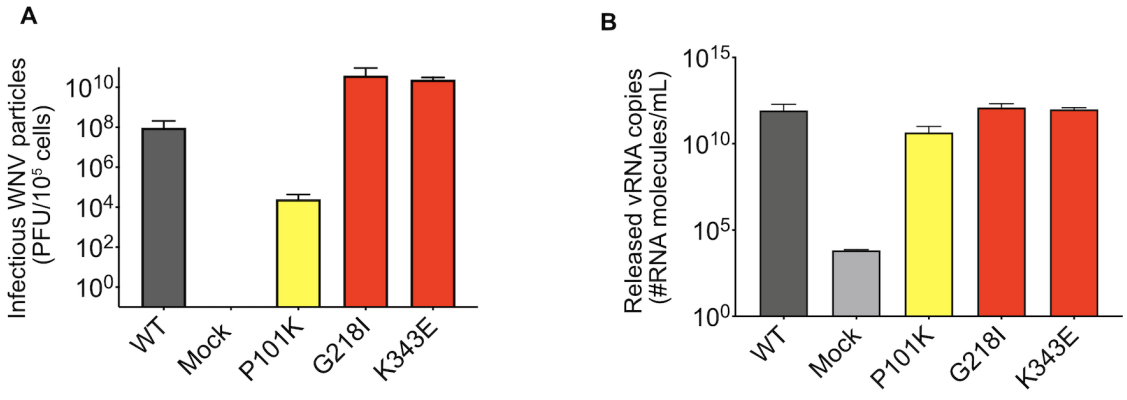

Fig. 2.3. Analysis of intracellular virus titer and released viral genomes. **(A)** Intracellular infectious virus titer. BHK cells were electroporated with the same amount of WT and mutant RNA (15μg). Lysates were collected at 72hpt and lysed by the freeze-thaw method three times. Cell lysates were used for plaque assays and plaque numbers were recorded on day 3 and calculated for virus titer. **(B)** Released viral RNA genome. The supernatants from electroporated samples were measured for vRNA copies by qRT-PCR. Values represent the average of two independent experiments. Error bars represent the standard deviation.

reduction in vRNA was released for 101 (Fig 2.3B). The specific infectivity of the WNV mutants was calculated as the amount of vRNA required to form an infectious particle, which showed WT level of specific infectivity for mutant 218 but increase in specific infectivity about 2 logs for mutant K343E, while the P101K substitution reduced the specific infectivity 3 logs compared to WT. From this analysis, it appeared that WNV to DENV changes led to either a reduction or increase in specific infectivity, depending on the residue.

2.4.3 Changes in E and NS1 expression and secretion level

To determine if the change in viral particle yield for WNV substitutions was related to E and NS1 expression and secretion, the levels of E and NS1 were determined by western blot and ELISA. Supernatants and lysates from transfected cells at 72 hpe were subjected to western blot and ELISA (supernatant only). Unlike DENV, WNV produced two forms of NS1, NS1 and NS1'. NS1' is an extended version of NS1 due to an alternative splicing of a pseudoknot-structure at the N-terminusinus of NS2A, resulting in an addition of 52 amino acids and producing a larger size (52-53 kDa) protein [94]. NS1' was found in both supernatants and lysates of mammalian and insects cells and and is suggested to share the same function as NS1, thus it was interchangeable for NS1 [95]. Western blot results of the lysates revealed that NS1' was produced in both WT and mutants. NS1 and NS1' were able to form homodimer (NS1-NS1 or NS1'-NS1') and heterodimers (NS1-NS1') (Fig 2.4 A). The NS1 and NS1' showed a slight reduction for mutants P101K and K343E, and WT and G218I were at similar intensity while the intracellular E protein was detected at similar level for all samples. NS1 and NS1' were not well separated in extracellular samples but were still consistent with the intracellular levels at the signal intensity, in which both P101K and K343E were lower in NS1/NS1' while the G218I was approximately similar to WT. E protein could not be detected in the NS1 sample of P101K, in

agreement with the low titer of the mutant but K343E showed extracellular E at a similar intensity as WT (Fig 2.4B).

To quantify the secretion of E and NS1 proteins, ELISA was performed for extracellular samples of WT and mutants. Secretion of E protein showed WT levels for G218I and K343E with a significantly lower level for P101K (Fig 2.4C). ELISA data for NS1 secretion, in contrast, showed differences among WT and all of the mutants (Fig 2.4D). All mutants released significantly less NS1 compared to WT, in which P101K was the lowest and K343E was also low in NS1 secretion (Fig 2.4D). The release of E protein from mutated viruses was consistent with the virus titer but NS1 secretion by the selected mutants was lower, suggesting these amino acid substitutions in WNV disrupt interactions with factor(s) specific for WNV NS1 secretion. The amount of secreted E protein for mutant K343E was consistent with the level of vRNA release, which confirmed the change in the virus infectivity was not because of increased virus production but instead the ability of the virus to infect cells. E and NS1 secretion were low or below the detection limit for the mutants at residue 101 for both DENV and WNV while the mutation caused no effect on virus replication, suggesting that mutating residue 101 of DENV and WNV may disrupt an interaction with host or virus proteins leading to NS1 secretion.

2.4.4 Mutations in NS1 alter virus infectivity via modulating virus entry

For virus infection, virus must first bind to cell (attachment) and then enter the cell and release its genome. To determine if entry was affected by these amino acid substitutions, an entry assay was used. BHK cells, the same cell line for virus transfection, and sample supernatants were pre-chilled at 4^oC for 1h before viruses were incubated with cells for 1h at 4^oC for virus attachment. The cells were then washed to remove unbound viruses. Attached viruses were allowed to enter via incubation at 37^oC for 1h (Fig 2.5A). After the entry assay, cells were washed with high salt buffer to detached surface-bound virus and cells were lysed to extract viral RNA genomes.

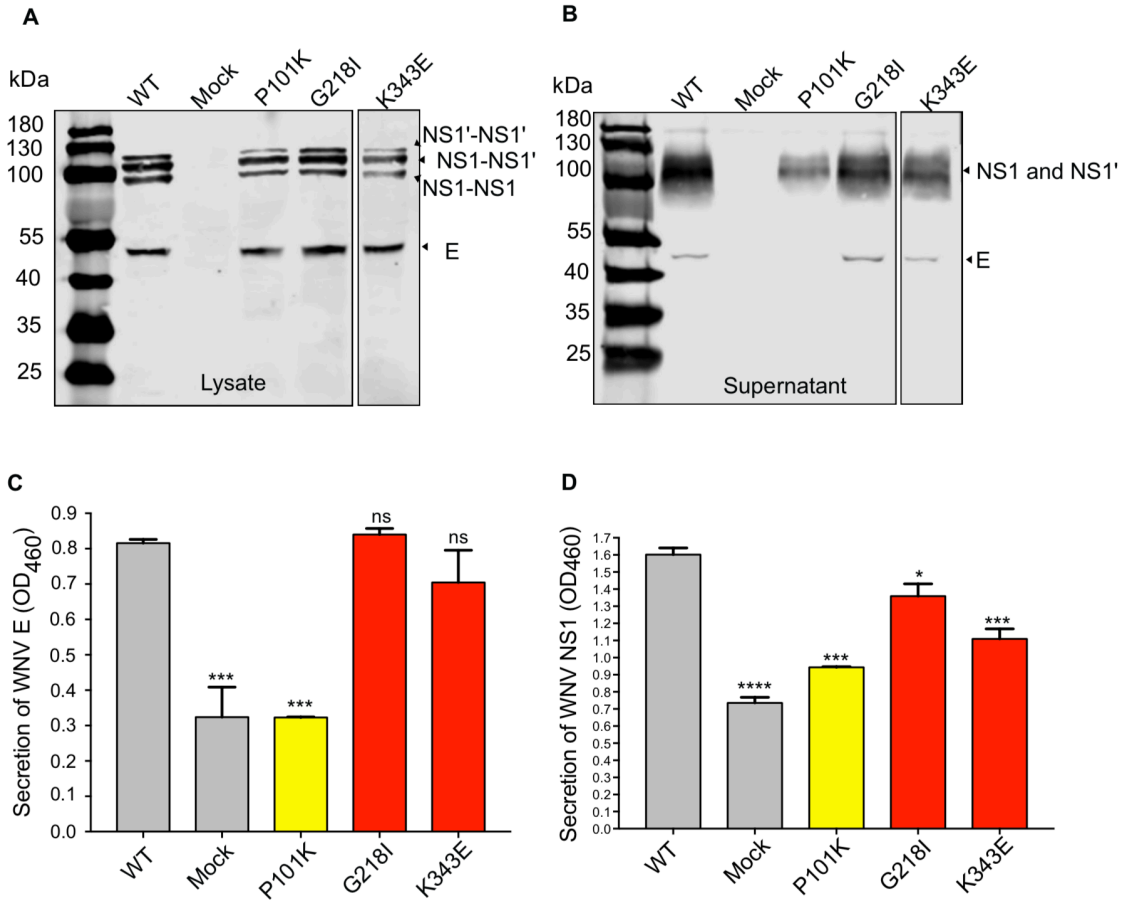

Fig. 2.4. Secretion of E and NS1 proteins. Analysis of E and NS1 proteins intracellular **(A)** and extracellular **(B)** by western blot assay. Lysate and supernatants of electroporated BHK cells were collected 3dpe and subjected to western blot assays. The membranes were probed with anti-NS1 antibody (Rb NS1) and anti-E antibody (E16). Molecular ladder is shown in kilodalton. Supernatants were quantified for secreted E **(C)** and NS1 **(D)** by ELISA. Direct ELISA assay was performed with supernatant samples coated at the bottom of a 96-well plate. Antibodies against E or NS1 were incubated with samples overnight and the absorbance were measured at 460 nm. Data were the average of two independent experiments.

Using the same amount of vRNA copies (10^8 copies), all virus particles entered cells at a rate of 1/1,000 (approximately 10^5 copies entered) after an hour attachment and entry. P101K showed WT level of entry while K343E was 3 fold higher than WT (Fig 2.5B), suggesting mutation K343E could enhance virus entry efficiency. The entry results supported the virus specific infectivity data of K343E as the virus was more infectious and the change may be driven through increase in virus entry. Corresponding mutations in DENV, in contrast, showed the reduction in virus entry, as well as the specific infectivity, indicating the residue may play critical roles in flavivirus viruses (DENV and WNV). Mutation P101K did not show change in virus entry, suggesting the mutated virus particles were able to get internalized to new cells as efficiently as WT and the change in virus infectivity was at a different step in virus life cycle. The corresponding mutation on DENV caused a virion formation defect, therefore, not producing any particle for virus entry.

2.4.5 Specific infectivity of purified virus particles were not affected by mutations on NS1

To determine if the mutations in NS1 caused changes in virus particles, leading to the alteration in the specific infectivity, secreted particles of WT and mutants were purified and separated from NS1 proteins and extracellular components. WNV particles were purified from supernatants of infected Vero cells at 72 hpi. The particles were analysed by SDS-PAGE and western blot. SDS-PAGE presented the viral structural proteins including bands at sizes corresponding to envelope, M/prM and capsid (Fig 2.6A). There was no NS1 band on the protein gel, thus western blot were performed to detect if NS1 co-purified with the virus particles (Fig 2.6B). The results confirmed that there was no NS1 in any purified virus particle sample. It also suggested that NS1 may not bind tightly with the particle in the extracellular environment.

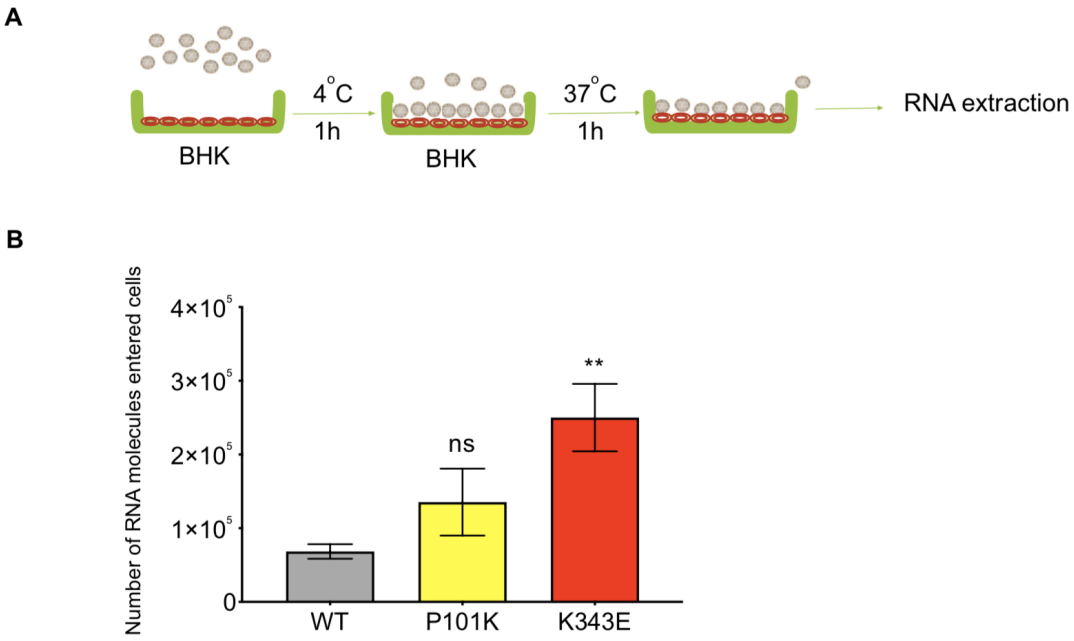

Fig. 2.5. Changes in virus entry. **(A)** Schematic diagram of entry assay. BHK and extracellular viruses were pre-chilled at 4^{o}C for 1h. Similar number of WNV vRNAs were added to BHK cells at 4^{o}C for 1hr. Plates were then washed 3 times with PBS then incubated at 37^{o}C for 1 hr to initiate viral entry. Plates were then washed with PBS and high salt wash buffer. RNA from cells was extracted by using Qiagen Rneasy extraction kit and quantified by qRT-PCR.**(B)** Entry assay. Supernatants of WT and mutants were calculated for 10^8 vRNA molecules for entry assay. Values were normalized to mock samples in the assay. The bars represent the average of three independent experiments.

The specific infectivity of purified viruses were examined. Plaque assay revealed the purified viruses of P101K and K343E were at WT titer and qRT data suggested all viruses also released WT levels of viral RNA (Fig 2.6B and C). The specific infectivity showed no significant difference between WT and mutants, indicating the mutations in NS1 did not affect the virus particle. The average specific infectivity for the virus particle was about 1.9 x 10^3 vRNA per infectious particle. The purified virus of WT had the specific infectivity of supernatant WT, suggesting the purified particles behaved as the the particles in the supernatant. The purified P101K particles , however, showed about 3 logs less vRNA required for an infectious particle, indicating the infectivity of virus paticles may be reduced by factor(s) in the extracellular environment. In contrast to P101K, the specific infectivity of K343E particles required more vRNA (1log) per a infectious particle compared to the particles in the supernatant, suggesting extracellular factor(s) may lessen the infectivity of particles in supernatant .

2.4.6 NS1 proteins modulate the entry of virus particles

The purified viruses were further characterized for the entry efficiency. Entry assay were performed using two different amounts of vRNA from WT and mutants to determine and evaluate the virus entry rate. Equal amounts (10^8 or 10^9) vRNA were used for each sample. Entry rates of WT in both were about 1/1,000 vRNA in an hour of attachment and entry. Both P101K and K343E purified viruses showed higher entry 2-5 fold higher than WT and there was no differences between P101K and K343E entry rate (Fig 2.7A and B). For K343E, the increase in entry rate of purified particles was at the same level as that of supernatant (Fig 2.5B), indicating the purified particle entered cells as efficiently as the particle in supernatant. The differences in specific infectivity of the K343E mutant suggested the increase in entry would not be the only causative reason for the increase in the specific infectivity. For P101K, the entry rate was better when there was only virus particles but at WT

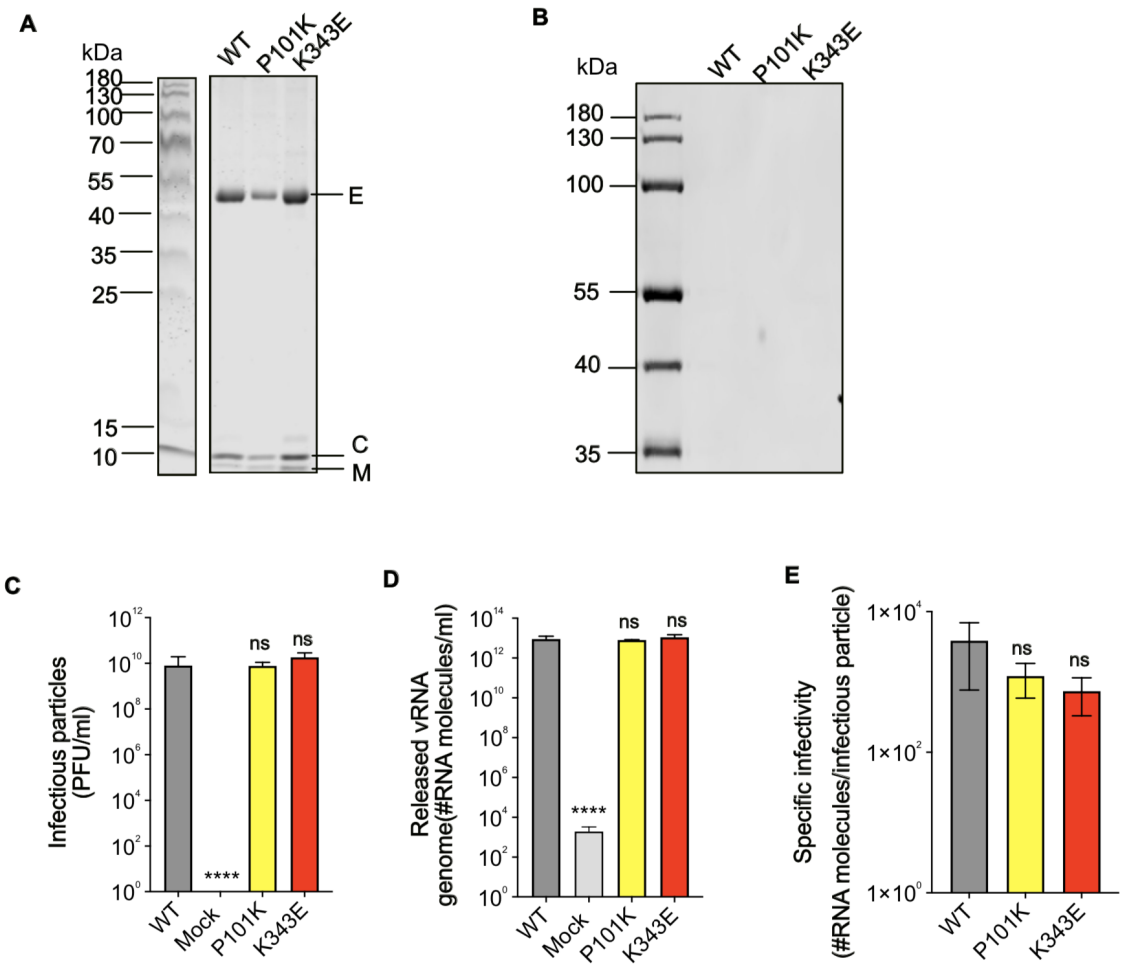

Fig. 2.6. Purified virus particles have the same specific infectivity and entry efficiency. **(A)** SDS-PAGE analysis of purified WNV particles from WT and mutants. WT and mutant samples were separated on SDS-PAGE for the presence of virus particles proteins including envelope (E), membrane (M) and capsid (C) proteins. **(B)** Western blot analysis of purified virus particles using anti-NS1 antibody for the presence of NS1 in purified virus particle samples. **(C)**Titer of purified viruses. Purified viruses were subjectd to plaque assays to determine the infectious particle titer.**(D)** Released vRNA of each purified virus were measured by qRT-PCR. **(E)** Specific infectivity of the virus particles were calculated as numbers of RNA molecules for each infectious particle. Number of released vRNA was normalized with mock samples before being used for the calculation. All graphs represent the average of three independent experiments.

level when there were other extracellular factors. The difference in the entry rate and infectivity of the mutants, therefore, was possibly the accumulation of extracellular factors over infection time.

Extracellular components of a virus infection contained both viral factors, such as virus particles and NS1 proteins, and host factors. Since the mutations were engineered in NS1, it is possible that the secreted protein may be the reason for the virus entry alteration. Virus particle entry levels were then examined in the presence of purified WNV NS1 at various concentrations. WNV NS1s were purified from BHK cells transfected with an expression system containing the whole NS1 gene with its signal sequence from E protein and a hexa-histidine tag at C-terminusinus. Mutated and WT proteins were collected at 72 hpt and separated from the supernatant mixture by Ni-NTA chromatography. Purified proteins were pre-chilled prior to co-incubation with virus particles and BHK cells. Virus particles from WT and mutants were diluted to approximately 10^{10} vRNA so we did not compare between WT and mutants but between the same virus particle group with different amount of NS1 supplement. Entry rate of the virus particles in all cases were similar to the range of the particles, about 1/1,000 vRNA. The addition of NS1 proteins from 1-10 μg/mL to the particles did not change the entry rate of P101K but slightly enhanced WT and K343E (1.2-1.6 fold higher) at the concentration of 10 μg/mL (Fig 2.7C). This result suggested that NS1 protein was able to enhance virus entry but mutation P101K may disrupt this activity of the protein.

2.5 Discussion

NS1 plays a myriad of important functions in the flavivirus lifecycle such as replication, assembly, immune evasion and pathogenesis, yet very little is understood about how it orchestrates these. Here we took an approach to investigate how NS1 might orchestrate these functions by making residue changes from DENV-WNV and WNV-DENV. In this study, we have found a panel of residues that can be used to

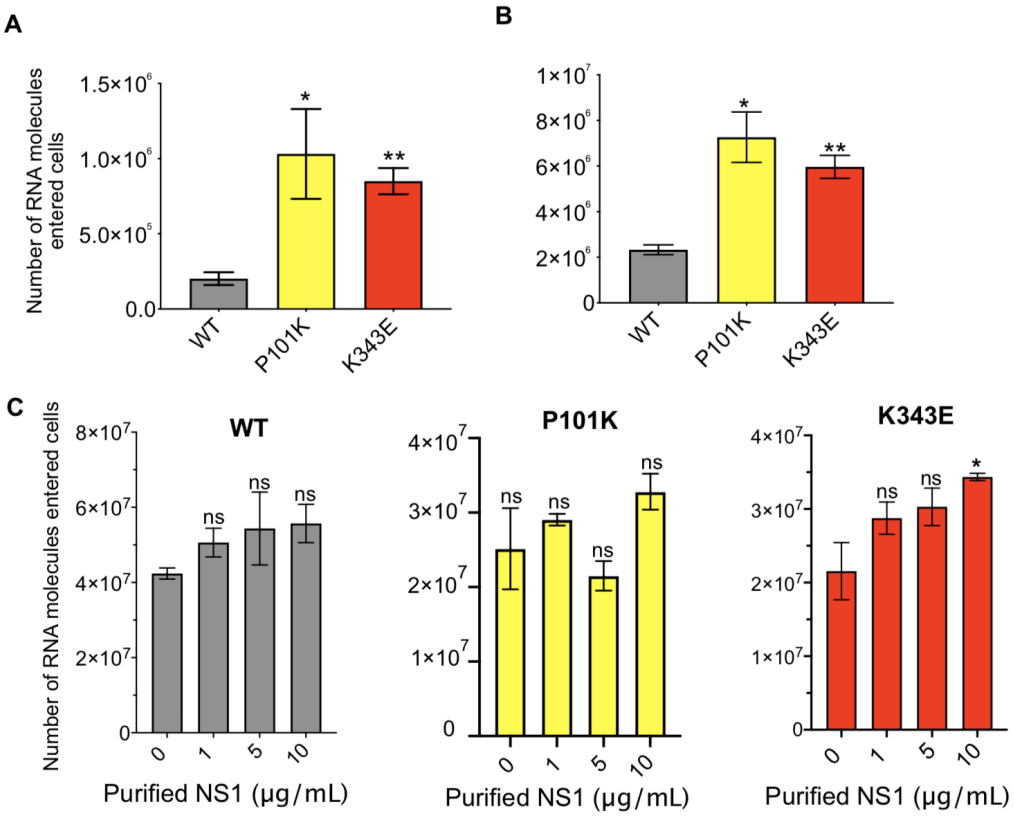

Fig. 2.7. Purified NS1 complement for virus particle entry. Entry assays of the purified virus particles using 10^8 **(A)** or 10^9 **(B)** vRNA genomes. **(C)**. Entry assay of virus particles with addition of homotypic NS1 proteins at concentrations from 1, 5, or 10 μg/mL. Results were normalized to mock samples in the entry assay. All graphs present the average of two independent experiments, duplicate for each experiment.

further probe the various functions of NS1 during a flavivirus infection. From our initial analysis of mutations in DENV, a group of mutations causing assembly defects without alterating virus replication were identified. DENV phenotypes were divided in two specific steps: (1) NS1 secretion or infectious virus release and (2) effects on virus specific infectivity. The reciprocal mutations on WNV also influenced trafficking of NS1 and virus particles, as well as virus specific infectivity, even though, there was differences in the effect of each mutation in different flaviviruses.

All mutations at residues 101, 218, 343 on DENV or WNV did not change virus RNA synthesis kinetics, but did alter the following steps in the virus life cycle. P101K on WNV caused reduction in virus titer and NS1 secretion. The intracellular and extracellular titer of P101K suggested the infectious viruses formed less intracellularly and less extracellularly, indicating the trafficking of the infectious particles was not affected by the the mutation on NS1. Unlike the infectious particles, secreted NS1 was less than the intracellular NS1. The differences in infectious particles and NS1 trafficking indicated the protein and particle traveled separately and had opposing secretion efficiency. The reduction of the intracellular infectious viruses also suggested that the NS1 mutation may affect virus at infectious particle formation or maturation. In the reciprocal mutation on DENV NS1 (performed by Michael J. White), K101P led to no infectious virus formation, and no NS1 secretion. In a previous report on DENV NS1, a single mutation on the NS1 wing domain (about 13-14 residues downstream of residue 101) caused a virus assembly defect via defect in interactions of NS1 and structural proteins including envelope, membrane, and capsid proteins [57]. Although a report suggested ER retained NS1 via KDEL-tag was trivial for the virion formation and release, the KDEL tagged protein could still travel from ER to cis-Golgi and retrograded to ER [96]. Therefore KDEL-NS1 may be still able to traffic to Golgi with the virion and allow NS1 to assist the virion formation and/or maturation. Thus residue 101 may disrupt NS1 secretion and virus formation via the loss in its interaction with viral and host proteins. In addition, the P101K supernatant showed that the mutation did not change the cellular entry ability and efficiency but puri-

fied infectious particles showed that without extracellular components, the particles could enter cells better than WT. Addition of P101K NS1 proteins to purified P101K particles did not enhance the particles entry while the WT NS1 protein enhanced the purified WT particles for its entry. This suggested there may be interaction of released particles and secreted NS1. As there was no NS1 detected in purified virus particles, the interaction may occur when they were released into the extracellular environment. The mutation P101K on NS1 may disrupt the interaction of NS1 and virus particles, and thus led to no enhancement in virus entry. This interaction of NS1 and virus for entry, was in line with emerging studies of extracellular NS1 functions in flavivirus infectivity. A recent study demonstrated that a single mutation on the wing domain, an adjunct residue of the greasy finger, led to an increase in NS1 secretion, and also an increase DENV load in the midgut of mosquitoes [97]. A DENV NS1 treatment prior to virus infection could also enhance the virus production [37]. Our study provided a new function of secreted NS1 in virus entry, thus can be used to explain its effect on virus infectivity.

We also identified a mutation, K343E, which showed the opposite effect on virus infectivity. Mutant K343E released less NS1 extracelularly, but a similar amount of E protein compared to WT. The intracellular traffic efficiency of the mutant infectious virus were not affected by the mutation but the virus infectivity. K343E had higher infectivity both intracellular and extracellular, confirming the function of NS1 in the formation of infectious particles. The particles were examined for their ability to infect cells in the presence of extracellular components (supernatant) or absence of all the components (purified particles). Virus entry occurred in both conditions, suggesting mutation K343E enhanced virus particles in entry capacity but also K343E NS1 could interact with the particles to enhance this capacity or have a direct effect on the cells. As the mutant produced less NS1 than WT but still had a better infectivity, the mutated protein may be improving in its ability to interact with the virus particles or structural proteins, thus required less proteins for increase in the infectivity. As the concentration of NS1 we examined for virus entry was limited to

10 μg/mL and there was an increase in virus entry at that concentration, higher NS1 supplements could be performed to determine the differences in the amount of NS1 for WT and mutants at the entry step. In addition, since the extracellular particles were shown to be interacting with NS1, it was possible that K343E NS1 could interact with intracellular particles to enhance its infectivity. The corresponding mutation on DENV showed the opposite effect as there were less infectious intracellular and extracellular viruses but there was no change in NS1 and E release. The contrasting results of the mutations on the same residue on DENV and WNV suggested the specificity of the residue for each virus. This specificity was related to NS1 secretion amount and functions as well as virus infectivity.

Another mutation G218I on WNV also supported the function of NS1 in the infectious particle formation and in virus trafficking. As reported for P101K and K343E, the trafficking of the infectious viruses was not influenced by the mutations. In the case of G218I, more infectious viruses were produced in cells but were secreted at WT level. There was no change in specific infectivity and protein secretion (both E and NS1). The results confirmed that the secretion pathway of the infectious particles and NS1 was separated. The mutant enhanced the particle assembly and/or infectious particle formation but led to inefficient release of the infectious particles. As the particles were infectious, they must have traveled to Golgi and matured via glycosylation and furin cleavage [35]. The reduction of infectious virus release would be from Golgi to extracellular environment. It was possible that the G218I mutation may affect the trafficking in this compartment via indirect or direct interaction with host proteins. The mutation on DENV showed an opposite effects on extracellular virus titer but similar trafficking and secretion rates.

NS1 functions in assembly was reported previously via its interaction with structural proteins to modulate virus formation [57]. In this study, we identified a group of mutations that are critical for NS1 function in virus assembly and beyond. Moreover, the reciprocal mutations on DENV and WNV were performed to dertermine if any residue was virus specific for NS1 function. All chosen mutations on DENV reduced

or disrupted the formation of infectious particles while the same residues on WNV could increase or reduce the amount of infectious virus formation. The substitutions from WNV to DENV amino acids were better for WNV virus and led to two possible outcomes: (1) an interaction of NS1 with viral structural proteins that would assist in particle assembly, and specific infectivity; and (2) an interaction of NS1 with host factors necessary to drive secretion of virus particle out of the cell. Furthermore, mutations on WNV NS1 caused reduction in NS1 secretion (mutations at 101 and 343). The secreted NS1 appears to be variable between different flaviviruses, in particular WNV NS1 is more surface expressed and less secreted when compared to DENV [39]. The secreted NS1 was found to be important for NS1 pathogenesis such as vascular leakage or virus transmission [73, 75]. In this study, the secretion of NS1 and E or virus particles seem to be separated in WNV but closely linked processes in DENV. Our study also found a novel function of NS1 in enhancing virus entry (WT and mutation 343) and P101K NS1 did not have this function may be via disruption of the interaction of NS1 and virus particles.

Taken together, these results demonstrate both differences and similarities between DENV and WNV at the level of virus infection and NS1 function. In particular, WNV residue change at 101 diminished virus infectivity while residue 343 enhanced virus infectivity but both were diminished in DENV. WNV NS1 residue change at 218 showed complex effects as it enhanced the infectious virus formation but reduced the release of infectious virus. Furthermore, we suggested a novel function of secreted NS1 in virus entry and a distinct function of residues in NS1 for similar function but produce opposing outcomes in virus infection. The model for NS1 functions was suggested in Fig 2.8.

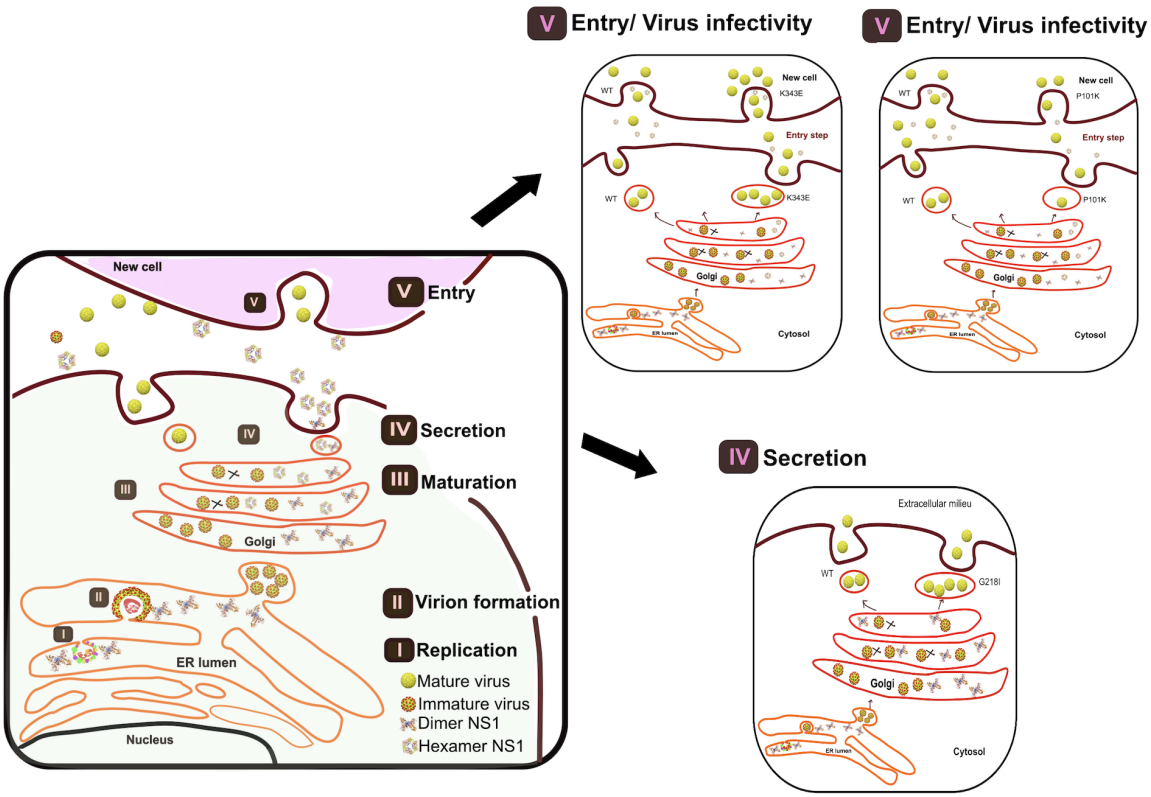

Fig. 2.8. Proposed model of NS1 roles in the WNV life cycle. In flavivirus life cycle, the NS1 protein plays important roles in not only replication but also assembly. In this study, substitution between DENV and WNV NS1 residue amino acids suggests roles of NS1 in multiple steps of virus assembly including infectious virus formation, virus trafficking, virus entry. The functions of NS1 in each step are suggested by different mutations on NS1. For WNV, mutation of residue 101 led to less infectious particle formation but increase in particle entry. Addition of NS1 protein to purified virus particles does not enhance the entry of the particles. Mutation of residue 343 led to increased infectious particle formation and enhanced virus entry with and without NS1 protein. On the other hand, mutation of residue 218 produced more infectious virus but reduced virus release efficiency, and led to WT levels of extracellular infectious virus. The differences in the effect of NS1 mutations in WNV suggests the particular roles of NS1 in virus assembly including infectious virus formation, virus release, and virus entry.

3. DENV NS1 MEMBRANE ASSOCIATION REGIONS CONTRIBUTE TO PROTEIN TRAFFICKING, OLIGOMERIZATION AND CELL ENTRY

3.1 Chapter summary

Flavivirus NS1 is a multifunctional protein with a peculiar ability to associate with lipid membranes. During the life cycle of NS1, the protein travels through the classical secretory pathway, similar to infectious virus particles, and is secreted into the extracellular space as mostly hexameric oligomers containing a lipid core. How the protein binds to lipids and whether such lipid binding is important for NS1 function and overall flavivirus pathology remains unknown. NS1 contains three hydrophobic regions, a β-roll domain, a flexible loop and a greasy finger and each of these domains were previously proposed to be membrane association regions. However, no molecular studies have been conducted to determine the significance of these regions in regard to NS1 function. In this chapter, we more fully define the role of each region within NS1 and their ability to associate with lipid membranes. Moreover, we relate the function of each region with two important steps in the NS1 life cycle, including protein secretion and new cell entry. We found that the flexible loop is the primary contributor to intracellular membrane binding, followed by the β-roll domain and then the greasy finger. NS1 was shown to require at least two hydrophobic regions in order to efficiently bind to lipid membranes and be secreted. There is a complex effect for the combination of these regions, suggesting possible redundancy in function, as membrane binding ability is also useful in protein secretion via the secretory pathway. In this chapter, we also determine the importance of the hydrophobic regions for NS1 cell-attachment and endocytosis. We found that NS1-cell surface binding is different from NS1-intracellular membrane binding between the different regions and each

hydrophobic region is able to limit cell endocytosis of the protein. In summary, we clarify the membrane binding properties of NS1 in mammalian cells and also suggest the molecular requirements in NS1 structure for its function and overall activity.

3.2 Introduction

Flavivirus NS1s are multifunctional proteins. They contribute as anchor and formation factor for the virus replication complex compartment [49, 54, 55]. It is suggested that the protein plays an important role in the very early step of viral RNA replication at negative strand synthesis [53, 54]. Intracellular NS1 proteins are also involved in virus particle assembly and maturation via interactions with the virus structural proteins (E, prM and C) [57]. NS1 traffics through the same secretory pathway as virus particles and gets secreted into the extracellular environment. The proteins then elicit the complement immune response to protect the virus infection [72, 91, 98]. DENV NS1 protein, without the infectious virus particle, causes vascular leakage both *in vitro* and *in vivo*. WNV NS1 protein, however, does not share the same function as DENV NS1 [75].

The native and recombinant NS1s travel to different cellular compartments in the secretory pathway and mature along the pathway via glycosylation [56, 99]. In addition, the protein can form different oligomers during its maturation. It is synthesized in ER as hydrophilic monomer, shortly after that, oligomerizes to a hydrophobic dimer and then to hexamer in the secretory pathway. The hexameric NS1 gets secreted as a soluble protein in a barrel shape with a lipid cargo in the central channel [44]. Structure studies of flavivirus NS1 revealed the three domains of the NS1 monomer that includes the β-roll (residues 1-29), wing (residues 30-180), and β-ladder (residues 181-352) [45]. When the protein forms a dimer, it creates two faces of NS1: an inner and outer face. The inner face consists of the β-roll domain and two sub-domains, flexible loop (residues 108-128) and greasy finger (residues 159-163), which are hydrophobic and facing towards cellular membranes. The inner face was proposed as

the membrane association surface of NS1. The outer face consists of the rest of the protein and facing outwards of the membrane, and available for all interactions [50].

Although the functions and structures of NS1 are established, the molecular mechanism related of the structre remains unclear. It is partly because of the interplay of NS1 functions and activities in the virus life cycle. Akey et al. reported the first full-length structure of flavivirus NS1 and suggested the possible function of the β-roll domain in interacting with ER and replication complex membranes. They further showed a single mutation on the greasy finger caused a lethal effect on virus replication but the mutants were still able to interact directly with liposome [45]. Other studies reported site directed mutagenesis on the flexible loop and greasy finger changed the interactions with viral structural and non-structural proteins and led to a reduction of new infectious virus [55,57]. The study did not determine if it was because of a loss of interaction of NS1 and the membrane, thus spacially separating NS1 from other proteins as NS1 remained in ER lumen and other viral proteins were either transmembrane proteins or stayed on the cytosolic side. The membrane association capacity of NS1 is mostly suggested via protein-lipid interaction assays [44,45,100,101]. However, how the peripheral NS1 interacts with cellular membranes and if this capacity is a prerequisite for NS1 activities and functions remain to be answered.

In this chapter, the aim is to gain insight of the structure and sequence on NS1 protein that plays roles in membrane binding. Individual hydrophobic regions in the inner face of NS1 were deleted and the truncated proteins were subjects for membrane and lipid binding. The structure requirements for membrane association ability of NS1 were established as co-intrusion of two hydrophobic regions. Moreover, the impact of each hydrophobic region on NS1 activities was defined in protein trafficking, secretion, oligomerization, new cell interaction and functions in virus system for virus replication.

3.3 Materials and methods

3.3.1 Cell lines

Baby hamster kidney (BHK) and Human embryonic kidney (HEK) 293T cells were maintained in Minimal Essential Medium (MEM) or Dulbelcco's modified Eagle medium (DMEM), respectively, containing 10% FBS at 37°C with 5% CO_2.

3.3.2 Site-directed mutagenesis (SDM)

Direct complementary primers for deletion or insertion were designed using PrimerX and synthesized via IDT. Mutations were made using a PCR protocol for Phusion high fidelity DNA polymerase (NEB). SDM PCR products were digested with DpnI at 37°C for 1 hr before being transformed into DH5alpha. Colonies were cultured for plasmid purification and plasmids were sent for sequencing. Two correct clones were chosen for each mutation for further characterization.

3.3.3 *In vitro* transcription and viral RNA electroporation

For DENV replicon and virus cDNA, five hundred nanograms of WT or mutated NS1 plasmids were used for in vitro transcription following XbaI linearization and T7 RNA polymerase with capA at 37^{o}C for 1 hour. RNA products were confirmed by agarose gel electrophoresis. For transfection into BHK cells, RNA (20 ng) of WT and mutants were electroporated into BHK cells (8 x 10^6 cells/sample) using the following settings: 1.5kV, 25F, 200 Ohms and 2 pulses for 3 seconds each. Electroporated cells were incubated at 37°C with 5% CO_2. Supernatants and lysates were harvested at 48 hpe and stored at -80^{o}C until use.

3.3.4 Transfection of plasmid DNA

293T cells were grown to 70%-80% confluency in 6-well plates at the time of transfection. Cells were transfected using Lipofectamine 2000 reagent (Thermo Fisher Scientific). Lipofectamine and DNA (pcDNA-NS1) were diluted in reduced serum Opti-MEM medium (ThermoFisher Scientific) and mixed at ratio 1:1. The complex of DNA and lipofectamine was incubated at room temperature for 30 minutes and added directly to each well. Supernatants and lysates were collected at 48 hpt.

3.3.5 Plaque assay

BHK cells were seeded into 6-well plates one day prior to plaque assay to achieve a monolayer. Serial ten-fold dilutions of virus samples were made in PBS and virus dilutions were added to each well. The plates were rocked at room temperature for 1 hour. A mixture of 1% agarose, MEM and 5% FBS was added to each well. The plates were incubated at 37^oC with 5% CO_2 for 72 hours. Plaques were stained with neutral red solutions (Sigma-Aldrich) for at least 8 hours and plaque number were reported.

3.3.6 Luciferease assay (Renilla luciferase and HiBiT luciferase)

The DENV replicon expressed Renilla Luciferase as a reporter for viral RNA synthesis. BHK cells were electroporated with WT and mutant RNA and plated onto 24 well plates. At 24-, 48-, and 72- hpt, cell lysates were collected using lysis buffer (Promega) and 20 μl of the lysed samples were incubated with Renilla substrate (Promega) in a 96-well plate SpectraMax L luminometer and measured with a Softmax Pro Software (Molecular Devices). Delta DD (DDD), a lethal mutation of NS5, was used as negative control for virus replication and background luciferase signal from the input RNA.

For the HiBiT luciferease assay, pcDNA-NS1 was engineered with HiBiT-tag and transfected into HEK 293T cells with Lipofectamine 2000 (Thermo Fisher Scientific) in the 6-well plate set-up. At 2 days post transfection (dpt), lysates were prepared using HiBiT lytic buffer and mixed with an equal volume of reaction mixture containing LgBiT according to the manufactures protocol (Promega). Supernatants were incubated with HiBiT extracellular buffer containing LgBiT for 10 minutes at room temperature. The luminescence signal was measured by SpectraMax L luminometer and measured with a Softmax Pro Software (Molecular Devices).

3.3.7 western blot

Transfected cells were collected for analyses of supernatants and lysates. Cell lysates were washed with PBS three times before being lysed by RIPA buffer with protease inHiBiTor cocktail (Millipore Sigma). Proteins from supernatants and lysates of WT and mutants were separated by SDS-PAGE and transferred to nitrocellulose membranes. The membranes were blocked with 5% skim milk in PBST (PBS with 1% Tween 20) for 1 hr, followed by three PBST washes, then incubated with rabbit polyclonal antibodies against NS1 (Kuhn lab), and/or beta-actin for actin (Abcam) for 1 hr and washed three times with PBST. Near infrared fluorescent secondary antibodies (Li-COR) were incubated with the membrane for 1 hr and visualized with Odyssey CLx Imager (Li-COR) and software Image Studio Lite 5.0.

3.3.8 Immunofluorescent assay (IFA)

HEK cells were transfected with pcDNA constructs by Lipofectamine 2000 reagent (Thermo Fisher Scientific). At 2dpt, cells were fixed with 3.7% paraformaldehyde for 10 minutes at room temperature. Fixed cells were permeabilized with PBS buffer containing 0.1% Triton X-100. Cells were then blocked in PBS buffer containing 1% BSA (blocking buffer) and incubated with primary antibodies including anti-NS1 antibody (Kuhn lab) and anti-Giantin antibody (Abcam) as a Golgi marker at

dilution 1:500 in blocking buffer. Cells were washed with PBS and incubated with secondary antibodies including goat anti-mouse Texas Red (Abcam) and goat anti-rabbit FITC (Abcam). Cells were rinsed with PBS and incubated with DAPI as blue-fluorescent DNA stain. Cells were washed further with PBS and mounted on coverslips for imaging with a fluorescent microscope (Nikon).

3.3.9 Triton X-114 phase-separation experiment

The Triton X-114 phase-separation protocol was adapted from Taguchi et al. 2014 [102]. HEK 293T cells in 6-well-plate were transfected with pcDNA-DENV-NS1 HiBiT constructs and cell lysates were collected at 2 days post transfection. Triton X-114lysis buffer (2% TX-114 in PBS) was added to each lysate and cells were incubated on ice for 30 min with vortexing for 5 seconds every 5 minutes. Cell suspensions were centrifuged at 13,200 rpm at benchtop centrifuge for 2 min at 4^oC. Supernatants were moved to new tubes as the TX-114 lysate. The lysates were incubated at 37^oC for 10 min, so the detergent phase (Det) precipitated. The tubes were centrifuged at max speed for 10 minutes at room temperature. The aqueous phase (Aq) on top was moved to the new tube. Triton X-114 wash buffer (0.1% TX-114 in PBS) was added to Det and mixed well. The Det was incubated at 37^oC for 10 min for phase- separation. This washing step was repeated 3-5 times to clean the Det. The Aq and Det were used for western blot to determine the presence of NS1.

3.3.10 Flotation assay

The flotation assay protocol was adapated from Noisakran et al. [100]. HEK 293T cells (10^7 cells) were transfected with WT or mutant plasmids. Cells were incubated for 48 hpt and washed with ice-cold PBS. Cell lysates were resuspended in 1ml lysis buffer (10 mM Tris-HCl, 150 mM NaCl, 5 mM EDTA, 1% Triton X-100, protease inhibitor cocktail) and incubated on ice for 30 min. Cell lysates were passed through a 26-gauge needle 15 times. The nuclei and cellular debris were removed by

centrifugation at 1000 g for 10 min at 4^{o}C. Clarified lysates were mixed with 1 ml of ice cold 85% sucrose and placed at the bottom of an ultracentrifuge tube, overlaid with 6 ml 35% sucrose and 3.5 ml of 5% sucrose. The lysates were ultracentrifuged at 35,000 rpm in an SW41 rotor (Beckman) for 18 hr at 4^{o}C. Each sample were collected from top to bottom of the gradient at 1 ml each fraction. All fractions from 2-10 were subjected to WB to determine the presence of NS1 and the lipid-raft marker.

3.3.11 NS1 deglycosylation

Lysates from transfected HEK cells were digested with PNGase F and EndoH (New England Biolabs) according to the manufacture protocol in non-denaturing conditions. Size of the deglycosylated NS1 proteins were determined by western blot.

3.3.12 Protein purification

HEK 293T cells were seeded one day prior to transfection with pcDNA-NS1-Flag. Transfected cells were incubated for 72 hpe and supernatants were collected, centrifuged at 3000 rpm for 5 mins at 4^{o}C. The clarified supernatants were incubated with ANTI-FLAG M2 affinity resin overnight at 4^{o}C on the rotator. The resins were collected by centrifugation at 9,000 rpm for 10 minutes and then washed with 40-50 bead volumes (CVs) wash buffer (0.05 M Tris HCl, pH 7.4, 0.15 M NaCl). The proteins were eluted with 150 ng/μL 3X Flag peptide solution. Eluates were concentrated using 10 kDa cut-off Amicon Ultra -15 centrifugal filter units (Milipore Sigma).

3.3.13 Size-exclusion chromatography (SEC)

. Concentrated purified NS1 proteins were loaded onto a Superdex 200 10/300 GL (GE Healthcare) at a rate of 0.3 ml/min with an AKTA FPLC. Fifteen fractions (2 ml each) were collected. The protein size markers (0.5 mg/ml, 200 μl), including

thyroglobulin (MW 670 kDa), γ -globulins from bovine blood ribonuclease A (MW 150 KDa), Albumin chicken egg grade VI (MW 44.3 kDa), Ribonuclease A type I-A from bovine pancreas (MW 13.7 kDa) and p-aminobenzoic acid (pABA) were separated in parallel.

3.3.14 Liposome assay

Liposome preparation were modified from the protocol [45]. Cholesterol (CHOL) (Avanti Polar) and 16:0 PC (DPPC) and 1, 2- dipalmitoyl-sn-glycero-3-phosphocholine (PC) were mixed in chloroform at ratios of 1:1 CHOL:PC. Portions of each solution were placed in glass tubes and dried under a stream of nitrogen. Liposomes were produced by adding 400 μL of buffer (50 mM Bis-Tris pH 5.5, 50 mM $(NH_4)_2SO_4$, 10% glycerol) to the dried lipids and then sonicating in a bath at 37^{o}C for approximately 5 min then a 50 μL sample of approximately 10 mg/mL NS1 protein was mixed with 150 μL of the liposome solution in 1.5 mL tubes followed by 2 hr incubation at 37^{o}C and 30 min centrifugation at 13,000 rpm.

3.3.15 Negative stain

Samples were liposome only and a mixture of liposome and NS1. For negative stain, a series of droplets were set up on parafilm, including 2 x 25 μL steamed distilled water, 1 x 10 μL 0.75% uranyl formate. Samples (3 μL each) were added to a grid for approximately 15-30 seconds and lipid was blotted away with Whatman paper. The grids were placed on water droplets, and blotted with Whatman paper. The process was repeated two times. The grid was then placed on an uranyl formate droplet for approximately 10 seconds and liquid was blotted away. The grid was air dried and ready for imaging. All grids were imaged at room temperature with a Tecnai T12 electron microscope (FEI) operated at 120 kV.

3.3.16 Statistical analysis

All analysises and graphs were generated using GraphPad Prism 8 software. Comparison between mutant groups and WT were analyzed using a one-way ANOVA. Differences between groups were considered significant when the p-value was less than 0.05.

3.4 Results

3.4.1 Hydrophobic regions on NS1 are critical for virus replication

The previously identified NS1 structures revealed hydrophobic regions within NS1 that putatively play roles in membrane association [45, 46] . To determine if these regions are important for NS1 function in viral RNA synthesis, and virus assembly, deletions of each region were generated in the viral cDNA, including a DENV replicon construct containing a luciferase reporter gene and a fully infectious virus construct. Hydrophobic regions including the beta-roll domain (residues 1-29), the flexible loop (residues 108-128) in the wing domain, and the greasy finger (residues 159-163) in the wing domain (Figs 1A and 1B) were individually deleted within the replicon and infectious virus cDNA systems. These constructs were then subjected to in vitro RNA synthesis to obtain viral RNA capable of generating viral RNA and virus particles. BHK cells were electroporated with wild-type (WT) or truncated mutant viral RNA. Using the replicon system, virus genome (RNA) synthesis was measured via luciferase activity at 48 hpe, while virus assembly and spreading were determined by plaque assay at 72 hpe using the full-length virus system. The results showed that all of the deletions (β-roll as $\triangle$B, $\triangle$flexible loop as $\triangle$F, and $\triangle$greasy finger as $\triangle$G) resulted in negetive control level of RNA synthesis in the virus replicon and displayed a lethal phenotype in the infectious virus system (Figs 3.1C and D), suggesting each hydrophobic region was crucial for an NS1 function, especially at the viral RNA synthesis step.

Because the deletion of the hydrophobic regions within NS1 demonstrated a lethal effect in both systems, we next determined if the deletions altered the expression or the stability of the protein, and if not, whether it affected the dimerization and secretion of NS1. This was accomplished using an NS1 expression plasmid, pcDNA-DENV-NS1. The deletions were engineered into the expression plasmid, which contained only the viral NS1 gene with its natural signal sequence (24 amino acids at the C-terminus of DENV envelope protein) (Fig 3.1E). The plasmids were transfected into the mammalian cell line (HEK 293T) via Lipofectamine 2000 and incubated for 48 hours. The supernatants and lysates were collected for western blot analysis to detect the presence of NS1 proteins. All samples were not boiled in order to maintain the dimer structure of NS1 for detection. Deletion of single hydrophobic region ($\triangle$B, $\triangle$F, and $\triangle$G) on NS1 not only showed the expression of the protein in its dimer form but the proteins were also shown to be secreted into the extracellular matrix (Fig 3.1F), suggesting that the deletion of each region did not impact NS1 expression, dimerization or trafficking through the secretory pathway. The molecular weights of the proteins were altered, however, due to their respective deletions. The size of these truncated NS1 proteins were observed as follows: The smallest protein was the truncated β-roll, followed by the truncated flexible loop mutant and then the $\triangle$G, the truncated greasy finger was about WT in size (Fig 3.1F). For quantification purposes, the NS1 expression system was engineered with HiBiT-tag at the C-terminus of the NS1 gene, labeled pcDNA-NS1-HiBiT (Fig 3.1E). HiBiT tag is a small tag (11 amino acid) having luciferase activity when incubated with its Large Bit (LgBit) counterpart and luciferase substrate (Promega). The same amounts of plasmids were transfected into the same number of HEK 293T cells, and the same volume from supernatant and lysate samples were subjected to HiBiT assays. Luciferase signals were recorded and compared with WT. The deletion of hydrophobic regions showed similar levels of intracellular NS1 but the secretion changed according to the deletion (Fig 3.1H and G). All the single hydrophobic deletions led to reduction in NS1 secretion, of which the least secreted was observed for $\triangle$B ($p<0.001$) at 7.5 times less than WT; second

least was △F ($p<0.001$) at 3.9 less than WT times; and last was △G ($p<0.005$) at 2.2 times less than WT (Fig 3.1H).

3.4.2 Complex interaction of any two hydrophobic regions on protein secretion

Our results indicated that deletion of any single hydrophobic region alone allowed NS1 protein to be expressed, dimerized and secreted. To further test if deletion of specific hydrophobic regions could impact protein activity, various combinations of deletions (any two individual regions or all regions simultaneously) were generated in the NS1 expression plasmid. These deletions showed that the loss of any two regions (△BF, △BG, or △FG) or all regions (△BFG) had no adverse effect on NS1 expression or dimerization of the truncated proteins (Fig 3.2B). This indicates that the hydrophobic regions of NS1 do not impact its biogenesis or dimerization processes. However, no NS1 was shown to be secreted in any of the constructs that deleted more than one hydrophobic region (Fig 3.2B). The retention of NS1 within the cell suggested that for NS1 to be secreted, it requires any two of its hydrophobic regions to be intact, suggesting possible redundancy in function of these regions for NS1 secretion.

To better define if specific deletion combinations contribute similarly to the lack of NS1 secretion, different truncations were performed on two large hydrophobic regions: β-roll (29 amino acids) and flexible loop (21 amino acids) in combination with the deletion on the whole greasy finger (5 amino acids). In the double deletion of both β-roll and greasy finger (△BG), the sequence of the β-roll was deleted from the C-terminus, with either the smaller deletion of residues 20-29, or larger deletion of residues 10-29. Extracellular NS1 proteins were observed in both constructs while the deletion of the whole β-roll and greasy finger showed no secreted NS1 (Fig 3.2B). We then deleted the 24 amino acids including residues 6-29 (keeping the first five residues of the protein) and 26 amino acids including 3-29 (keeping the first two

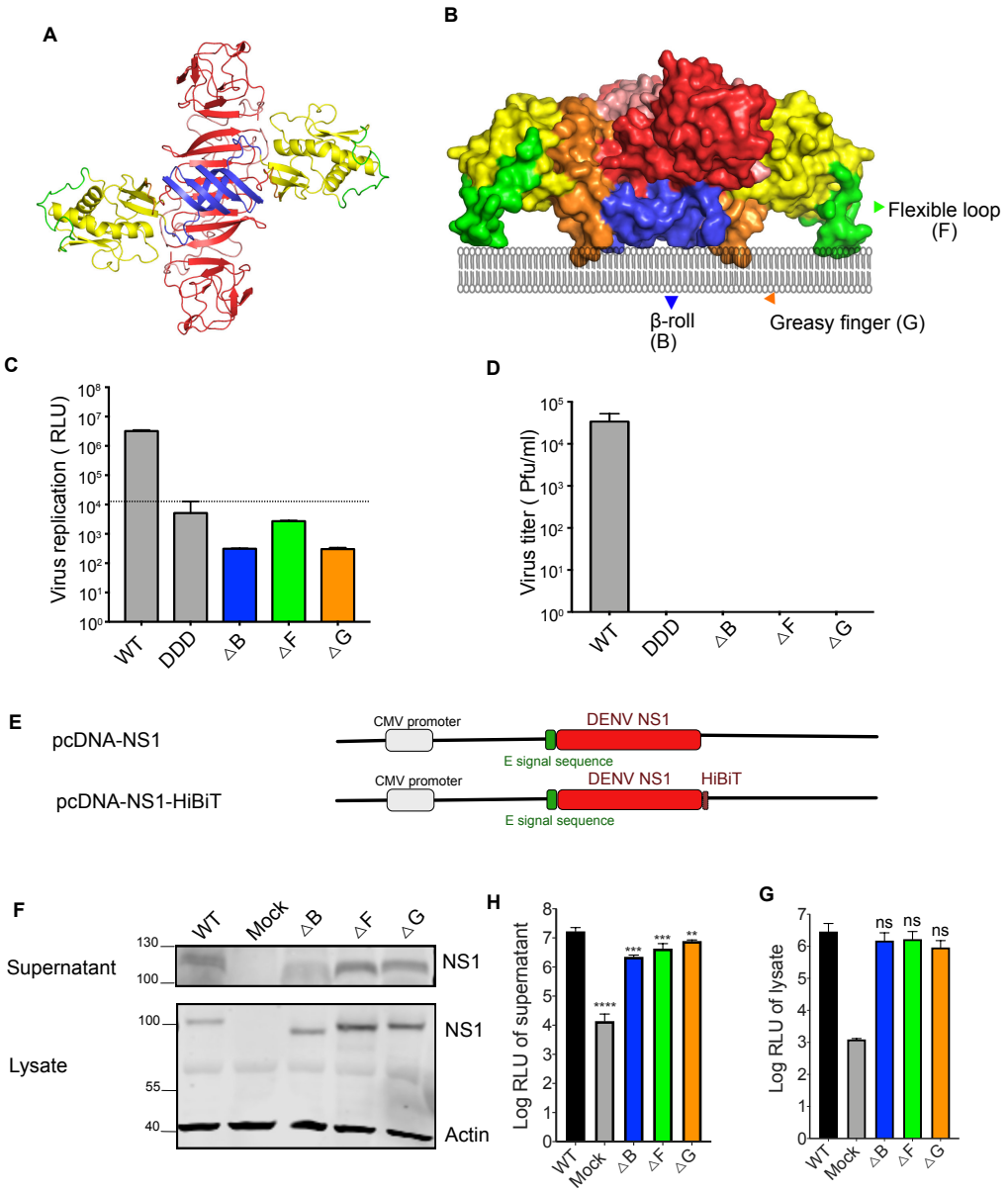

Fig. 3.1. Deletion of hydrophobic regions on NS1 caused lethal effect on virus replication but not NS1 biosynthesis and secretion ability. **(A)** Front view of dimeric NS1 (PDB ID 5K6K) with arranged domains in color codes as blue- β-roll, yellow-wing (green- flexible loop) and red- β-ladder. **(B)** Perpendicular view of dimer with membrane. Individual domains of each monomer in color code in contact with bilayer membrane. **(C)** Effect of hydrophobic region deletions on viral RNA synthesis. **(D)** Effect of hydrophobic region deletions on virus titer. **(E)** Schematic representation of the expression systems pcDNA-DENV-NS1 and NS1 with HiBiT-tag at C-terminus. **(F)** Effect of deletion of single hydrophobic region on NS1 synthesis and dimerization. **(H and G)** Luciferase assays for WT and truncated NS1 with HiBiT-tag in supernatants and lysates.

residues). The presence of the first five residues on the N-terminusinus of the β-roll showed extracellular NS1, suggesting the first 3-4 residues on β-roll were sufficient for the secretion of the protein with a combination of deletions in the greasy finger (Fig 3.2C).

The combined deletions in the flexible loop and greasy finger showed completely different requirements for protein secretion. The flexible loop was truncated in half generating two constructs, each retaining either the first half of the flexible loop (residues 108-118) or the second half (residues 118-128), in combination with the deletion of the whole greasy finger. Extracellular NS1 was observed in both cases (Fig 3.2D). While the two constructs of the truncated flexible loop did not share sequence homology, they did share one half of the flexible loop each containing 10 residues. This may indicate that for NS1 to be secreted, the flexible loop may act as the natural spacer for the protein during secretion. On the other hand, the results show that the presence of the whole β-roll domain and half of the flexible loop were sufficient for NS1 secretion, suggesting that their combined presence alone is sufficient for secretion, superseding any hypothesized length requirements for the flexible loop.

We further examined if the deletion of the β-roll domain and half of the flexible loop would yield the same results. This truncation combination, however, showed no extracellular NS1 (Fig 3.2E). Moreover, the deletion of the whole flexible loop and the last twenty amino acids at the C-terminus of the β-roll domain showed no extracellular NS1 (Fig 3.2E). These results suggested that even though there was redundancy in hydrophobic regions for NS1 secretion, each region may possess distinctive features for this function.

3.4.3 Hydrophobic regions on NS1 do not determine NS1 intracellular colocalization

The double and triple truncated proteins were retained intracellularly, thus we investigated where in the secretory pathway the proteins remained. Immunofluorescent

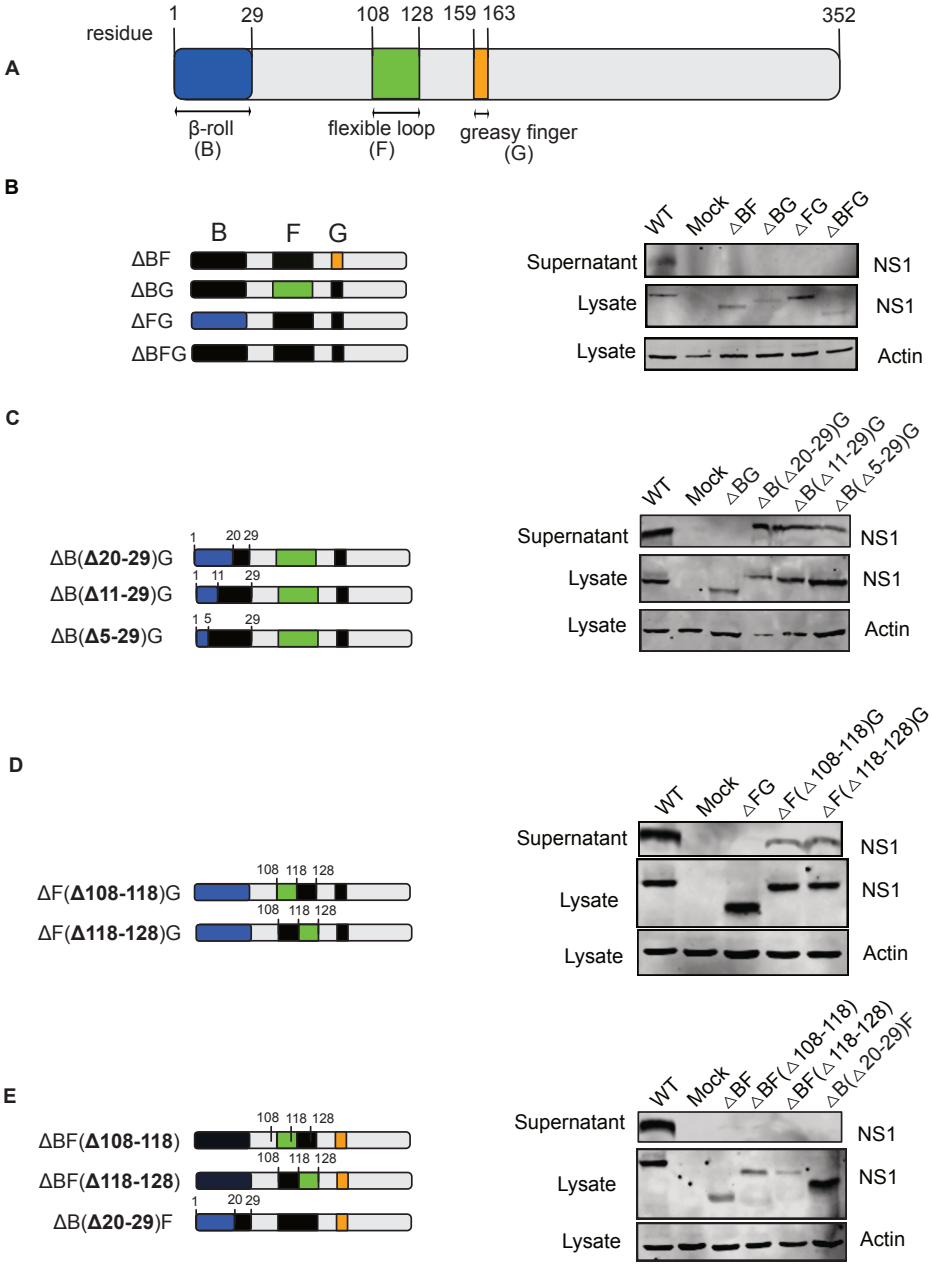

Fig. 3.2. Hydrophobic regions contribute distinctively for NS1 secretion but no impact on NS1 expression and dimerization. **(A)** Schematic representation of the three hydrophobic regions on NS1 in color codes: blue- β-roll, green- flexible loop and orange- greasy finger.**(B)** Combination of truncation of two and three hydrophobic regions on NS1. **(C)** Truncation of β-roll in different length and greasy finger **(D)** Truncation of flexible loop with different lengths and greasy finger. **(E)** Truncation of β-roll and flexible loop in different lengths.

assays (IFA) were performed to examine the subcellular localization of the proteins. The proteins were expressed in the same cell line (HEK 293T) for 48hpt before being fixed with paraformaldehyde and stained for intracellular colocalization. Antibodies against NS1, Rb NS1 (Kuhn lab) and the Golgi marker, gigantin (Abcam), were used to discern localization. All of the hydrophobic region deleted proteins were distributed similar to intracellular WT NS1 and also colocalized with the Golgi marker (Fig 3.3), suggesting that after being synthesized, the proteins could traffic from ER to Golgi, however, they could not travel into the extracellular matrix.

To validate our findings that NS1 is able to enter the Golgi, glycosylation assays were performed. NS1 proteins have two glycosylation sites at residues 130 and 207. The protein is glycosylated with a complex sugar at residue 130 and high-mannose glycan at residue 207 [99]. Both endoH and PNGase F endoglycosidase enzymes were used to cleave the N-glycosylation decorations on the proteins. The protein was expected to be sensitive to both EndoH and PNGase F, but a greater change in molecular weight would be seen after cleavage from PNGase F treatment if the protein did indeed travel into Golgi where it would be processed to a complex sugar. The results revealed that all the truncated proteins were glycosylated similar to WT and suggested the proteins obtained complex sugars in the Golgi, confirming that the protein was retained in Golgi (Fig 3.4).

3.4.4 Deletion of hydrophobic regions of NS1 reduced membrane association

Previous studies have shown evidence of NS1 interacting directly or indirectly with cellular membranes. Here, we performed three different sets of experiments to study different interactions between NS1, cellular membranes and lipids. DENV NS1 proteins from all four serotypes were found to associate with lipid rafts, a lipid rich microdomain on the membrane [100, 103]. In this study, we investigated the impact of each hydrophobic region on NS1-lipid raft association. WT and truncated

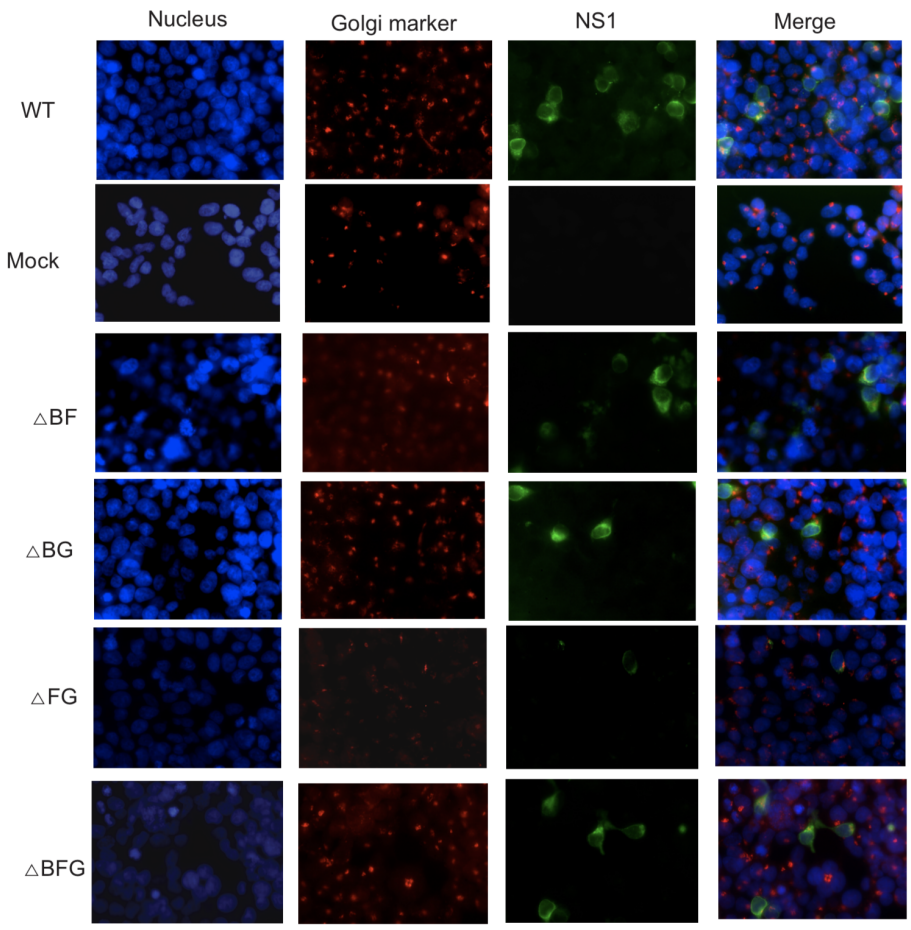

Fig. 3.3. Double and triple hydrophobic region truncated proteins travel to and remain at Golgi. NS1 protein from WT and deletion of double and triple hydrophobic regions on NS1 were expressed in HEK 293T. At 48hpt, the cells was fixed and stained with antibodies against NS1 and the Golgi marker (gigantin). DAPI (blue) stain was used to visualize the cell nucleus. Golgi stained in red and NS1 in green.

proteins were expressed in HEK 293T cells for 48 hpt and the lysates were collected for flotation assays. Cell lysates were lysed and loaded at the bottom of a sucrose cushion where they were subsequently centrifuged at high speed to separate various components within the lysates. Sample fractions were collected from the top of the centrifuge tube to the bottom. In total, 10 fractions were collected and fractions 2-10 were used in western blot analyses. The lipid raft marker (flotilin-1) was seen in

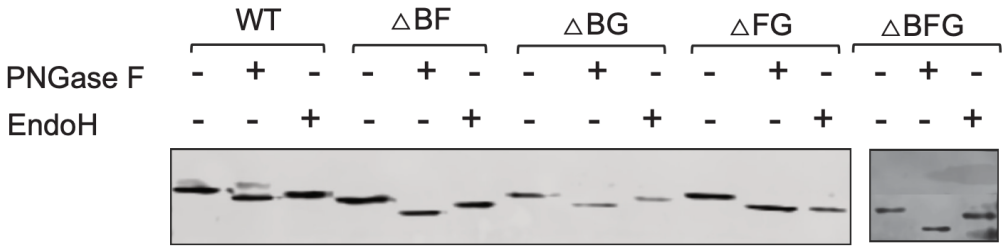

Fig. 3.4. Deglycosylation of double and triple hydrophobic region truncated proteins. NS1 protein from WT and deletion of double and triple hydrophobic regions on NS1 were expressed in HEK 293T. At 48 hpt, the lysates were collected and treated with Endo H and PNGase F in non-denaturing conditions. Samples were subjected to western blot using antibodies against NS1.

fractions 3-5, and WT NS1 proteins were present in both raft containing and non-raft containing fractions (fractions 4-10) (Fig 3.5). Truncated proteins, △B, △F, and △G all showed NS1 in the same fractions as WT, including both raft and non-raft containing fractions, suggesting the association of those truncated proteins with the lipid rafts or plasma membrane remained intact. It was noticed, however, that the signal of NS1 proteins in raft fractions was weaker than that in non-raft fractions, indicating just a small fraction of the NS1 population associated with the lipid raft.

Flavivirus NS1 proteins were found to be cell membrane associated since they have amphiphilic features and appear in both detergent (Det) and aqueous (Aq) phases in the Triton X-114 phase separation assay of both mammalian and insect host cells [44, 101, 104]. Triton X-114 (TX 114) phase-separation assays were performed to examine the impact of hydrophobic regions on NS1 amphiphilicity. In order to quantify the change in the hydrophobicity of the protein, NS1 expression plasmids with HiBiT tag were used. All the single, double and triple hydrophobic region deletions on NS1 were also subjected to the assay. WT and mutant plasmids were transfected into HEK 293T cells and lysates were lysed by TX114 and separated by

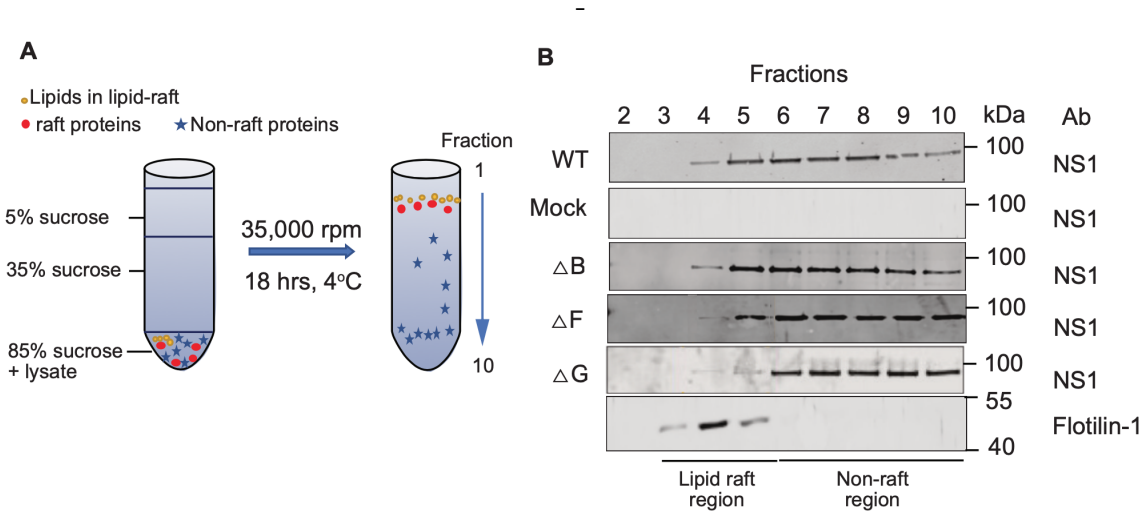

Fig. 3.5. Flotation assay. **(A)**Schematic representative of flotation assay. WT and mutant NS1 were expressed in HEK cells (9 x 10^7 cells). Lysates were subject for flotation assay using sucrose cushion centrifugation. Each sample were collected in 10 fractions from top. western blot was performed to detect the presence of NS1 in fraction 2-10.**(B)** western blot of WT and mutant proteins with antibodies against NS1 (100kDa) and lipid raft marker, flotilin-1 (49kDa). All samples were run in reduced condition without boil step. Images represent data from two independent experiments.

temperatures and centrifugation. Both aqueous detergent phases were collected and diluted to the same volume. The same volume of each phase from WT and mutants were quantified by HiBiT assay. Single deletions showed the presence of NS1 in both phases but there was significant loss in the proteins hydrophobicity. WT showed about equal amounts of Det and Aq phase of NS1 while in △B, Det showed about 14.8% (±3.0%) and Aq phase showed 85.2%(±3.0%). △F proteins changed the percentage of Det to 6.7% (±2.9%) and Aq phase to 95.2% (±4.4%). △G proteins changed the percentage of Det to 27.0% (±10.7%) and Aq phase at 73.0% (±10.7%)(Fig 3.6). The results suggested the deletion of the flexible loop (20 amino acids) caused the greatest reduction in NS1 membrane association, followed by deletion of the β-roll domain (29 amino acids) and lastly by the deletion of the greasy finger (4 amino

acids). All the double and triple deletions of hydrophobic regions showed the Det phase with less than 3.0% ($\pm 1.2 - 2.3\%$) and the Aq at 97.7%-99.7% (($\pm 1.2 - 2.3\%$). As the loss of hydrophobicity in any combination of any two regions was higher than its accumulative value, any combination would sufficiently change the amphiphilic nature of the proteins.

Direct interaction of a protein and lipids can be studied by liposome assay. The NS1 protein was suggested to directly interact with the lipid membrane of liposomes and able to rearrange a huge liposome into small lipo-particles [45]. To examine if the hydrophobic-truncated NS1 proteins were able to directly bind to and rearrange a liposome, liposome assays were performed and the size of the liposome or lipo-particles were measured via photon correlation spectroscopy and imaged with negative stain EM. Large unilamellar vesicles (liposomes) containing only phospholipid (DOPC) and cholesterol were generated at the size of about 600 nm. Purified DENV-NS1s in WT and single deletion forms were incubated with liposomes at the molar ratio of 100:1 (lipid:protein). The control included WT proteins and monomer WT, which were boiled at 95^{o}C for 10 min to dissociate high oligomer forms to monomer, and mock buffer purified in the same process as purified NS1 proteins. The monomer form was confirmed in size exclusion chromatography. Both WT and monomer forms of WT affected the size of the liposomes and remodeled it to smaller lipid particles (about 300 nm), while the mock sample showed no effect. All truncated proteins were found to associate with the liposome and rearrange the large liposomes into smaller lipid particles (about 300-400nm) and there was no significant difference in the size of altered lipid particles between WT proteins or truncated proteins (Fig 3.7A). The monomer WT proteins caused the rearrangement of the liposome alone, suggesting the oligomer form of NS1 was not critical for the protein-lipid interaction. The results were validated by negative stain electron microscopy, which showed changes in the liposome size when incubated with NS1 proteins. We did observe a small particle and possibly NS1 hexamer in the background for WT NS1 proteins (in the form of an oligomer), $\triangle$F, and $\triangle$G (Fig 3.7B). Only tiny particles with clear backgrounds were

seen in samples including liposomes and monomer WT and △B, suggesting either all the used NS1 was bound to the lipo-particles or the NS1 proteins of monomer form or △B were too small to be visible at the resolution used. The results confirmed that NS1 proteins are capable of interacting with lipid and cellular membranes without individual hydrophobic regions.

3.4.5 Beta-roll domain is crucial for hexamer formation but not flexible loop or greasy finger

Flavivirus NS1 proteins were known to be secreted as soluble proteins, mostly in hexameric form containing three homodimers with a central lipid core [43, 44, 105]. The hexamer DENV NS1 proteins are not only important as biomarkers for virus infections, but also crucial for virus pathogenesis, immune-evasion, and vascular leakage [37, 75, 98, 106]. To examine the importance of hydrophobic regions on NS1 oligomer formation, purified NS1 proteins were subjected to size exclusion chromatography (SEC). Two major peaks were observed from fractions 4-6 for WT, △F, and △G NS1 proteins (Fig 3.8A, C and D). However, the △B NS1 protein produced 3 peaks at fractions 4-6 and at fractions 7-8, which was the highest peak of all three. The molecular mass of these peaks was estimated from protein standard at about 1140 kDa (higher order oligomer), 320 kDa (hexamer), and 130 kDa (dimer). Each fraction was subjected to western blot analysis without heat treatment for detecting dimer and with antibody against NS1. Data showed the presence of NS1 proteins in fractions for both higher order oligomer forms and hexamers for all samples WT, △F, and △G; only △B showed NS1 in lower molecular weight fraction (dimer). The change in the oligomer profile of truncated NS1 from the β-roll deletion indicated that the β-roll domain is critical for the hexamer formation, while neither the flexible loop or greasy finger of the wing domain was required for hexamer formation. All of the fractions were subjected to western blot analysis with antibodies against NS1. NS1 was mostly present in fractions 4-7 (WT, △F, and △G) and 8 (for △B) as dimer (Fig

3.8F), this suggested that the hexamer and higher order oligomer forms were sensitive to SDS detergent since their interface interaction is weak and hydrophobic [44].

3.4.6 All membrane association regions are critical for NS1 cellular endocytosis but not cell attachment

Similar to virus particles, secreted NS1 proteins bind to new cells and are capable of being endocytosed [36,37]. To assess whether hydrophobic regions on NS1 are critical for its capacity to attach to cell surfaces and become endocytosed, supernatants of NS1-HiBiT tagged proteins were incubated with cells and the attachment and entry were measured by HiBiT luciferease assay. The percentage of attached NS1 was measured by the percentage of the luciferase value of the bound NS1 over that of the total supernatant used for the attachment. For cell binding, the supernatant of NS1-HiBiT was incubated with HEK 293T at 4^oC for 1h. Cells were then washed and subjected to HiBiT assay. The results showed all proteins bound to cells at very low levels, which was less than 1% of the total (Fig 9A). The WT NS1 bound to new cells less than all the truncated proteins, with the highest binding capacity coming from $\triangle$G, which showed 2 times higher binding activity than WT. $\triangle$B and $\triangle$F were about 1.5 times and 1.2 times higher than WT, respectively. These results suggested that without each hydrophobic region, the protein attached better to cells. However, differences among the values was in the low range from 0.1%-0.5%, thus the statistical value may reflect the reproducibility of the experiment rather than any real biological differences, indicating without any hydrophobic region, NS1 can attach to cells.

After attachment, cells were washed so that only cell-bound NS1 remained, and incubated at 37^oC for 1h to allow for the entry of NS1 into the cells. To normalize the amount of NS1, the entry of NS1 was measured as a percentage of entry signal over the attachment signal. The deletion of hydrophobic regions showed reduction in NS1 entering new cells. WT NS1 showed 25% of attached proteins endocytosed, while $\triangle$B

showed 14% internalization, and 7.3% and 5.4% for △F and △G, respectively (Fig 9B). This highlighted the importance of those regions for NS1 endocytosis.

3.5 Discussion

The flavivirus NS1 protein contains no transmembrane sequences but is still able to interact with host membranes and behaves as an amphiphilic protein. The structure of flavivirus NS1 revealed three hydrophobic regions which were predicted to be responsible for its membrane association ability. There is no molecular study on how these regions effect the membrane association of NS1 or how they contribute to NS1 activities. Therefore, in this study, we sought to provide details of the significance of these hydrophobic regions, namely the β-roll domain, the flexible loop, and the greasy finger, in DENV NS1 membrane association activities. We first examined the impact of these regions on NS1 function through the use of virus cDNA constructs, including replicon and infectious virus plasmids, which were used to introduce various deletions into the NS1 protein. The data generated revealed the significance of the afore mentioned regions on NS1 function in RNA synthesis as both systems showed lethal effects when combinations of hydrophobic regions were deleted. Our results are consistent with previous studies using site directed mutagenesis within the hydrophobic regions [45, 57]. In these studies, single mutations in the greasy finger inHiBiTed viral RNA replication within the cell, while maintaining expression ability, interaction with liposomes and continued support of the formation of replication complexes in virus expression systems [45, 57]. Even though the three regions were well studied in mutagenesis studies, it remained unclear if any of the regions impacted the membrane association ability and if these regions worked in a synergistic manner for NS1 functions and activity. Our study, therefore, used a deletion strategy to investigate the contribution of each individual region separately, as well as in combination with one another.

The first question we aimed to answer was whether all three hydrophobic regions were equally important for NS1-membrane interaction. We used different membrane-binding methods to evaluate their functions. Our results were in agreement with the membrane interacting function of all three regions. Without individual hydrophobic regions, the proteins were still found to colocalize with lipid-rafts. However, the population of NS1 that travels to the lipid raft is a small fraction of total intracellular NS1. Our results are consistent with reports of infectious DENV NS1 being found located with lipid raft. However, the same report suggested the absence of NS1 in lipid-rafts in the transient system in HEK 293T [100, 103]. As the raft-NS1 is a small fraction of the intracellular NS1 population and the expression of protein in cell lines may vary, the conflicting data may merely reflect the amount of NS1 in the cell lysate used for flotation centrifugation assays and not any discrepancy in function. Our study suggests that recombinant NS1 proteins behave similar to the native NS1 obtained from virus infection and no individual hydrophobic region inHiBiTs the interaction of NS1 and lipid-rich microdomains. Moreover, we found that for membrane binding, DENV NS1 requires that at least two regions remain intact in any combination, but not all the regions contribute equally to the protein membrane association. Among them, the flexible loop has the greatest impact in membrane binding, the second is the β-roll domain and lastly is the greasy finger. Deletion of more than one hydrophobic region turned NS1 into a soluble protein (more than 97% of total NS1). This is the first quantification for the detergent resistant and aqueous portions of intracellular NS1. The WT protein showed equal distribution of those populations, and loss of hydrophobic regions showed loss in its hydrophobicity. It was noticed that the β-roll and loop structure showed to be important for membrane binding as membrane interaction regions are usually helical structure. The structure pattern of NS1 for membrane binding support the model of membrane protrusion on peripheral protein which suggests the co-insertable hydrophobic protrusion [107].

The next question for the membrane association of NS1 is whether each hydrophobic region is critical for NS1 membrane remodeling ability. WT NS1 purified from a

baculovirus system rearranges large liposomes into small lipid particles [45]. Purified NS1 from mammalian cells was used in this study and demonstrated the same effect. The protein can also be seen in the background of negative stain EM. In the previous study, no NS1 was observed in the background and suggested the proteins all bound to the lipid. As we used smaller lipid to protein ratios (100:1) compared to the published ratio (358:1), unbound NS1 was observed. However, the monomer WT or $\triangle$B (in dimer form) showed no NS1 in the background but did change the liposome size. It is possible that the proteins all bind to the lipids as its change in molecular weight led to less monomer/dimer compared to WT. Another possibility is that the monomer and dimer forms of NS1 are too small to be visible in negative stain EM, therefore it cannot be observed in the negative stain. As all the truncated proteins showed effects on liposomes, individual hydrophobic regions may not be critical for NS1 ability to change the curvature of the membrane. This also suggests a redundancy in function of each region and the membrane binding property may be significant for cellular membrane structure modification. During the preparation of this chapter, a recent study on those membrane association regions on NS1 was published [108]. Purified ZIKV NS1 was incubated with liposomes of smaller size (100nm in diameter) and the mixture was separated by co-flotation assay. WT ZIKV NS1 was shown to co-float with liposomes but not $\triangle$B. However, the negative stain EM of $\triangle$B with liposome at 400 nm in diameter was shown to generate smaller particles (200 nm) compared to the liposome only sample. WT, however, does not reduce liposome size but forms tubular structures [108]. Although ZIKV NS1 may behave differently from DENV NS1, the ability to remodel liposomes may be consistent. Further studies on the two flavivirus NS1s as well as the condition in size and composition of the liposomes used may be useful to clarify these differences.

As the membrane association function of the hydrophobic regions were established, the impact of these regions were investigated in NS1 activity. NS1 exists in various oligomeric forms intracellularly, but when secreted, the proteins are mostly in hexamer form. The secreted oligomer profile of truncated NS1 revealed that the flexible loop

and greasy finger of NS1 showed no effect on oligomerization. Different oligomer forms of NS1 were able to remodel the liposome or interact directly with the lipids, suggesting the lipid binding ability may be an intrinsic property of NS1.

It is noted that the greatest reduction in membrane binding ($\triangle$F) can still lead to the hexamerization of NS1, while the second reduction in membrane binding ($\triangle$B) lead to a reduction in hexamers. Both truncated proteins can still directly interact with lipids, suggesting lipid binding ability of NS1 may not be essential for the hexamer formation. This conclusion is consistent with hexamer formation from virus infected NS1 from mosquitoes, which has less lipid compared to mammalian cells [70].

We also investigated the effect of the membrane binding regions on NS1 trafficking and secretion. NS1 intracellular trafficking does not need the hydrophobic regions, but NS1 protein is retained in the Golgi when it is not able to bind to membrane. Without the β-roll domain, the protein remains in dimer form and is secreted seven times less compared to WT. Without the flexible loop and greasy finger, the proteins still form hexamers and are secreted 3 or 2 times less, respectively. Without any two membrane binding regions, the proteins are retained in the secretory pathway after trafficking from ER to Golgi. Without the hydrophobic regions, the NS1 protein is completely soluble, suggesting the hydrophobicity or membrane binding is important for the protein to be secreted. It is possible that the deletion may change the structure of the protein, resulting in a defect in the binding ability. The importance of the two membrane binding regions, the β-roll and flexible loop, were further characterized to determine if the length or amino acid specificity were responsible for the retention. The results show the two regions contribute distinctly for NS1 secretion. The β-roll only requires the first three amino acids (DSG) for secretion while the flexible loop may behave as a distance spacer ($<$10 amino acids) for protein interaction or structural stability. We did observe the change in the level of intracellular NS1 in double or triple deletion in membrane regions, indicating the instability of the proteins or protein structures. The change is not due to the glycosylation of the truncated proteins. However, the combination of the first three-four amino acids of the β-roll

and ten-amino-acid length (about 38Å) suggests the complexity in function of each region and as a whole as the combination results in no secretion.

Lastly, the effect of each hydrophobic region on cell entry was determined using an entry assay. The secreted NS1 proteins were able to bind to the cell surface of various mammalian cells [36,106]. The entry of NS1 into cells enhances virus entry and could facilitate virus infection and cause vascular leakage [37]. In this study, all NS1 proteins showed low levels of cell attachment. As reported, the oligomeric form of NS1, $\triangle$B proteins stays mostly in dimer form, thus the oligomer forms of NS1 are not critical for membrane attachment. This data is consistent with the lipid binding and Triton X114 data as with single deletion, truncated proteins can still interact directly with lipid and remain capable of membrane association. However, as individual regions have different membrane association levels, the similar rate of attachment suggests that surface binding is not driven by the NS1 hydrophobic regions and this interaction is different from intracellular membrane binding. All the truncated proteins showed a reduction in endocytosis, suggesting these membrane binding regions are essential for the internalization of the protein.

Collectively, our data provide not only the confirmation and detail of the membrane association contribution of each hydrophobic region of NS1 but also the relation of membrane binding and NS1 oligomerization, secretion and cell entry. Although our study provides answers for the membrane association of DENV NS1, there are questions that remain to be clarified. How does the protein interact to form hexamers? Are any of the hydrophobic regions required for replication complex formation? Is the structure of the protein stable without the membrane binding regions? Does each region bind to distinct lipid groups or species? Are those lipids significant for the surface binding vs the intracellular membrane binding? This information may elucidate the mechanism of membrane association of NS1 hexamer formation and binding of the protein to cellular membranes.

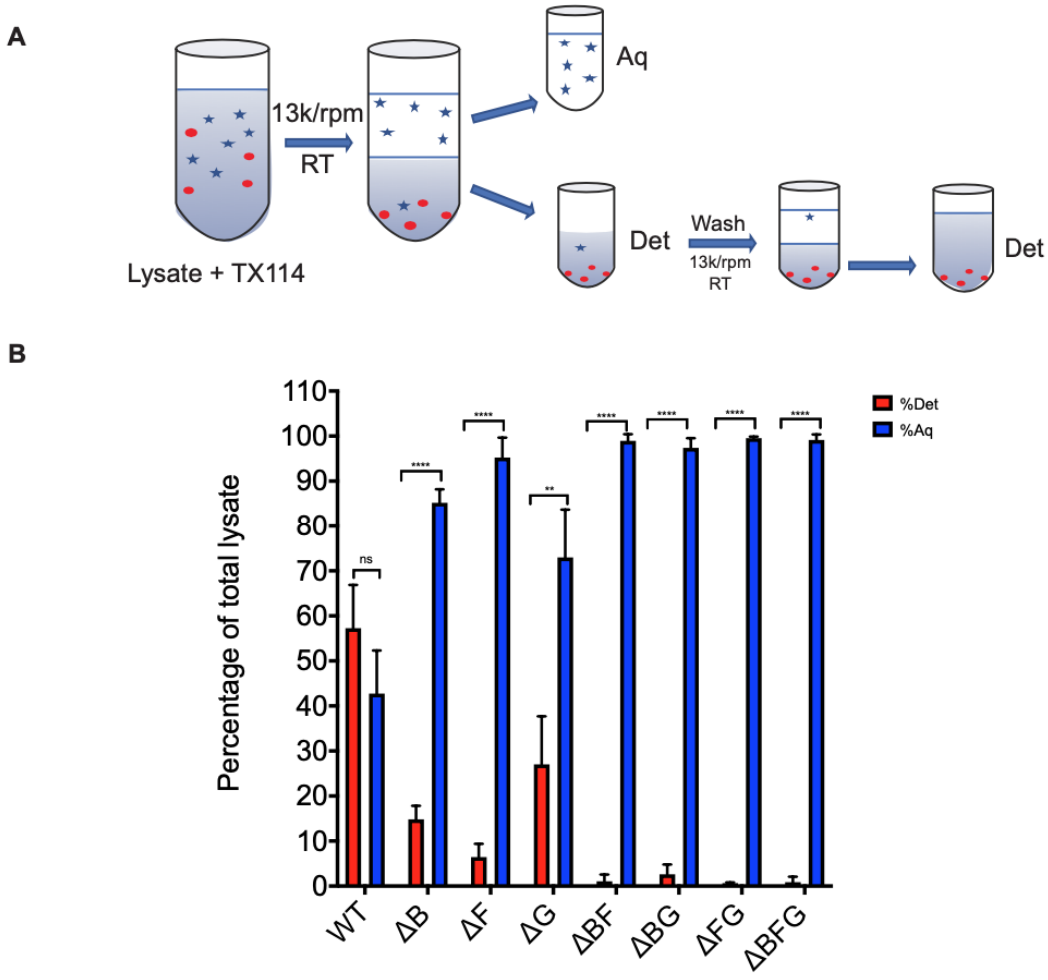

Fig. 3.6. Triton X114 assay. **(A)** Schematic representative of Triton X-114 phase separation assay. WT and mutant NS1s were expressed in HEK cells (10^6 cells). Lysates were lysed by TX114 and separated at room temperature and centrifugated. Each sample were separated into a detergent phase (Det) and an aqueous phase (Aq) at the same volume. Det samples were washed 4 times with TX114 wash buffer and diluted to the same volume as the Aq. HiBiT assays were performed to measure the level of NS1 in each samples. **(B)** Percentage of each phase on total lysate. Luciferease assay was measured and calculated as percentage of each phase over the total value of both detergent and aqueous phases. Data were from three independent experiments.

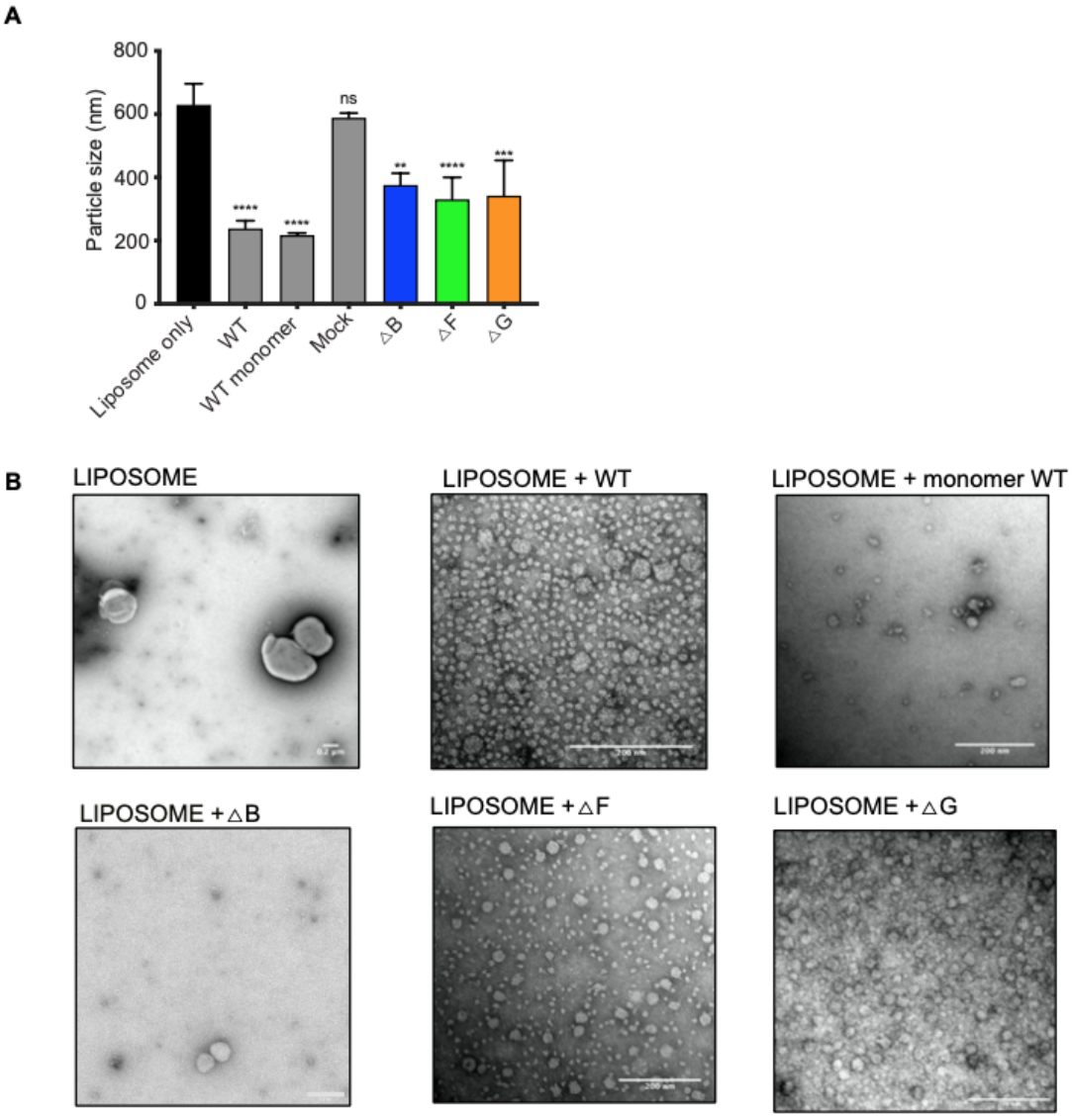

Fig. 3.7. Liposome assay. **(A)** Particle size of the mix of liposome and purified NS1 proteins. WT and mutant NS1 were transfected and purified from supernatants of HEK cells. Liposome were incubated with purified WT or truncated NS1 proteins for 1hr at 37^o and subjected to photon correlation spectroscopy to measure the particle size. **(B)** Negative stain of the mixtures of liposomes and purified NS1 proteins.

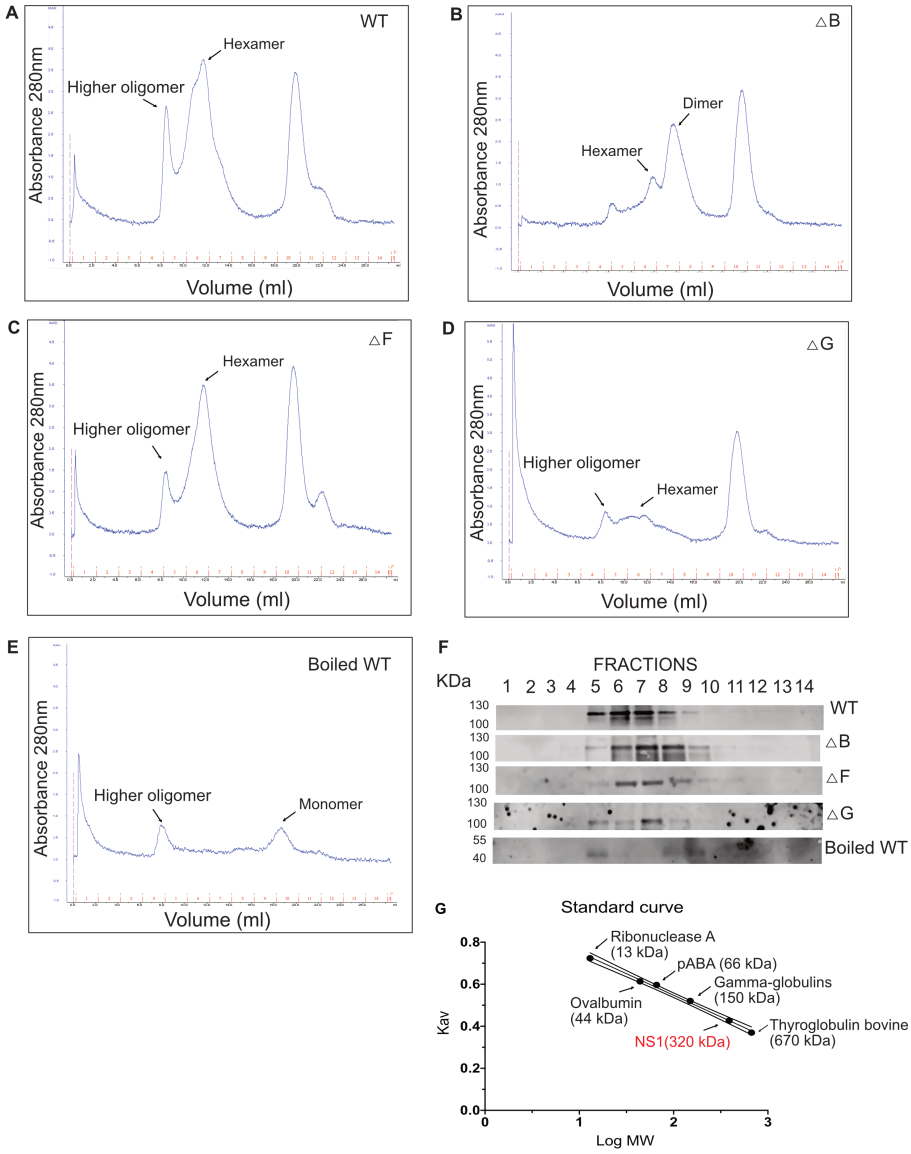

Fig. 3.8. Deletion of the β-roll domain disrupts the formation of NS1 hexamer but deletion of flexible loop and greasy finger do not change the oligomer profile. NS1 proteins from different constructs with single deletion of β-roll, flexible loop, or greasy finger were purified with one-step Flag purification and subjected to size-exlusion chromatography. The chromatogram of each deletion and WT in native form and in heat denatured form are shown in **(A)** native WT, **(B)** $\triangle$ β-roll ($\triangle$B), **(C)** $\triangle$ flexible loop ($\triangle$F), **(D)** $\triangle$ greasy finger ($\triangle$G), **(E)** heat denatured WT, **(F)** western blot for the presence of NS1 proteins in different fractions from size-exclusion chromatography. **(G)** Standard curve of the size exclusion chromatography with standard proteins and NS1 protein as hexamer. Chromatograms represent samples from 3 independent experiments.

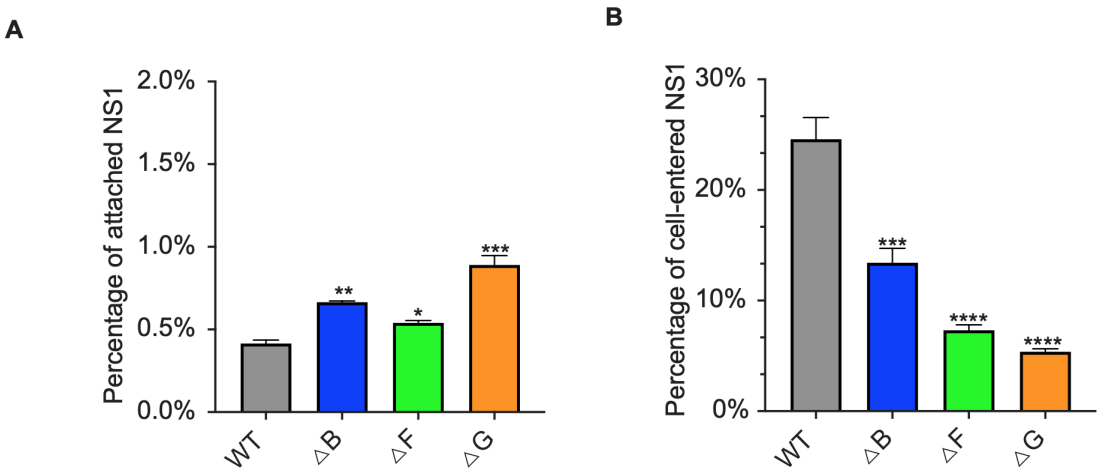

Fig. 3.9. Effect of the deletion of hydrophobic regions on NS1 attachment and entry to cells. NS1 proteins from different constructs with a single deletion of β-roll, flexible loop, or greasy finger with HiBiT tags were expressed in HEK 293T cells. Supernatants were collected at 48hpt and used for attachment and entry assays. **(A)** Attachment of WT and truncated NS1 proteins to HEK 293T cells. Supernatants were incubated with pre-cooled cells in 96 well-plates for 1h at 4^oC. HiBiT assays were performed to measure the signal of HiBiT after 1h incubation and calculated as percentage of the original samples. **(B)** Entry ability of WT and truncated NS1. After the attachment, cells were washed to remove all the unbound NS1 and plates were move to 37^oC for 1h. The cells were washed afterward to remove NS1 and subjected for HiBiT assay. Entry level were determined by the percentage of internalized NS1 over attached NS1 from previous assay. Results show the mean of two independent experiments. The error bars indicate the standard deviation.

4. COMPARISON OF FLAVIVIRUS NS1 LIPIDOMIC PROFILES

4.1 Chapter summary

Flavivirus NS1 is known as multifunctional protein, which plays roles in virus replication, assembly and pathogenesis. The secreted flavivirus NS1 is a lipoprotein with a central lipid core. As lipids are critical in flavivirus infection for various roles in the virus life cycle, the lipid composition of NS1 protein may be important for the functions and activities of the proteins. However, the composition of the lipid core was not fully investigated. There are many questions remaining to be clarified such as lipid classes and species that are present in the proteins or lipid target of each membrane association region on NS1. In the study, we used multiple reaction monitoring (MRM) profiling mass-spectometry to profile the lipid classes and species of DENV2-NS1 (strain 16681). We quantified the composition of lipid classes in WT NS1 as well as truncated NS1, which was deleted in a single membrane association region. Beside determining the change in the amount of lipid classes, we also identified the lipid target of each hydrophobic region of the DENV NS1 protein. The β-roll domain is the main carrier of lipids including both surface lipids and lipid at the core. The lipid composition reduced when there was no flexible loop and increased in case of no greasy finger. The change in classes and species of lipid of all cases are reported. The finding provides the foundation for the composition of lipids of DENV NS1 proteins, and presents a new target for NS1 function study as well as a potential new therapeutic target for flavivirus infection.

4.2 Introduction

Flavivirus infection triggers significant changes in host lipid metablolism and the global lipid profile [31,109–111]. Lipid classes are critical in virus infection as they are involved in every step of the flavivirus virus life cycle including entry, viral protein translation, viral RNA synthesis, assembly and virion egress [112]. Different flaviviruses may demand different lipid classes. For example, the replication and virus production of WNV requires an increase in the metabolism of sphingomyelin from ceramide and phosphocholine classes, while DENV replication and virus production increases when the metabolism of sphingomyelin is inHiBiTed [113].

NS1 proteins are peripheral and able to interact with cellular membranes and carry lipids in the lipid cargo when secreted [44]. The secreted NS1 are mostly in a barrel-shaped hexameric form having a lipid core. The size of the lipid core is 20Å in diameter, accommodating about 70 lipid molecules [44, 45]. The lipid classes of the core were only reported for DENV NS1 with the composition similar to high density lipoprotein (HDL) [44]. HDL, interestingly, also showed the ability to cause endothelial dysfunction as the vascular leakage. As NS1 is conserved among flavivirus, the structures of DENV NS1, WNV NS1 and ZIKV NS1 show similar arrangement and size of the lipid core [45, 46]. It remains unclear if the other flavivirus NS1 proteins share similar composition as DENV NS1. DENV NS1 lipid composition, although being reported about ten years ago, was not fully investigated for its lipid classes and species [44]. The NS1 structure suggests the protein interacts with cellular membranes or lipids via three membrane association regions: β-roll domain (residues 1-29), flexible loop (residues 108-128), and greasy finger (residues 159-163). In the previous chapter, we confirmed the membrane interaction function of these regions and also suggested differences in oligomeric forms, membrane binding and secretion of these regions. In this chapter we further characterize the importance of each region on lipid binding. Since lipids and NS1 proteins both play various roles in the virus life cycle, it is possible that the protein functions may related to the lipids it interacts. We

identified and quantified the lipidome of DENV2-NS1 via multiple reaction monitoring profiling (MRM-Profiling). Furthermore, we provided the lipidome of NS1 without each membrane association region. Based on the alteration or absence of each lipid class or species, we suggested the lipid targets of each membrane association region. In combination with the data for the oligomer formation of each truncation, the flexibility of the lipid core and the relation of the lipid core and hexamer form were revealed. The lipidomic results in the chapter give detail in the lipid species and lipid mass from the NS1 protein, which is missing in previous report and aim to give foundation for further lipid-function studies for flavivirus NS1.

4.3 Materials and methods

4.3.1 Cell cultures

Human embryonic kidney 293T (HEK 293T) cells were cultured in Dulbecco's Modified Eagle Medium (DMEM). Cells were grown in 10% fetal bovine serum (FBS) at 37^{o}C with 5% CO_2 .

4.3.2 Plasmid constructions

DENV2 NS1 (strain 16681) including the last 72 nucleotides at the C-terminusinus of E protein (signal sequence) and the whole NS1 gene (1052 nucleotides), was amplified in PCR reaction with primers containing the restriction sites BamHI and XbaI (for pcDNA 3.1(+). The reverse primers for pcDNA 3.1(+) system were engineered with the FLAG-tag (peptide sequence DYKDDDK) with linker in between the NS1 and Flag and stop codon after the tag. The NS1 gene was purified via PCR extraction kit (Qiagen). NS1 genes and plasmids were digested with a set of restriction enzymes (NEB) for 3hrs at 37^{o}C. The digested genes and plasmids were purified from the gel via a gel purification kit (Qiagen). The genes and plasmid backbones were ligated overnight at 16^{o}C and transformed into competent cells DH5α. Four to five colonies

were grown and examined for insertion via restriction digestion before being sent for sequencing (Low Throughput Genomics core at Purdue University) to determine the presence of NS1 gene . The correct clones were determined by both digestion reaction and sequencing results for NS1 sequences.

The truncation clones were generated on the pcDNA-DENV-NS1-Flag backbone, using site directed mutation PCR with primers targeting deletion of the β-roll domain (residues 1-29), flexible loop (residues 108-128) and greasy finger (residues 159-163). PCR products were incubated with DpnI for 3 hr at 37^{o}C and transformed into the competent cells DH5α. Four clones from each deletion were sent for sequencing at Low Throughput Genomics core at Purdue University with sequencing primers identifying the DENV NS1 sequence. Correct clones were chosen and kept for next experiments.

4.3.3 Transfection

pcDNA-DENV-NS1-Flag, pcDNA-NS1-$\triangle$B-Flag (β-roll deletion) , pcDNA-NS1-$\triangle$F-Flag (flexible loop deletion), pcDNA-NS1-$\triangle$G-Flag (greasy finger deletion), and mock (no plasmid) were transfected into HEK 293T cells via lipofectamine 2000 (Thermo Fisher Scientific) at ratio of 1:1. The transfected cells were incubated with 5% FBS in the incubator at 37^{o}C with 5% CO_2. Each purified sample was from the supernatant of 10 T150 flasks (5 x 10^7 cells), which were transfected with 300μg DNA in total.

4.3.4 Protein purification

HEK 293T cells were transfected with pcDNA-DENV-NS1-Flag WT and truncated mutants ($\triangle$B, $\triangle$F and $\triangle$G). Transfected cells were incubated for 72 hpe and supernatants were collected, centrifuged at 3000 rpm for 5 mins at 4^{o}C. The clarified supernatants were incubated with anti-FLAG M2 affinity resin (Sigma-Aldrich) overnight at 4^{o}C on the rotator. The resins were collected by centrifugation at 9,000 rpm for 10 minutes and washed with 20-30 bead volumes wash buffer (0.05 M Tris

HCl, pH 7.4, 0.15 M NaCl). The proteins were eluted with 150 ng/μl 3X Flag peptide solution. Eluates were concentrated using 10 kDa cut-off Amicon Ultra -15 centrifugal filter units at 3,000 rpm for 30-60 mins.

All purified proteins were checked on SDS-PAGE with 10% acrylamide gels with BSA standard. Protein mass was determined based on the protein assay (Biorad).

4.3.5 Lipid extraction

Lipids from purified NS1 were extracted by the Bligh and Dyer protocol [114]. Purified protein (about 9.12 x 10^{12} molecules, except for $\triangle$B at both 9.12 x 10^{12} molecules (1:1 ratio) and 2.73 x 10^{13} (3:1 ratio)) were incubated with chloroform ($CHCl_3$) and methanol (MeOH), followed by vortexing (10s) and incubation on ice for 5 mins. After that, 250 μl of ultrapure water and 125 μl of $CHCl_3$ were added to the sample microtubes and samples were centrifuged at 5,000xg for 5 mins at room temperature. The lipids were concentrated at the bottom phase and transferred to a new tube. The lipid extracts were dried in a speedvac centrifuge and kept at -80^{o}C until use.

4.3.6 LC-MS analysis

Lipid extracts were diluted in the solvent Acetonitrile (ACN): MeOH: Ammonium-acetate (NH_4AC) at ratio of 3.00 : 6.65 : 0.35 together with a lipid internal standard (EquiSPLASH LIPIDOMIX Quantitative Mass Spec Internal Standard, Avanti Polar lipids, Inc.) at 0.6 ng of each internal standard lipid. The samples were injected using an autosampler (Agilent G1367A 1100 series) to the ion source of a triple quadrupole mass spectrometer (Agilent QQQ 6410) to reach an ion signal of 2.0 - 5.0 x 10^6 ion counts for the chromatogram peak ion of phosphatidylcholine (PC) lipids, which are expected to be abundant. The PC lipid profile was obtained by operating the mass spectrometer in neutral loss scan of 141 mass units with collision energy previously optimized to this lipid class. Samples were screening by flow injection of 8 μL of diluted

lipid extract by MRM methods for phosphatidylethanolamine (PE), phosphatidylserine (PS), phosphatidylglycerol (PG), phosphatidylcholines (PC), phosphatidylinositol (PI), Ceramide (Cer), Sphingomyelin (SM) cholesteryl ester (Ch-E), triacylglyceride (TAG)listed at the LipidMaps database (The LIPID MAPS Lipidomics Gateway, http://www.lipidmaps.org/). The lipid annotation were conducted by The Metabolite Profiling Facility from Bindley Bioscience Center at Purdue University.

4.3.7 Data processing and statistical analysis

Lipid mass were calculated from the internal standard. Final lipid abundance was the value of subtraction of each sample weight and water samples. Experimented data were from three independent purified protein experiments, except WT was from two independent experiments. Prism8 software was used to present and analyze the processed MS data in peak intensity from lipid mass and concentration. All data were considered to be significantly different with p value <0.05.

4.4 Results

Flavivirus NS1s are secreted as a hexamer with a lipid core. The only lipid profile report is for DENV NS1, which suggested the composition of the lipid core is similar between DENV serotypes 1 and 2 [44]. Hydrophobic regions on the NS1 protein contributes differently to NS1 membrane association. It is still unclear how each region contributes to the lipid cagro composition. To unravel this question, the three hydrophobic regions, β-roll domain (residues 1-29), flexible loop (residues 108-128), and greasy finger (residues 159-163), were individually deleted and expressed in HEK 293T cells. All proteins were expressed and secreted. The recombinant proteins were purified and lipids from secreted NS1 proteins were extracted and subjected to triple quadrupole mass spectrometer for untargeted (global) lipidomic analysis. Internal lipid standard containing known amounts of different lipids in each class including phospholipids (PC, PG, PE, PS, and PI), sphingolipids (ceramide, and SM) , TAG

and Ch-E were used for lipid concentration quantification of each class. The lipid mass, lipid composition and distribution were then compared between the lipid cargo of the truncated proteins and that of the WT.

4.4.1 Without β-roll domain, the proteins contained low amount of phospholipids, sphingolipids and no cholesteryl ester

Lipid amounts of WT and $\triangle$B were compared at equivalent molar ratios of the two proteins. Each lipid class was measured in relative abundance of weight (nanogram) using the internal standard, except the cholesteryl ester class was calculated in total ion counts (subtraction of sample intensity to water intensity) since there was no standard for the cholesteryl ester in the internal standard kit. With equivalent amounts of molecules of WT, $\triangle$B contained about mock level of all examined lipid classes, including both lipid cargo surface phospholipids and sphingolipids and lipid cargo core lipids, TAG and Ch-E (Fig 4.1). In the graph 4.1, this comparison was shown in weight only (ng), not in concentration ng lipid/μg protein.

As reported in Chapter 3, the deletion of β-roll domain led to mostly the dimer form of secreted NS1, therefore, the lipidome of the molar ratio comparison showed $\triangle$B at three times less dimer than WT. Thus, we compared WT and $\triangle$B at the ratio 1:3 (WT:$\triangle$B) to achieve the same amount of dimer molecules. The lipid concentration increased in four lipid classes such as PG, PS, TAG, Cer but consistently at mock level in four lipid classes PC, PE, SM and Ch-E (Fig 4.1). The lipid value was calculated in concentration ng lipid/μg protein for this set-up. The lipid classes increased in the 3x ratio, including PG, PE, PS, Cer, and TAG (Fig 4.1A, D, E, G, and I), indicated that the truncated proteins did carry those lipids but at low amount in the comparison at ratio 1:1 and intensifying when there were more molecules. The lipid classes that remained at the mock level, were PC, SM and Ch-E (Fig 1D, H, and J), suggesting the $\triangle$B protein did not carry or had below detectable amount of those lipids.

Among all the lipid classes, the most abundant was the phospholipid, PC, which had 210 (± 22.6) ng lipid/μg protein (Fig 4.1B) in WT samples, while the △B showed no value of the lipid class. The second abundant class were also phospholipids, PG and PI at 43.6 (± 8.4) ng lipid/μg protein and 40(± 12.9) ng lipid/μg protein, respectively, in the WT samples. Lipids of △B samples showed no significant difference to WT in △B (at the ratio 1:3) (Fig 4.1A and C). The lipids were further characterized in total chain length and amount of unsaturation to determine if the distribution of each lipid class was altered between WT and mutant (△B). Both lipid classes, PG and PI, showed the same pattern of WT in distribution of the species in chain length and amount of unsaturation (Fig 4.2A,B,C, and D). The next phospholipid, PS, showed no significant difference between WT and △B but at less concentration, 19.7(±6.2) ng lipid/μg protein and 15.4 ((±10.6) ng lipid/μg protein, respectively (Fig 4.1D). The distribution of PS species also showed no change in chain length or amount of unsaturation between WT and △B (Fig 4.2E and F). The last phospholipid, PE, was at concentration 1.35(±0.7) ng lipid/μg protein for WT, while △B contained PE at about mock level, at 0.1(±0.07) ng lipid/μg protein. The reduction of PE was found mostly in the species with chain length from 32-40 with more than 4 unsaturation in the lipid structure (Fig 4.2G and H).

Sphingolipids from the lipid cargo of WT NS1 showed a high concentration of SM, 77.2 (±9.2) ng lipid/μg protein, and low concentration of Cer, 0.8(±0.2) ng lipid/μg protein (Fig 4.1H and I). The sphingolipids from △B showed no SM and lower concentration of Cer, at 0.16(±0.07) ng lipid/μg protein (Fig 4.1H and I). The reduction of Cer were on species of chain length 18 with 11 or more of △B samples (Fig 4.3C and D).

The hydrophobic lipids organized at the core of the lipid core were examined including TAG and Ch-E. TAG concentration of △B was significantly lower than that of WT, at a concentration 4.3(±0.4) ng lipid/μg protein and 10.8(±1.6) ng lipid/μg protein, respectively (Fig 4.1 G and H). TAG species at chain length from

48-54 with fatty acid chain length 20:0 were significantly reduced in △B samples (Fig 4.3A and B).

All together, the data provided the lipid profile of △B NS1. The main lipids from △B were phospholipids, PG, PI, and PS. Sphingolipid was present at low amount of Cer and there was no SM.

4.4.2 Without flexible loop, the lipidome reduced in mass and lacked of PS, PE, and less TAG and Cer

The deletion of the flexible loop caused changes in the presence of phospholipids, PC, PS and PE but not PG, and PI. The two phospholipid classes, PG and PI showed no significant difference in concentration between WT and the mutant (Fig 4.4A and C). All the detected species of the two classes showed the similar pattern of distribution in chain length and amount of unsaturation (Fig 4.5A, B, E and F). The PC class, the most abundant phospholipid, showed reduction in △F samples compared to WT. The distribution of PC species revealed the change in only species with chain length from 30-40 and number of unsaturation from 1-2 (Fig 4.5C and D). PS and PE concentrations were at mock level, suggesting the absence of the two classes in the composition of △F lipid composition (Fig 4.4 D and E).

The sphingolipids, SM and Cer, were in lower concentration compared to the WT. SM was more abundant than the Cer in the lipid composition, at 58.2 (±6.1) ng lipid/μg protein and 0.24(±0.02) ng lipid/μg protein, respectively (Fig 4.4H and I). The reduction in SM was from the species at 18 sphingoid chain length with more than 20 fatty acid chain length (Fig 4.6A and B). Cer showed reduction in species at 18 sphingoid chain length with more than 11 fatty acid chain length (Fig 4.6C and D).

Lipid composition of △F showed the presence of TAG and Ch-E, the lipids at core of the lipid cargo, even though both lipid classes were reduced in concentration and total ion count (Fig 4.4G and J). The reduction of TAG was from all the chain

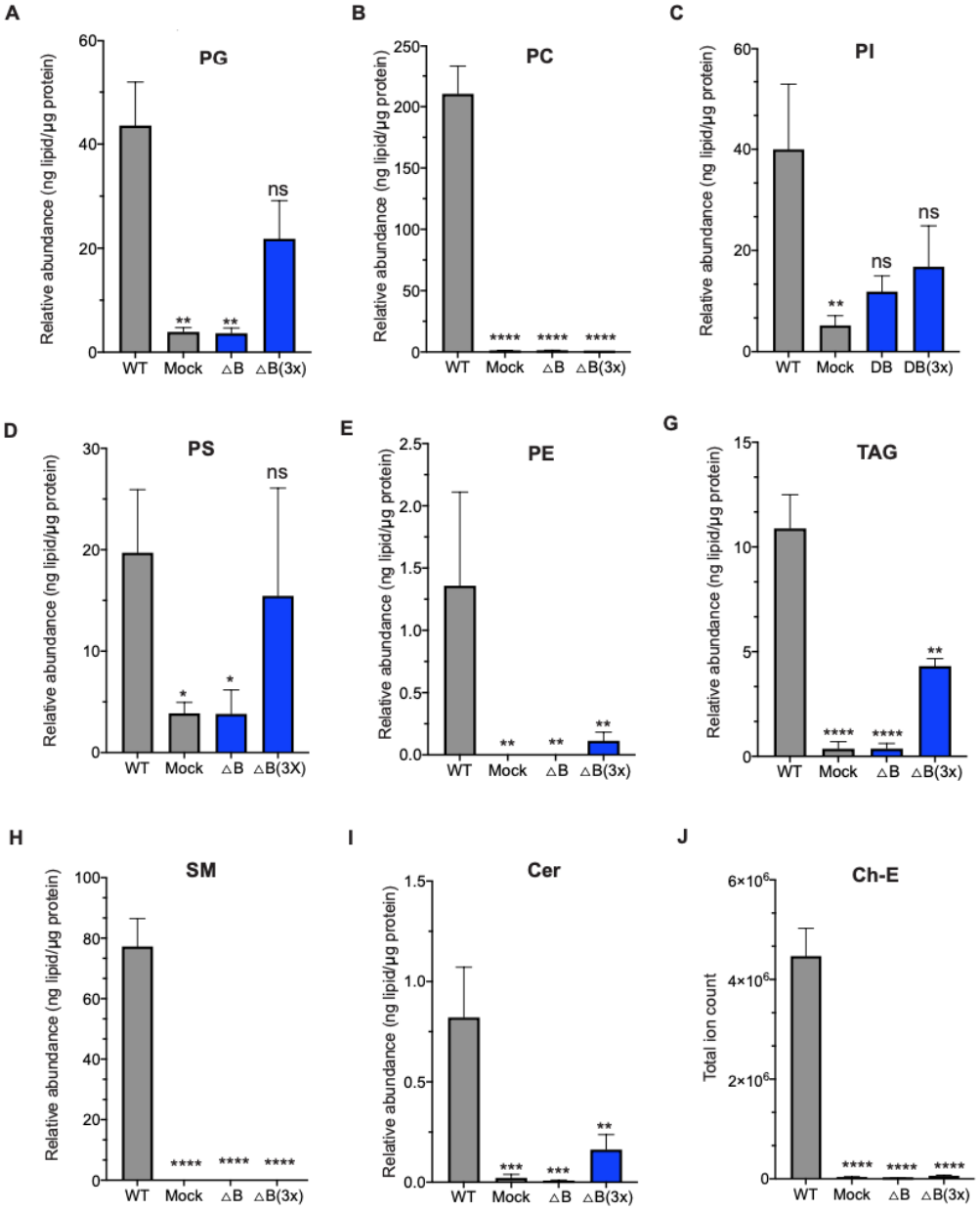

Fig. 4.1. Lipid class changes in DEN2 NS1 lacking the β-roll domain. Amount of lipids (ng lipid/μg protein) by lipid class for WT, mock and $\triangle$B. The amount the each lipid classes was calculated via internal standards, except the quantification of Ch-E. Ch-E amount was shown in total ion count and obtained by subtracting the sample ion counts from a blank sample. $\triangle$B (n=3) was samples in the same amount of molecules as WT. $\triangle$B(3x) (n=3) was samples at 3 times more molecules than WT.

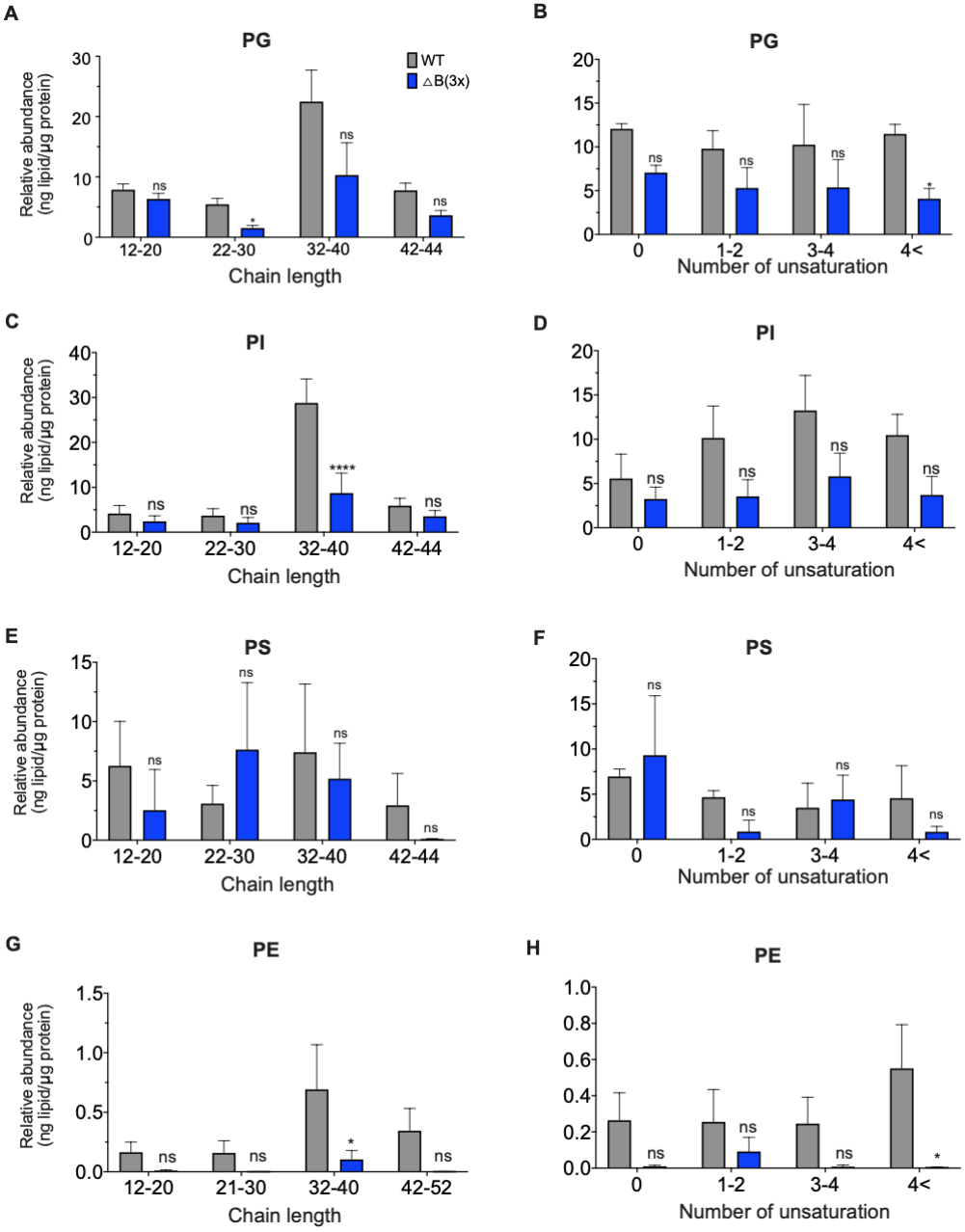

Fig. 4.2. Changes in distribution by chain length and number of unsaturation of phospholipid classes (PG, PI, PS, and PE) from DEN2 NS1 lacking the β-roll domain. Lipid species in each phospholipid class were grouped by their chain length or number of unsaturation. Samples $\triangle$B(3x) (n=3) were 3 times more molecules than WT to make the total number of dimer NS1 the same as WT.

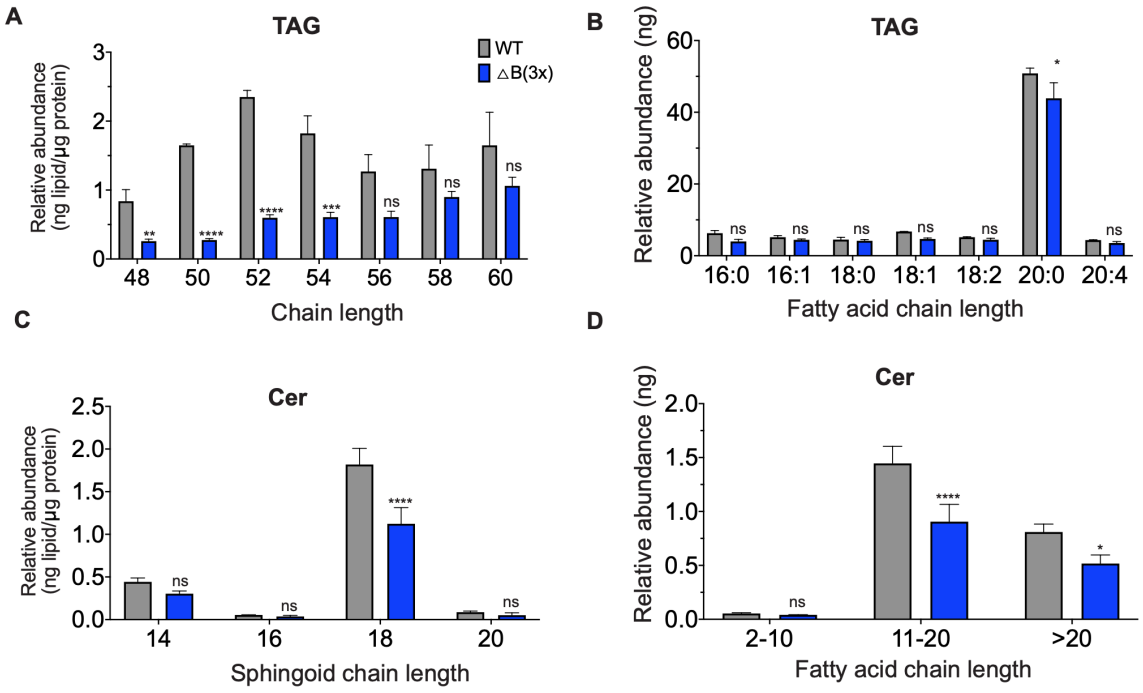

Fig. 4.3. Changes in distribution by sphingoid chain length and fatty acid chain length of TAG and Cer from DEN2 NS1 without β-roll domain. Lipid species in each lipid class were grouped by their sphingoid chain chain length or fatty acid chain length. Samples $\triangle$B(3x) (n=3) were 3 times more molecules than WT to make the total number of dimer NS1 the same as WT.

length from 48-60 and all fatty acid chain length except 18:0 (Fig 4.6E and F). Ch-E also showed reduction in almost all the species, chain length 12-20 and number of saturation more than 1. CH-E species with chain length 21-24 and saturation remained in WT total ion count level (Fig 4.6G and H).

Taken together, deletion of the flexible loop led to the reduction of PC, all examined sphingolipids and lipids at the core, TAG and Ch-E. PG and PI were not affected by the deletion of this region, suggesting that the flexible loop may not be binding to those lipids or lipids were bound by β-roll and greasy finger. The loss of PS, PE, Cer and TAG in the lipid composition indicated these classes would be the target lipids for the flexible loop.

4.4.3 Deletion of greasy finger intensifies the lipid profile of the lipid cargo

The deletion of the greasy finger enriched the lipid composition including both surface lipids and core lipids. Phospholipid classes, PG, PC, PS and PE, remained at WT concentration, while PI was about 2.4 times higher in $\triangle$G than in WT (Figs 4.7 A-E). Analysis of chain length and amount of saturation of those lipid classes showed the same distribution of lipid species as WT and $\triangle$G (Figs 4.8A-J). The PI in $\triangle$G contained more species at chain length 32-40 with all amount of unsaturation (Figs 4.8E and F). Sphingolipids, SM and Cer, showed different effects in $\triangle$G samples. SM concentration increased 1.6 times compared to WT (Fig 4.7H). The distribution of SM species was similar to WT but the concentration of all species were higher in $\triangle$G samples (Fig 4.9A and B). Cer, on the other hand, showed no difference between samples from WT and the truncated protein (Fig 4.7I). Distribution and concentration of all the Cer species from WT and $\triangle$G shared the same pattern and value (Figs 4.9C and D). Core lipids from the lipid cargo of $\triangle$G showed the increase in concentration (TAG) and total ion count (Ch-E) (Figs 4.7G and J).

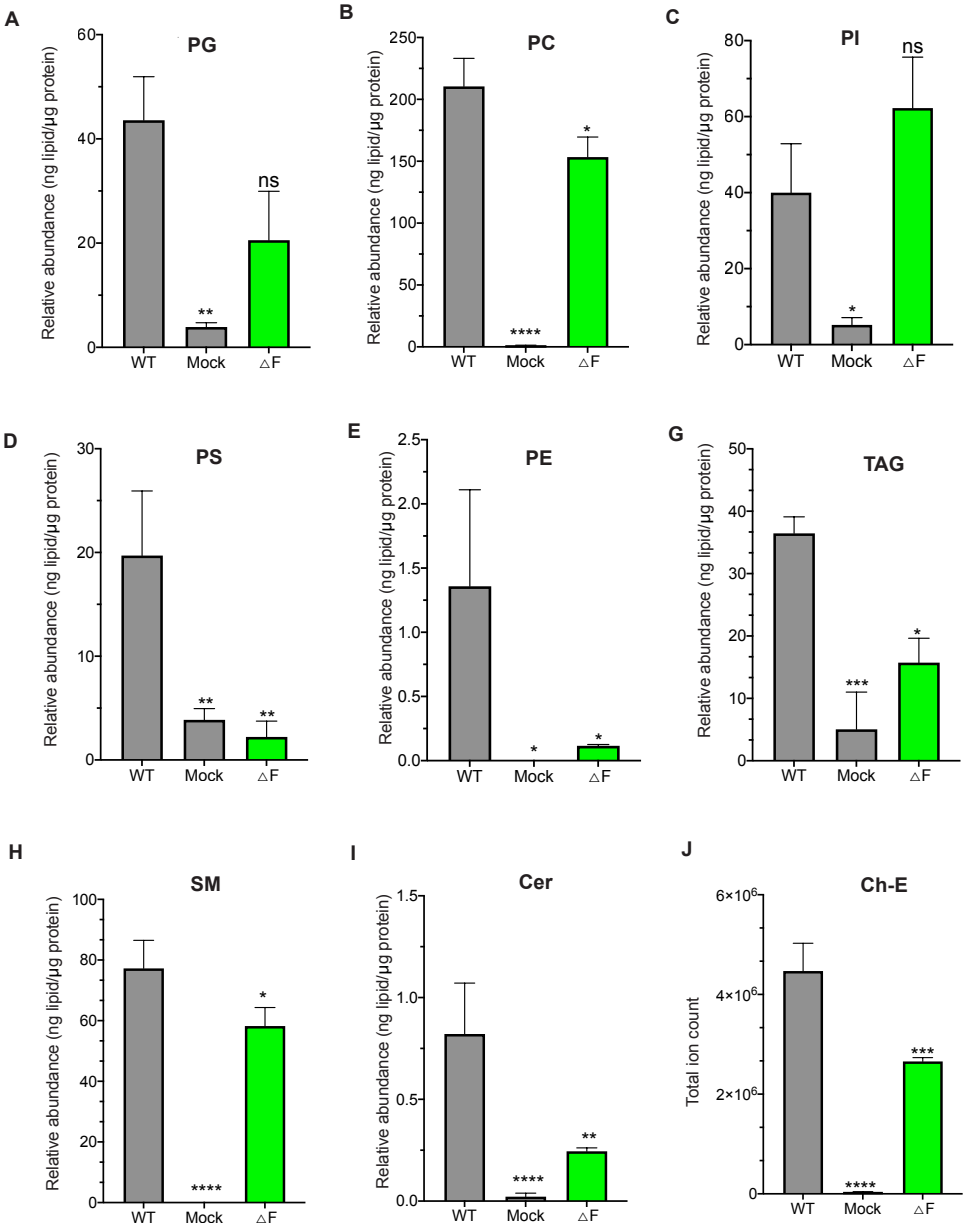

Fig 1: Change in lipid classes from △F protein

Fig. 4.4. Lipid class changes in DEN2 NS1 lacking the flexible loop. Amount of lipids (ng lipid/μg protein) by lipid class for WT, mock and $\triangle$F. The amount the each lipid classes was calculated via internal standards, except the quantification of Ch-E. Ch-E amount was shown in total ion count and obtained by subtracting the sample ion counts from a blank sample.

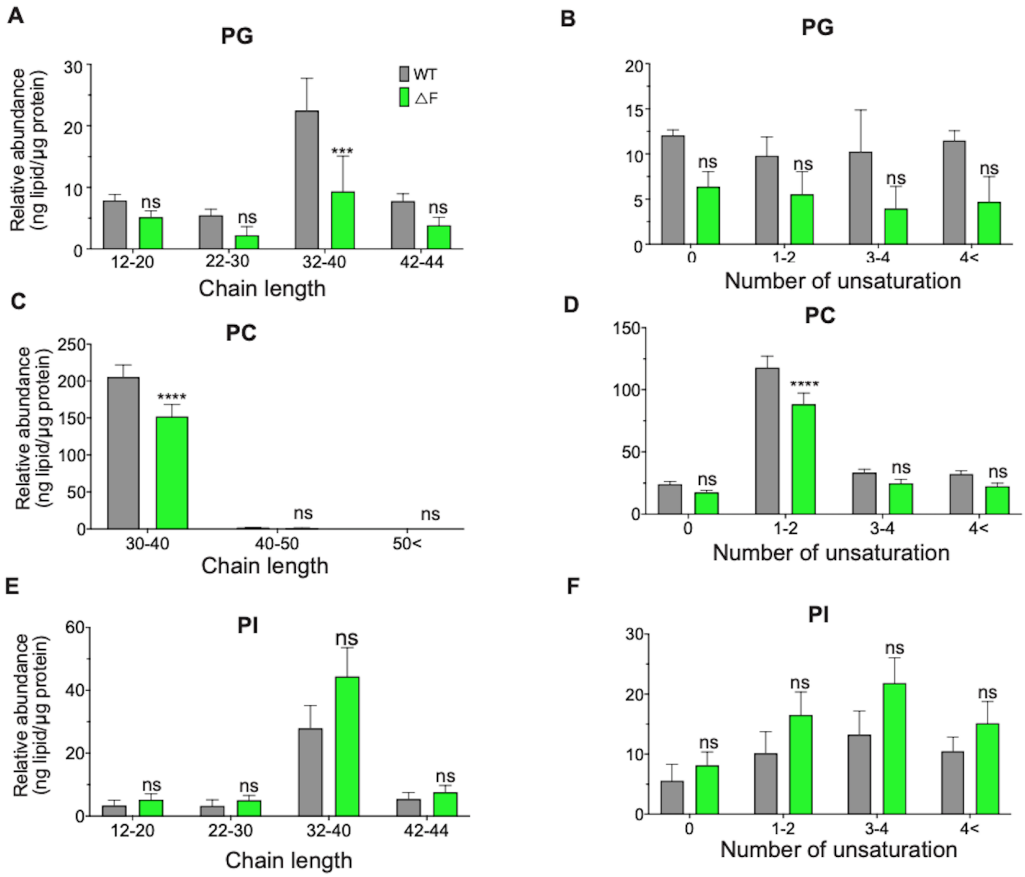

Fig. 4.5. Changes in distribution by chain length and unsaturation level of phospholipid classes (PG, PC, and PI) from DEN2 NS1 lacking the flexible loop. Lipid species in each phospholipid class were grouped by their chain length or number of unsaturation.

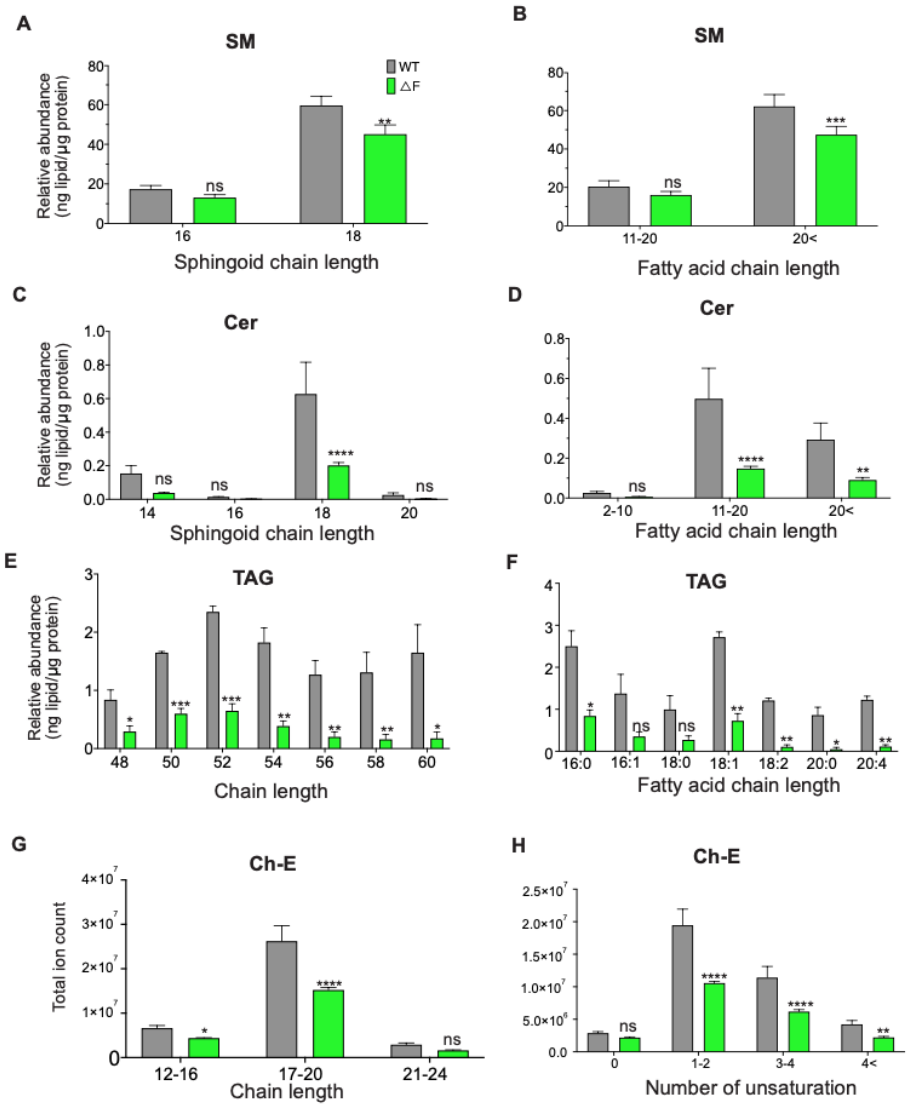

Fig. 4.6. Changes in distribution of sphingolipid classes (SM and Cer) and core lipids (TAG and Ch-E) from DEN2 NS1 lacking the flexible loop. Phospholipid species were grouped by their sphingoid chain length and fatty acid chain length. TAG species were grouped by the chain length and fatty acid chain length. Ch-E species were grouped by chain length and number of unsaturation.

Table 4.1.
Membrane association region deletions alter the lipid profile of NS1. Different lipid groups were analysed and color code for their effects compared to WT, including WT Absence Decrease Increase

NS1	Phospholipids	Sphingolipids	Core lipids
WT	PC, PG, PI, PE, PS	SM and Cer	TAG and Ch-E
△B	PC, PG, PI, PE, PS	SM and Cer	TAG and Ch-E
△F	PC, PG, PI, PE, PS	SM and Cer	TAG and Ch-E
△G	PC, PG, PI, PE, PS	SM and Cer	TAG and Ch-E

Taken together, deletion of greasy finger enhanced the lipidome of the NS1 cargo while retaining a similar distribution of lipid species.

4.5 Discussion

Molecular and mouse model studies on flavivirus NS1 revealed immense information of NS1 pathogenesis *in vitro* and *in vivo*. There is abundance of proteomic analysis for NS1 and host interactome networks to determine how NS1 hijacks host machinery for its various functions. However, lipidomic analysis of the protein is very limited although lipids recently are considered as indispensable factors for flavivirus infection [115]. In this study, the lipidomic profile of secreted NS1 proteins was examined via multiple reaction monitoring profiling (MRM-Profiling)- tandem mass spectrometry. We sought to characterize and quantify the lipid composition of the lipid cargo from recombinant DENV NS1 in mammalian cells (HEK 293T). Moreover, lipid classes and species that bind to different membrane association regions were compared with WT to determine the lipid targets for each region. Based on the oligomeric characterization of the deletion of each membrane association region, we looked for the lipid class or species that differentiate the dimer and hexamer NS1 as well as the compositional diveristy of the hexamer.

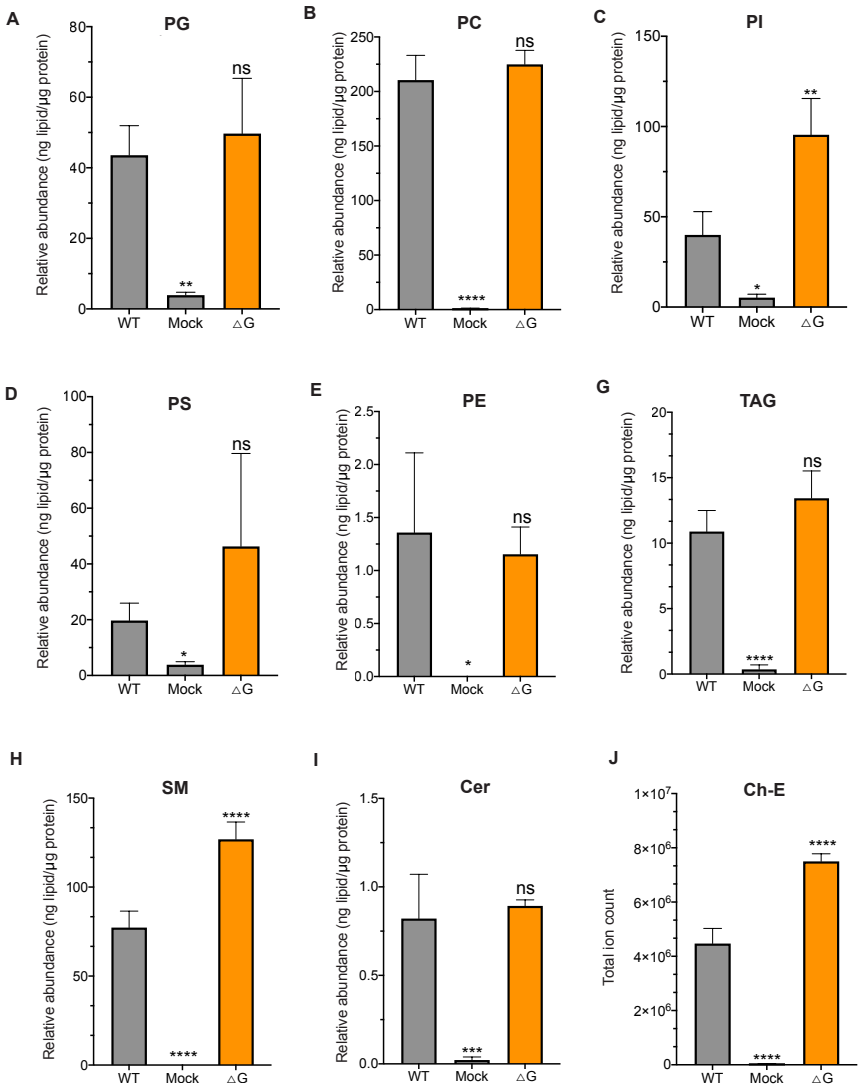

Fig. 4.7. Lipid class changes in DEN2 NS1 lacking the greasy finger. Amount of lipids (ng lipid/μg protein) by lipid class for WT, mock and $\triangle$G. The amount the each lipid classes was calculated via internal standards, except the quantification of Ch-E. Ch-E amount was shown in total ion count and obtained by subtracting the sample ion counts from a blank sample.

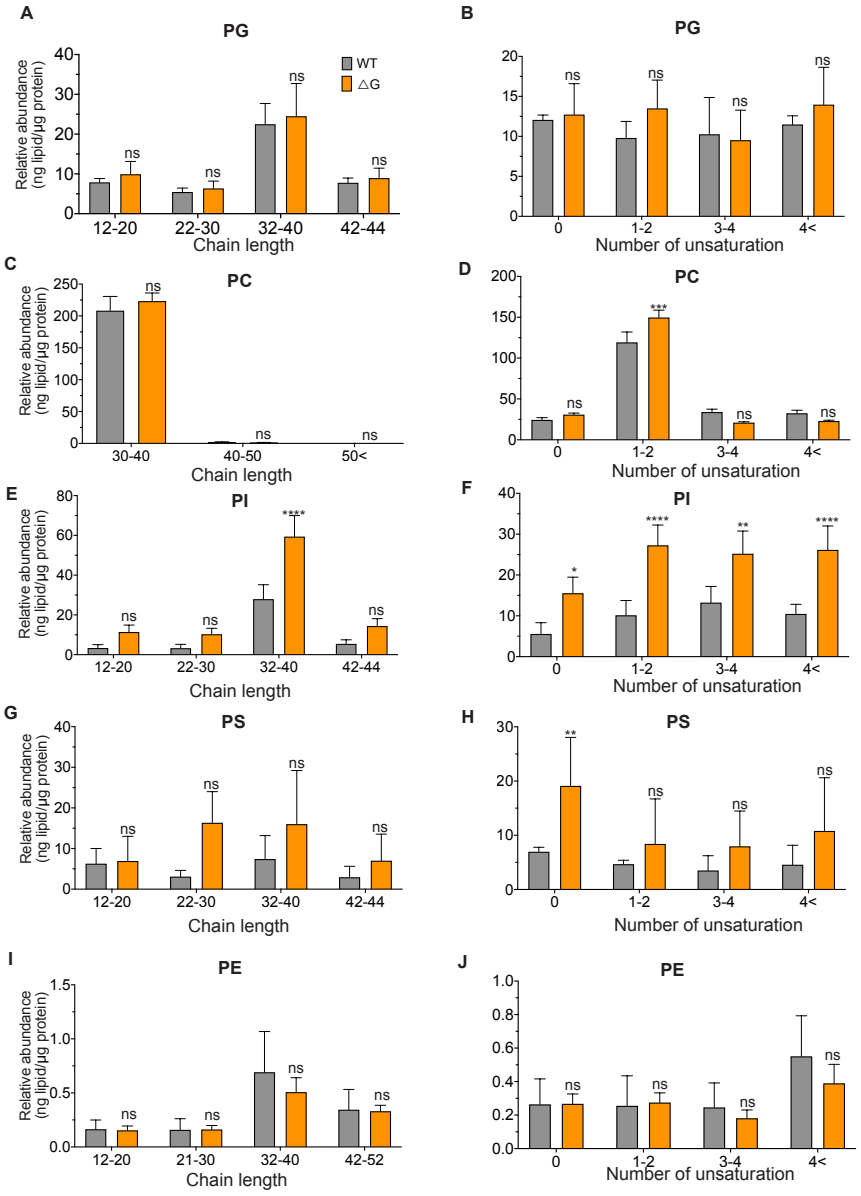

Fig. 4.8. Changes in distribution by chain length and unsaturation level of phospholipid classes (PG, PC, PI, PS and PE) from DEN2 NS1 lacking the greasy finger. Lipid species in each phospholipid class were grouped by their chain length or number of unsaturation.

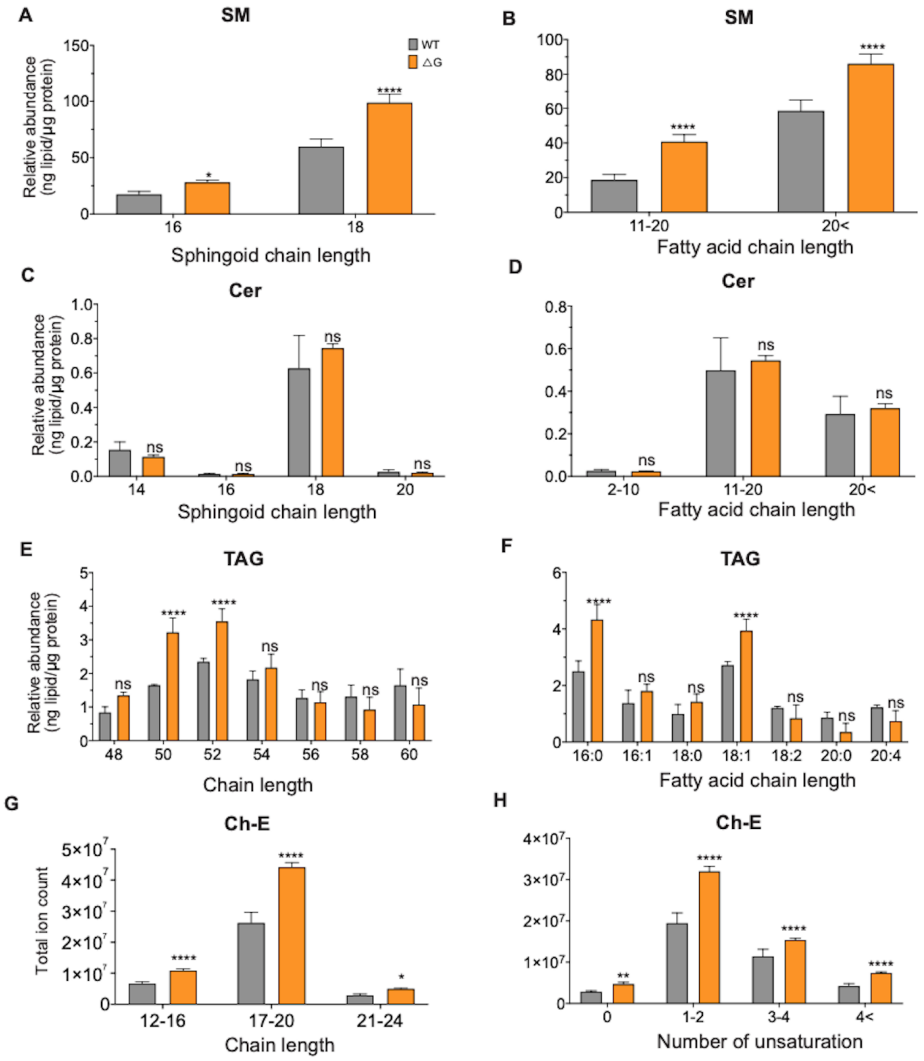

Fig. 4.9. Changes in distribution of sphingolipid classes (SM and Cer) and core lipids (TAG and Ch-E) from DEN2 NS1 lacking the greasy finger. Phospholipid species were grouped by their sphingoid chain length and fatty acid chain length. TAG species were grouped by the chain length and fatty acid chain length. Ch-E species were grouped by chain length and number of unsaturation.

The composition of lipids in the lipid cargo of DENV NS1 revealed the most abundant lipid is phosphatidylcholine (PC), about 200 ng lipid/ μg protein. The most abundant species of this phospholipid class are at 32-40 chain length. The next abundant lipids are also phospholipids, phosphatidylglycerol (PG) and phosphatidylinositol (PI), at about 40 ng lipid/ μg protein. The most abundant species of both phospholipid classes are also at 32-40 chain length. PS was at about 20 ng lipid/ μg protein, at about half concentration of PI and PG. PE is the least phospholipid, at 1.2 ng lipid/ μg protein. In the previous study, the composition of the cargo were found to be similar to that of high-density lipoproteins (HDLs) [44]. Phospholipids is the most dominant lipid group in the lipid cargo of NS1. It is similar to the composition of HDL, in which phospholipids are at 40-60 weight% of total HDL lipid [116]. PC is also the predominant phospholipid class in HDL, at 33-45 weight% of total HDL lipid. However HDL contains lower amounts of PI, at 0.5-1.5 weight% of total HDL lipid [116]. Sphingolipids, sphingomyelin (SM) and ceramide (Cer), are the second most abundant group in the cargo. SM is at 70 ng lipid/ μg protein and Cer is at 0.7 ng lipid/ μg protein. Sphingolipids in HDL are also at lower level than phospholipid, at 5-10 weight% of total HDL lipid, however the Cer is less than SM. At the core of the lipid cargo, there are lipid classes, cholesteryl ester (Ch-E) and triacylglyceride (TAG). Cholesteryl ester is dominated HDL core lipids at 30-40 weight% of total HDL lipid and triacylglyceridelycerides is about 5-10 weight% of total HDL lipid [116]. Triacylglyceride species found in the study are also at low amount, at 10 ng lipid/μg protein, including species saturated palmitic acid, stearic acid and unsaturated oleic acid with the carbon length from 48 to 56. The Ch-E is not quantified as there was no internal standard in the study. Cholesteryl ester species were not report in the literature but here we provided species including molecules with chain length from 12-24 with the number of unsaturated from 0-6. Our analyses of lipid profile of the DENV NS1 suggests the abundance of different lipid groups of the lipid cargo but also the distribution and abundance of the lipid species. The composition of DENV NS1 is similar to HDL as previously reported but not identical as the ratio of lipids

from the same lipid groups varies from values reported in the HDL lipidome. It is noted that alteration in the HDL lipidome can lead to diseases, such as cardiovascular risk via inducing endothelial hypertension [117–119]. NS1 is also able to cause hyperpermeability of human cells [79], indicating the change in lipidome of the protein may play a role in this function.

NS1 proteins are able to bind to cellular membranes via three hydrophobic regions; the lipidomes of secreted proteins without individual hydrophobic regions were investigated and compared with WT. The β-roll domain, which is the largest hydrophobic region with 29 amino acids (residues 1-29), caused the greatest reduction in the lipidome of secreted NS1. As reported in chapter 3, the $\triangle$B proteins stay mostly in dimer form, the comparisons were performed at both molar ratios 1:1 (WT:$\triangle$B) and 1:3 (WT:$\triangle$B) to get to the same amount of dimer as WT. The absence of the β-roll domain led to an undetectable level of PC, PE, SM, Cer, and Ch-E, which are the most abundant phospholipids, sphingolipids and the core lipid in the NS1 cargo, suggesting these lipids were bound by the β-roll domain. Undetectable Ch-E in the truncated protein is consistent with the oligomeric status of $\triangle$B, and confirms that the hexamer form may require the presence of Ch-E. Other lipid classes, including PG, PI, PS, and TAG, showed lower level or WT level in the truncated protein, indicating the other membrane association region(s) binds to these lipids.

In the absence of the flexible loop, the lipid profile reveals that the region may not target PG and PI, but binds to PS, and PE. The flexible loop may also bind to PC, SM, Cer, TAG, and Ch-E but as the level of these lipid classes were reduced but still present in $\triangle$F samples. It is possible that the other membrane association regions bind to these as well. The $\triangle$F protein was reported in a previous chapter as mainly hexamer. Thus the decrease of the highly hydrophobic lipid Ch-E at the core of the lipid cargo may indicate that the level of CH-E can be varied in the cargo core, without changing the hexameric form.

Lastly, the lipidome of NS1 lacking the greasy finger showed an increase in lipid binding. It is surprising as none of the lipid classes is reduced and most of them remain

unchanged, such as PG, PC, PS, PE, Cer, and TAG. The three classes augmented their levels at about 2 times, including PI, SM, and Ch-E. It is noted that unlike WT, the ratio of PI:PG converted to 2:1, which was usually at ratio 1:1 in HEK 293T cells [120]. The increase of lipid classes in the truncated protein may be due to one of these possibilities. The first possibility is that NS1 can sense the membrane properties and the truncation on NS1 leads to the change in the sensing of the lipid composition on the membrane and therefore, interact with different membrane area. The second possibility is that the NS1 protein is able to alter the lipid composition of the cellular membrane, thus the truncation on the greasy finger results in changing this ability, and the lipid composition of the binding membrane change. The last possibility is that NS1 expression is able to alter lipid metabolism of transfected cells, leading to the lipid change in the cellular level, thus the lipid composition of the membranes in $\triangle$G contains more the PI and SM than the WT. In any case, the $\triangle$G showed more lipids and still formed hexamers. This may be in agreement with the $\triangle$F results, which suggesting that the lipid composition of the lipid cargo can vary without affecting the hexamer formation.

All together, the data suggest the β-roll domain plays the main role in membrane binding (phospholipids, sphingolipids) and formation of the lipid core (cholesteryl ester and triacylglyceridelyceride). The main lipid targets for the β-roll domain might be PC, PE, SM, Cer, and Ch-E. The flexible loop may target PS, and PE. The two phospholipids, PG and PI may bind to protein in unspecific manner. As the greasy finger deletion did not show absence of lipid binding, this region may contribute to the membrane association in unspecific binding or sensing the composition of the membranes for the other regions to interact with. In this investigation, we provided the list of lipid species that change with different truncated NS1s for further NS1-lipid study. As there is not much information on the species of each lipid class in NS1 cargo, the lipidome was not compared with previous studies. The only report showed that native (infection) purified DENV-1 NS1 contained TAG with species such as

palmitic acid, oleic acid, and linoleic acid [44], which was also shown in our study, it is unclear if the other lipid classes were the same as that in the recombinant NS1.

In addition, this study suggested the flexibility of lipid composition within hexameric NS1. The lipid mass of the lipid cargo is able to increase or decrease (Table 4.1) but the distribution of the species showed no change in the species presence and ratio . To date, there are limited reports on the composition of the lipid cargo or the flexibility of the composition for the NS1 hexamer formation. A report of recombinant DENV-2 NS1 serum-free condition of Baculovirus suggested the proteins contained low lipid levels while the hexameric form and structure were similar to the mammalian-derived protein [121]. Together with data from a previous chapter, the lipid cargo of DENV NS1 showed to be varied in the lipid level and cargo composition, and it is not critical for its secretion ability and hexamer formation. However, the composition showed some effects on NS1 secretion level and hexamer stability. Mutant T164S on NS1 (the residue adjacent to the greasy finger) formed hexamers with a lipid composition reduced in PE but increased in ether lysophosphatidylcholines (LPC-O). The mutant was secreted more in mammalian cells and facilitated mosquito infection [97]. Thus, lipid composition in NS1 may affect the protein activity as well as its functions in virus infection. Further study may be required to understand these lipids effects in NS1 as well as function of NS1 in virus life cycle.

This lipidomics study provided insight for NS1 specific lipid targets as well as variety of lipid cargo composition in dimer and hexamer forms. This hopefully can guide further research direction for NS1 functions. We did not determine the size of the lipid cargo in the structure of each truncated protein. The mass and amount of species in the cargo, together with the size or volume of its structure can suggest more detail of number of lipids and limit of lipid amount for the lipid core. It is also helpful to determine if recombinant NS1 from different mammalian cell lines such as Chinese hamster ovary (CHO) or baby hamster kidney (BHK) may share similar lipidomes or may reflect the differences in cellular lipid composition. Moreover, the differences in lipidomes from native and recombinant NS1 could also be useful to distinguish the

lipids for virus infection and NS1 expression. These differences in lipid may be used for further investigation of lipid requirements for hexamer formation and pathogenesis of NS1. This lipid study can aid for better NS1-disease related diagnosis as well as NS1-target antiviral therapeutics.

5. CONCLUSION AND FUTURE DIRECTIONS

In this chapter, we aim to use the new knowledge from the studies to clarify some specific steps in the virus and NS1 life cycles at a molecular level. Since the flavivirus NS1 proteins are multifaceted in structures and functions, they serve as a potential therapeutic target and a vaccine candidate. However, antibodies against NS1 can play both protective and pathogenic functions, thus the usage of NS1 as antigen or antibody should be proceeded with caution. Therefore, the molecular information of NS1 residues or domains that critical for different NS1 functions can be used to consider for the design of the future study or vaccine development. We also suggest some potential future experiments to answer questions remaining in our studies.

5.1 Differences of flavivivirus NS1

Flavivirus NS1 contributes greatly to the virus infection. As the proteins are highly conserved in their structures and sequences in flavivirus genus, they are expected to share similar functions. However, several reports suggest there are differences of the flavivirus NS1 in the same activity such as secretion kinetics, tissue tropism, and interaction with complement components [39, 40, 91, 122–124]. However there are limited comparative studies on different NS1 in flavivirus systems. Youn et al. suggested that a deletion of the NS1 gene in WNV can be rescued by trans-complementation of homologous or heterologous flavivirus NS1 (YFV, DENV, JEV, and SLEV) [54]. In previous work by Lindenbach et al, deletion of the NS1 gene in YFV cannot be rescued by trans-complementation of DENV NS1, suggesting the specific interaction of NS1 and the virus system [58]. Our study aims to provide evidence for differences in activity of specific flavivirus NS1s in the flavivirus infection. Using reciprocal substitutions between DENV and WNV amino acids at the

same residue, we identified three residues that influence virus titers, dependent on the specific virus amino acid. Switching the DENV to WNV amino acids on these residues causes defects on the virion formation, maturation and virus entry, while the reciprocal substitutions enhance infectious particle formation and entry or affect the virus secretion. Furthermore, our study suggested the release of the DENV virus particle is related to DENV NS1 secretion while WNV particles travel independently of the WNV NS1. These differences demonstrate specificity of NS1 activity in each virus system and suggest the two viruses may interact distinctly with the host at the molecular level. It is possible that each virus system has different fitness level of their genome or viral protein interactions, therefore, amino acids from a better fitness system can enhance the infectious progeny or if they are from a strict fitness system, the infectious progeny would be less adapted or lose their fitness.

5.2 Flavivirus NS1 functions

5.2.1 Replication

NS1 functions in viral RNA synthesis include the synthesis of negative and positive strand RNA and anchor of the replication complex [54]. The anchor function is suggested via its interaction with other viral non-structural proteins, NS4A, NS4B and the precursor of the NS4A-2K-NS4B [49, 55, 58, 60]. The interaction of NS1 and the precursor NS4A-2K-NS4B is via two residues on the NS1 wing domain, G161 and W168, which are located on the greasy finger (residues 159-163) and adjacent sites. The mutations, G161A and W168A, inHiBiT viral RNA synthesis but still allow the formation of the replication complex in virus expression [55], suggesting the interaction of NS1 and the precursor nonstructural proteins is not critical for replication complex formation. The study gives details into the two separate functions of NS1 including assembly of the replication complex and viral RNA synthesis. The same study further suggested the mutations did not affect the membrane association ability of NS1 but merely disrupts the viral protein interaction. Our study on membrane

association provides valuable information for the study of NS1 function related to its ability to interact with cellular membrane. We suggested the deletion of each hydrophobic region (β-roll, flexible loop, and greasy finger) reduced the interaction of NS1 and membrane and secretion but do not completely abrogate the function and activity. Thus any site-directed mutation on each region will not inHiBiT the membrane binding or NS1 secretion. The defect, therefore, would be due to the disruption of other interactions of NS1 and viral or host proteins. Further study may be required to determine how NS1 separates the two functions of assembly of the replication complex and assisting RNA synthesis as NS1 is spatially separated from the rest of the viral replication proteins.

5.2.2 Assembly

NS1 function in virus assembly is recently investigated. It was suggested to influence infectious particle formation via interaction with viral structural proteins, capsid, prM and envelope via residues S114, W115 on NS1 [57]. Our study suggested in details other steps in the virus life cycle for NS1 function with a different set of mutations. Those mutations on NS1 can disrupt virion formation, virus maturation, trafficking and release. These functions of NS1 are independent from its functions in viral RNA synthesis. These steps are caused by a single mutation on either wing or β-ladder domains, suggesting the protein may use distinct domains for its functions. It is also interesting that the previous study and our study found single mutation on NS1 affecting individual steps after replication. This possibly reflects different populations of NS1 that do different functions in the virus life cycle. Further study is required to explain how NS1 uses different domains or residues for each specific step in the virus life cycle. As the protein affects virion formation and intracellular maturation, how these happen and how NS1 separates from the particle in the extracellular environment are interesting questions for the mechanism of NS1.

5.2.3 Cell entry

Extracellular NS1 has been intensively studied for its functions *in vitro* and *in vivo*. DENV NS1 and virus particles are found to bind to cell lines via glycoaminglycan (GAG) and flavivirus NS1s bind to tissues reflecting its specific disease tropism [40, 92, 125]. NS1 treatment prior to virus infection could enhance virus production [37]. The protein can enter new cells and be stable in late endosomes up to 48 hour after entry [37]. Our study provide a new function of NS1 in virus entry. We suggest that extracellular NS1 can enhance virus entry in dose-dependent manner and a mutation (K101) in NS1 can disrupt this function. This could be used to explain why NS1 treatment can enhance virus infection. A study on a DENV NS1 mutation, T164S, led to increase in NS1 secretion and decrease in infectious particle formation but caused tissue inflammation and severe disease in mice compared to WT [97]. The results indicate that even with less infectious particles, more NS1 can enhance virus infection and consequently cause severe disease.

5.3 Membrane association capacity

NS1 is an enigmatic protein with an ability to associate with membranes. This ability is suggested to be critical for the protein for its function, however how membrane binding contributes to NS1 behavior and function was not determined. Based on the NS1 structure, we investigated the contribution of NS1 hydrophobic regions, including the β-roll, flexible loop, and greasy finger, on membrane binding. We found that each region can bind to lipids and cellular membrane and the deletion of each of them can reduce the level of membrane binding. The protein requires a cooperation of any two regions for the function, thus there is a redundancy in membrane association regions. Moreover, the protein can dimerize and be secreted as long as it is able to bind to cellular membranes. The flexible loop and greasy finger are dispensable for hexamer formation but the β-roll is critical for both hexamer formation and also stability. The β-roll is found to target all the abundant lipids on the membrane including

phospholipids (PC, PE) and sphingolipids (SM, Cer). As the protein without β-roll stays mainly in dimer form, there is no cholesteryl ester, which is more hydrophobic and usually stays at the core of the lipid channel, was found from β-roll lipid extraction. The flexible loop targets phospholipids, PS and PE, which are both less abundant then PC, and may not bind to sphingolipids. The greasy finger surprisingly causes an increase in lipid profile when it is deleted. We suggest that this region may play role in lipid sensing or regulating the binding of the other two regions. As each region seeks different lipids, it is possible that the protein binds to membrane with certain lipid composition, such as lipid raft, a lipid-rich microdomain on Golgi and plasma membrane. Collectively, our study provided a molecular study of membrane binding regions on NS1 and suggested the lipid target for each. This may serve as a foundation to study how NS1 contributes to replication complex formation or location of NS1 in different cell compartments based on the lipid composition of the membrane. Further study on composition of virus particles and NS1 may reveal if they form in the same compartment as well as if NS1 targets the lipid of the virus particle or merely interacts with E protein as suggested from previous studies.

REFERENCES

REFERENCES

[1] S. Bhatt, P. W. Gething, O. J. Brady, J. P. Messina, A. W. Farlow, C. L. Moyes, J. M. Drake, J. S. Brownstein, A. G. Hoen, O. Sankoh *et al.*, "The global distribution and burden of dengue," *Nature*, vol. 496, no. 7446, p. 504, 2013.

[2] T. Solomon and D. Vaughn, "Pathogenesis and clinical features of japanese encephalitis and west nile virus infections," in *Japanese encephalitis and West Nile viruses*. Springer, 2002, pp. 171–194.

[3] V.-M. Cao-Lormeau, A. Blake, S. Mons, S. Lastère, C. Roche, J. Vanhomwegen, T. Dub, L. Baudouin, A. Teissier, P. Larre *et al.*, "Guillain-barré syndrome outbreak associated with zika virus infection in french polynesia: a case-control study," *The Lancet*, vol. 387, no. 10027, pp. 1531–1539, 2016.

[4] J. Mlakar, M. Korva, N. Tul, M. Popović, M. Poljšak-Prijatelj, J. Mraz, M. Kolenc, K. Resman Rus, T. Vesnaver Vipotnik, V. Fabjan Vodušek *et al.*, "Zika virus associated with microcephaly," *New England Journal of Medicine*, vol. 374, no. 10, pp. 951–958, 2016.

[5] T. M. Colpitts, M. J. Conway, R. R. Montgomery, and E. Fikrig, "West nile virus: biology, transmission, and human infection," *Clinical microbiology reviews*, vol. 25, no. 4, pp. 635–648, 2012.

[6] J. R. Powell, A. Gloria-Soria, and P. Kotsakiozi, "Recent history of aedes aegypti: vector genomics and epidemiology records," *Bioscience*, vol. 68, no. 11, pp. 854–860, 2018.

[7] M. Besnard, S. Lastere, A. Teissier, V. Cao-Lormeau, and D. Musso, "Evidence of perinatal transmission of zika virus, french polynesia, december 2013 and february 2014," *Eurosurveillance*, vol. 19, no. 13, p. 20751, 2014.

[8] D. Musso, C. Roche, E. Robin, T. Nhan, A. Teissier, and V.-M. Cao-Lormeau, "Potential sexual transmission of zika virus," *Emerging infectious diseases*, vol. 21, no. 2, p. 359, 2015.

[9] P. S. Pandit, M. M. Doyle, K. M. Smart, C. C. Young, G. W. Drape, and C. K. Johnson, "Predicting wildlife reservoirs and global vulnerability to zoonotic flaviviruses," *Nature communications*, vol. 9, 2018.

[10] S. Thongyuan and P. Kittayapong, "First evidence of dengue infection in domestic dogs living in different ecological settings in thailand," *PloS one*, vol. 12, no. 8, p. e0180013, 2017.

[11] C. DeCarlo, A. H. Omar, M. I. Haroun, L. Bigler, M. N. Bin Rais, J. Abu, A. R. Omar, and H. O. Mohammed, "Potential reservoir and associated factors for west nile virus in three distinct climatological zones," *Vector-Borne and Zoonotic Diseases*, vol. 17, no. 10, pp. 709–713, 2017.

[12] R. Vorou, "Zika virus, vectors, reservoirs, amplifying hosts, and their potential to spread worldwide: what we know and what we should investigate urgently," *International Journal of Infectious Diseases*, vol. 48, pp. 85–90, 2016.

[13] A. W. Franz, A. M. Kantor, A. L. Passarelli, and R. J. Clem, "Tissue barriers to arbovirus infection in mosquitoes," *Viruses*, vol. 7, no. 7, pp. 3741–3767, 2015.

[14] L. A. Alonso-Palomares, M. Moreno-García, H. Lanz-Mendoza, and M. I. Salazar, "Molecular basis for arbovirus transmission by aedes aegypti mosquitoes," *Intervirology*, vol. 61, no. 6, pp. 255–264, 2018.

[15] B. E. Martina, P. Koraka, and A. D. Osterhaus, "Dengue virus pathogenesis: an integrated view," *Clinical microbiology reviews*, vol. 22, no. 4, pp. 564–581, 2009.

[16] A. N. Brown, K. A. Kent, C. J. Bennett, and K. A. Bernard, "Tissue tropism and neuroinvasion of west nile virus do not differ for two mouse strains with different survival rates," *Virology*, vol. 368, no. 2, pp. 422–430, 2007.

[17] J. J. Miner and M. S. Diamond, "Zika virus pathogenesis and tissue tropism," *Cell host & microbe*, vol. 21, no. 2, pp. 134–142, 2017.

[18] R. J. Kuhn, W. Zhang, M. G. Rossmann, S. V. Pletnev, J. Corver, E. Lenches, C. T. Jones, S. Mukhopadhyay, P. R. Chipman, E. G. Strauss *et al.*, "Structure of dengue virus: implications for flavivirus organization, maturation, and fusion," *Cell*, vol. 108, no. 5, pp. 717–725, 2002.

[19] D. Sirohi, Z. Chen, L. Sun, T. Klose, T. C. Pierson, M. G. Rossmann, and R. J. Kuhn, "The 3.8 å resolution cryo-em structure of zika virus," *Science*, vol. 352, no. 6284, pp. 467–470, 2016.

[20] S. Mukhopadhyay, B.-S. Kim, P. R. Chipman, M. G. Rossmann, and R. J. Kuhn, "Structure of west nile virus," *Science*, vol. 302, no. 5643, pp. 248–248, 2003.

[21] S. Mukhopadhyay, R. J. Kuhn, and M. G. Rossmann, "A structural perspective of the flavivirus life cycle," *Nature Reviews Microbiology*, vol. 3, no. 1, pp. 13–22, 2005.

[22] C. J. Neufeldt, M. Cortese, E. G. Acosta, and R. Bartenschlager, "Rewiring cellular networks by members of the flaviviridae family," *Nature Reviews Microbiology*, vol. 16, no. 3, p. 125, 2018.

[23] P. Hilgard and R. Stockert, "Heparan sulfate proteoglycans initiate dengue virus infection of hepatocytes," *Hepatology*, vol. 32, no. 5, pp. 1069–1077, 2000.

[24] J. Reyes-del Valle, S. Chávez-Salinas, F. Medina, and R. M. Del Angel, "Heat shock protein 90 and heat shock protein 70 are components of dengue virus receptor complex in human cells," *Journal of virology*, vol. 79, no. 8, pp. 4557–4567, 2005.

[25] L. Meertens, X. Carnec, M. P. Lecoin, R. Ramdasi, F. Guivel-Benhassine, E. Lew, G. Lemke, O. Schwartz, and A. Amara, "The tim and tam families of phosphatidylserine receptors mediate dengue virus entry," *Cell host & microbe*, vol. 12, no. 4, pp. 544–557, 2012.

[26] R. Hamel, O. Dejarnac, S. Wichit, P. Ekchariyawat, A. Neyret, N. Luplertlop, M. Perera-Lecoin, P. Surasombatpattana, L. Talignani, F. Thomas *et al.*, "Biology of zika virus infection in human skin cells," *Journal of virology*, vol. 89, no. 17, pp. 8880–8896, 2015.

[27] J. Chu, P. Leong, and M. Ng, "Analysis of the endocytic pathway mediating the infectious entry of mosquito-borne flavivirus west nile into aedes albopictus mosquito (c6/36) cells," *Virology*, vol. 349, no. 2, pp. 463–475, 2006.

[28] B. A. Hackett and S. Cherry, "Flavivirus internalization is regulated by a size-dependent endocytic pathway," *Proceedings of the National Academy of Sciences*, vol. 115, no. 16, pp. 4246–4251, 2018.

[29] A. Agrelli, R. R. de Moura, S. Crovella, and L. A. C. Brandão, "Zika virus entry mechanisms in human cells," *Infection, Genetics and Evolution*, 2019.

[30] H. M. Van Der Schaar, M. J. Rust, C. Chen, H. van der Ende-Metselaar, J. Wilschut, X. Zhuang, and J. M. Smit, "Dissecting the cell entry pathway of dengue virus by single-particle tracking in living cells," *PLoS pathogens*, vol. 4, no. 12, p. e1000244, 2008.

[31] E. Zaitseva, S.-T. Yang, K. Melikov, S. Pourmal, and L. V. Chernomordik, "Dengue virus ensures its fusion in late endosomes using compartment-specific lipids," *PLoS pathogens*, vol. 6, no. 10, p. e1001131, 2010.

[32] L. K. Gillespie, A. Hoenen, G. Morgan, and J. M. Mackenzie, "The endoplasmic reticulum provides the membrane platform for biogenesis of the flavivirus replication complex," *Journal of virology*, vol. 84, no. 20, pp. 10 438–10 447, 2010.

[33] S. Welsch, S. Miller, I. Romero-Brey, A. Merz, C. K. Bleck, P. Walther, S. D. Fuller, C. Antony, J. Krijnse-Locker, and R. Bartenschlager, "Composition and three-dimensional architecture of the dengue virus replication and assembly sites," *Cell host & microbe*, vol. 5, no. 4, pp. 365–375, 2009.

[34] S. Apte-Sengupta, D. Sirohi, and R. J. Kuhn, "Coupling of replication and assembly in flaviviruses," *Current opinion in virology*, vol. 9, pp. 134–142, 2014.

[35] S. Mukherjee, D. Sirohi, K. A. Dowd, Z. Chen, M. S. Diamond, R. J. Kuhn, and T. C. Pierson, "Enhancing dengue virus maturation using a stable furin over-expressing cell line," *Virology*, vol. 497, pp. 33–40, 2016.

[36] P. Avirutnan, L. Zhang, N. Punyadee, A. Manuyakorn, C. Puttikhunt, W. Kasinrerk, P. Malasit, J. P. Atkinson, and M. S. Diamond, "Secreted ns1 of dengue virus attaches to the surface of cells via interactions with heparan sulfate and chondroitin sulfate e," *PLoS pathogens*, vol. 3, no. 11, p. e183, 2007.

[37] S. Alcon-LePoder, M.-T. Drouet, P. Roux, M.-P. Frenkiel, M. Arborio, A.-M. Durand-Schneider, M. Maurice, I. Le Blanc, J. Gruenberg, and M. Flamand, "The secreted form of dengue virus nonstructural protein ns1 is endocytosed by hepatocytes and accumulates in late endosomes: implications for viral infectivity," *Journal of virology*, vol. 79, no. 17, pp. 11 403–11 411, 2005.

[38] S. Alcon, A. Talarmin, M. Debruyne, A. Falconar, V. Deubel, and M. Flamand, "Enzyme-linked immunosorbent assay specific to dengue virus type 1 nonstructural protein ns1 reveals circulation of the antigen in the blood during the acute phase of disease in patients experiencing primary or secondary infections," *Journal of clinical microbiology*, vol. 40, no. 2, pp. 376–381, 2002.

[39] S. Youn, H. Cho, D. H. Fremont, and M. S. Diamond, "A short n-terminal peptide motif on flavivirus nonstructural protein ns1 modulates cellular targeting and immune recognition," *Journal of virology*, vol. 84, no. 18, pp. 9516–9532, 2010.

[40] H. Puerta-Guardo, D. R. Glasner, D. A. Espinosa, S. B. Biering, M. Patana, K. Ratnasiri, C. Wang, P. R. Beatty, and E. Harris, "Flavivirus ns1 triggers tissue-specific vascular endothelial dysfunction reflecting disease tropism," *Cell reports*, vol. 26, no. 6, pp. 1598–1613, 2019.

[41] B. Falgout, R. Chanock, and C. Lai, "Proper processing of dengue virus nonstructural glycoprotein ns1 requires the n-terminal hydrophobic signal sequence and the downstream nonstructural protein ns2a." *Journal of virology*, vol. 63, no. 5, pp. 1852–1860, 1989.

[42] H. Hori and C. Lai, "Cleavage of dengue virus ns1-ns2a requires an octapeptide sequence at the c terminus of ns1." *Journal of virology*, vol. 64, no. 9, pp. 4573–4577, 1990.

[43] M. Flamand, F. Megret, M. Mathieu, J. Lepault, F. A. Rey, and V. Deubel, "Dengue virus type 1 nonstructural glycoprotein ns1 is secreted from mammalian cells as a soluble hexamer in a glycosylation-dependent fashion," *Journal of virology*, vol. 73, no. 7, pp. 6104–6110, 1999.

[44] I. Gutsche, F. Coulibaly, J. E. Voss, J. Salmon, J. d'Alayer, M. Ermonval, E. Larquet, P. Charneau, T. Krey, F. Mégret *et al.*, "Secreted dengue virus nonstructural protein ns1 is an atypical barrel-shaped high-density lipoprotein," *Proceedings of the National Academy of Sciences*, vol. 108, no. 19, pp. 8003–8008, 2011.

[45] D. L. Akey, W. C. Brown, S. Dutta, J. Konwerski, J. Jose, T. J. Jurkiw, J. DelProposto, C. M. Ogata, G. Skiniotis, R. J. Kuhn *et al.*, "Flavivirus ns1 structures reveal surfaces for associations with membranes and the immune system," *Science*, vol. 343, no. 6173, pp. 881–885, 2014.

[46] W. C. Brown, D. L. Akey, J. R. Konwerski, J. T. Tarrasch, G. Skiniotis, R. J. Kuhn, and J. L. Smith, "Extended surface for membrane association in zika virus ns1 structure," *Nature structural & molecular biology*, vol. 23, no. 9, p. 865, 2016.

[47] H. Song, J. Qi, J. Haywood, Y. Shi, and G. F. Gao, "Zika virus ns1 structure reveals diversity of electrostatic surfaces among flaviviruses," *Nature structural & molecular biology*, vol. 23, no. 5, p. 456, 2016.

[48] X. Xu, H. Song, J. Qi, Y. Liu, H. Wang, C. Su, Y. Shi, and G. F. Gao, "Contribution of intertwined loop to membrane association revealed by zika virus full-length ns1 structure," *The EMBO journal*, vol. 35, no. 20, pp. 2170–2178, 2016.

[49] S. Youn, T. Li, B. T. McCune, M. A. Edeling, D. H. Fremont, I. M. Cristea, and M. S. Diamond, "Evidence for a genetic and physical interaction between nonstructural proteins ns1 and ns4b that modulates replication of west nile virus," *Journal of virology*, vol. 86, no. 13, pp. 7360–7371, 2012.

[50] D. L. Akey, W. C. Brown, J. Jose, R. J. Kuhn, and J. L. Smith, "Structure-guided insights on the role of ns1 in flavivirus infection," *Bioessays*, vol. 37, no. 5, pp. 489–494, 2015.

[51] T. Poonsiri, G. S. Wright, M. S. Diamond, L. Turtle, T. Solomon, and S. V. Antonyuk, "Structural study of the c-terminal domain of nonstructural protein 1 from japanese encephalitis virus," *Journal of virology*, vol. 92, no. 7, pp. e01 868–17, 2018.

[52] E. G. Westaway, J. M. Mackenzie, M. T. Kenney, M. K. Jones, and A. A. Khromykh, "Ultrastructure of kunjin virus-infected cells: colocalization of ns1 and ns3 with double-stranded rna, and of ns2b with ns3, in virus-induced membrane structures." *Journal of virology*, vol. 71, no. 9, pp. 6650–6661, 1997.

[53] B. D. Lindenbach and C. M. Rice, "trans-complementation of yellow fever virus ns1 reveals a role in early rna replication." *Journal of virology*, vol. 71, no. 12, pp. 9608–9617, 1997.

[54] S. Youn, R. L. Ambrose, J. M. Mackenzie, and M. S. Diamond, "Non-structural protein-1 is required for west nile virus replication complex formation and viral rna synthesis," *Virology journal*, vol. 10, no. 1, p. 339, 2013.

[55] A. Płaszczyca, P. Scaturro, C. J. Neufeldt, M. Cortese, B. Cerikan, S. Ferla, A. Brancale, A. Pichlmair, and R. Bartenschlager, "A novel interaction between dengue virus nonstructural protein 1 and the ns4a-2k-4b precursor is required for viral rna replication but not for formation of the membranous replication organelle," *PLoS pathogens*, vol. 15, no. 5, p. e1007736, 2019.

[56] P. Somnuke, R. E. Hauhart, J. P. Atkinson, M. S. Diamond, and P. Avirutnan, "N-linked glycosylation of dengue virus ns1 protein modulates secretion, cell-surface expression, hexamer stability, and interactions with human complement," *Virology*, vol. 413, no. 2, pp. 253–264, 2011.

[57] P. Scaturro, M. Cortese, L. Chatel-Chaix, W. Fischl, and R. Bartenschlager, "Dengue virus non-structural protein 1 modulates infectious particle production via interaction with the structural proteins," *PLoS pathogens*, vol. 11, no. 11, p. e1005277, 2015.

[58] B. D. Lindenbach and C. M. Rice, "Genetic interaction of flavivirus nonstructural proteins ns1 and ns4a as a determinant of replicase function," *Journal of virology*, vol. 73, no. 6, pp. 4611–4621, 1999.

[59] I. Umareddy, A. Chao, A. Sampath, F. Gu, and S. G. Vasudevan, "Dengue virus ns4b interacts with ns3 and dissociates it from single-stranded rna," *Journal of general virology*, vol. 87, no. 9, pp. 2605–2614, 2006.

[60] M. I. Giraldo, O. Vargas-Cuartas, J. C. Gallego-Gomez, P.-Y. Shi, L. Padilla-Sanabria, J. C. Castaño-Osorio, and R. Rajsbaum, "K48-linked polyubiquitination of dengue virus ns1 protein inhibits its interaction with the viral partner ns4b," *Virus research*, vol. 246, pp. 1–11, 2018.

[61] S. Noisakran, S. Sengsai, V. Thongboonkerd, R. Kanlaya, S. Sinchaikul, S.-T. Chen, C. Puttikhunt, W. Kasinrerk, T. Limjindaporn, W. Wongwiwat *et al.*, "Identification of human hnrnp c1/c2 as a dengue virus ns1-interacting protein," *Biochemical and biophysical research communications*, vol. 372, no. 1, pp. 67–72, 2008.

[62] M. Cervantes-Salazar, A. H. Angel-Ambrocio, R. Soto-Acosta, P. Bautista-Carbajal, A. M. Hurtado-Monzon, S. L. Alcaraz-Estrada, J. E. Ludert, and R. M. Del Angel, "Dengue virus ns1 protein interacts with the ribosomal protein rpl18: this interaction is required for viral translation and replication in huh-7 cells," *Virology*, vol. 484, pp. 113–126, 2015.

[63] D. Allonso, I. S. Andrade, J. N. Conde, D. R. Coelho, D. C. Rocha, M. L. da Silva, G. T. Ventura, E. M. Silva, and R. Mohana-Borges, "Dengue virus ns1 protein modulates cellular energy metabolism by increasing glyceraldehyde-3-phosphate dehydrogenase activity," *Journal of virology*, vol. 89, no. 23, pp. 11 871–11 883, 2015.

[64] S.-H. Yang, M.-L. Liu, C.-F. Tien, S.-J. Chou, and R.-Y. Chang, "Glyceraldehyde-3-phosphate dehydrogenase (gapdh) interaction with 3'ends of japanese encephalitis virus rna and colocalization with the viral ns5 protein," *Journal of biomedical science*, vol. 16, no. 1, p. 40, 2009.

[65] M. L. Hafirassou, L. Meertens, C. Umaña-Diaz, A. Labeau, O. Dejarnac, L. Bonnet-Madin, B. M. Kümmerer, C. Delaugerre, P. Roingeard, P.-O. Vidalain *et al.*, "A global interactome map of the dengue virus ns1 identifies virus restriction and dependency host factors," *Cell reports*, vol. 21, no. 13, pp. 3900–3913, 2017.

[66] Y. Yang, C. Shan, J. Zou, A. E. Muruato, D. N. Bruno, B. d. A. M. Daniele, P. F. Vasconcelos, S. L. Rossi, S. C. Weaver, X. Xie *et al.*, "A cdna clone-launched platform for high-yield production of inactivated zika vaccine," *EBioMedicine*, vol. 17, pp. 145–156, 2017.

[67] T. Fukuhara, T. Tamura, C. Ono, M. Shiokawa, H. Mori, K. Uemura, S. Yamamoto, T. Kurihara, T. Okamoto, R. Suzuki *et al.*, "Host-derived apolipoproteins play comparable roles with viral secretory proteins erns and ns1 in the infectious particle formation of flaviviridae," *PLoS pathogens*, vol. 13, no. 6, p. e1006475, 2017.

[68] D. A. Muller and P. R. Young, "The flavivirus ns1 protein: molecular and structural biology, immunology, role in pathogenesis and application as a diagnostic biomarker," *Antiviral research*, vol. 98, no. 2, pp. 192–208, 2013.

[69] S. Thiemmeca, C. Tamdet, N. Punyadee, T. Prommool, A. Songjaeng, S. Noisakran, C. Puttikhunt, J. P. Atkinson, M. S. Diamond, A. Ponlawat *et al.*, "Secreted ns1 protects dengue virus from mannose-binding lectin–mediated neutralization," *The Journal of Immunology*, vol. 197, no. 10, pp. 4053–4065, 2016.

[70] A. C. Alcalá, F. Medina, A. González-Robles, L. Salazar-Villatoro, R. J. Fragoso-Soriano, C. Vásquez, M. Cervantes-Salazar, R. M. del Angel, and J. E. Ludert, "The dengue virus non-structural protein 1 (ns1) is secreted efficiently from infected mosquito cells," *Virology*, vol. 488, pp. 278–287, 2016.

[71] A. C. Alcala, R. Hernandez-Bravo, F. Medina, D. S. Coll, J. L. Zambrano, R. M. Del Angel, and J. E. Ludert, "The dengue virus non-structural protein 1 (ns1) is secreted from infected mosquito cells via a non-classical caveolin-1-dependent pathway," *Journal of General Virology*, vol. 98, no. 8, pp. 2088–2099, 2017.

[72] P. Avirutnan, A. Fuchs, R. E. Hauhart, P. Somnuke, S. Youn, M. S. Diamond, and J. P. Atkinson, "Antagonism of the complement component c4 by flavivirus nonstructural protein ns1," *Journal of Experimental Medicine*, vol. 207, no. 4, pp. 793–806, 2010.

[73] J. Liu, Y. Liu, K. Nie, S. Du, J. Qiu, X. Pang, P. Wang, and G. Cheng, "Flavivirus ns1 protein in infected host sera enhances viral acquisition by mosquitoes," *Nature microbiology*, vol. 1, no. 9, pp. 1–11, 2016.

[74] Y. Liu, J. Liu, S. Du, C. Shan, K. Nie, R. Zhang, X.-F. Li, R. Zhang, T. Wang, C.-F. Qin *et al.*, "Evolutionary enhancement of zika virus infectivity in aedes aegypti mosquitoes," *Nature*, vol. 545, no. 7655, pp. 482–486, 2017.

[75] P. R. Beatty, H. Puerta-Guardo, S. S. Killingbeck, D. R. Glasner, K. Hopkins, and E. Harris, "Dengue virus ns1 triggers endothelial permeability and vascular leak that is prevented by ns1 vaccination," *Science translational medicine*, vol. 7, no. 304, pp. 304ra141–304ra141, 2015.

[76] N. Modhiran, D. Watterson, D. A. Muller, A. K. Panetta, D. P. Sester, L. Liu, D. A. Hume, K. J. Stacey, and P. R. Young, "Dengue virus ns1 protein activates cells via toll-like receptor 4 and disrupts endothelial cell monolayer integrity," *Science translational medicine*, vol. 7, no. 304, pp. 304ra142–304ra142, 2015.

[77] H.-R. Chen, Y.-C. Chuang, Y.-S. Lin, H.-S. Liu, C.-C. Liu, G.-C. Perng, and T.-M. Yeh, "Dengue virus nonstructural protein 1 induces vascular leakage through macrophage migration inhibitory factor and autophagy," *PLoS neglected tropical diseases*, vol. 10, no. 7, p. e0004828, 2016.

[78] H.-R. Chen, Y.-C. Chuang, C.-H. Chao, and T.-M. Yeh, "Macrophage migration inhibitory factor induces vascular leakage via autophagy," *Biology open*, vol. 4, no. 2, pp. 244–252, 2015.

[79] H. Puerta-Guardo, D. R. Glasner, and E. Harris, "Dengue virus ns1 disrupts the endothelial glycocalyx, leading to hyperpermeability," *PLoS pathogens*, vol. 12, no. 7, p. e1005738, 2016.

[80] D. R. Glasner, K. Ratnasiri, H. Puerta-Guardo, D. A. Espinosa, P. R. Beatty, and E. Harris, "Dengue virus ns1 cytokine-independent vascular leak is dependent on endothelial glycocalyx components," *PLoS pathogens*, vol. 13, no. 11, p. e1006673, 2017.

[81] H. T. Duyen, T. V. Ngoc, D. T. Ha, V. T. Hang, N. T. Kieu, P. R. Young, J. J. Farrar, C. P. Simmons, M. Wolbers, and B. A. Wills, "Kinetics of plasma viremia and soluble nonstructural protein 1 concentrations in dengue: differential effects according to serotype and immune status," *Journal of Infectious Diseases*, vol. 203, no. 9, pp. 1292–1300, 2011.

[82] F. A. Orsi, R. N. Angerami, B. M. Mazetto, S. K. Quaino, F. Santiago-Bassora, V. Castro, E. V. de Paula, and J. M. Annichino-Bizzacchi, "Reduced thrombin formation and excessive fibrinolysis are associated with bleeding complications in patients with dengue fever: a case–control study comparing dengue fever patients with and without bleeding manifestations," *BMC infectious diseases*, vol. 13, no. 1, p. 350, 2013.

[83] I.-J. Liu, C.-Y. Chiu, Y.-C. Chen, and H.-C. Wu, "Molecular mimicry of human endothelial cell antigen by autoantibodies to nonstructural protein 1 of dengue virus," *Journal of Biological Chemistry*, vol. 286, no. 11, pp. 9726–9736, 2011.

[84] Y.-C. Chuang, J. Lin, Y.-S. Lin, S. Wang, and T.-M. Yeh, "Dengue virus nonstructural protein 1–induced antibodies cross-react with human plasminogen and enhance its activation," *The Journal of Immunology*, vol. 196, no. 3, pp. 1218–1226, 2016.

[85] D.-S. Sun, C.-C. King, H.-S. Huang, Y.-L. SHIH, C.-C. LEE, W.-J. TSAI, C.-C. YU, and H.-H. CHANG, "Antiplatelet autoantibodies elicited by dengue virus non-structural protein 1 cause thrombocytopenia and mortality in mice," *Journal of Thrombosis and Haemostasis*, vol. 5, no. 11, pp. 2291–2299, 2007.

[86] M.-C. Chen, C.-F. Lin, H.-Y. Lei, S.-C. Lin, H.-S. Liu, T.-M. Yeh, R. Anderson, and Y.-S. Lin, "Deletion of the c-terminal region of dengue virus nonstructural protein 1 (ns1) abolishes anti-ns1-mediated platelet dysfunction and bleeding tendency," *The Journal of Immunology*, vol. 183, no. 3, pp. 1797–1803, 2009.

[87] W. E. Brandt, D. Chiewsilp, D. L. Harris, and P. K. Russell, "Partial purification and characterization of a dengue virus soluble complement-fixing antigen," *The Journal of Immunology*, vol. 105, no. 6, pp. 1565–1568, 1970.

[88] D. S. Shepard, E. A. Undurraga, Y. A. Halasa, and J. D. Stanaway, "The global economic burden of dengue: a systematic analysis," *The Lancet infectious diseases*, vol. 16, no. 8, pp. 935–941, 2016.

[89] S. B. Halstead, "Dengvaxia sensitizes seronegatives to vaccine enhanced disease regardless of age," *Vaccine*, vol. 35, no. 47, pp. 6355–6358, 2017.

[90] D. H. Libraty, P. R. Young, D. Pickering, T. P. Endy, S. Kalayanarooj, S. Green, D. W. Vaughn, A. Nisalak, F. A. Ennis, and A. L. Rothman, "High circulating levels of the dengue virus nonstructural protein ns1 early in dengue illness correlate with the development of dengue hemorrhagic fever," *The Journal of infectious diseases*, vol. 186, no. 8, pp. 1165–1168, 2002.

[91] K. M. Chung, M. K. Liszewski, G. Nybakken, A. E. Davis, R. R. Townsend, D. H. Fremont, J. P. Atkinson, and M. S. Diamond, "West nile virus nonstructural protein ns1 inhibits complement activation by binding the regulatory protein factor h," *Proceedings of the National Academy of Sciences*, vol. 103, no. 50, pp. 19 111–19 116, 2006.

[92] P. Avirutnan, R. E. Hauhart, P. Somnuke, A. M. Blom, M. S. Diamond, and J. P. Atkinson, "Binding of flavivirus nonstructural protein ns1 to c4b binding protein modulates complement activation," *The Journal of Immunology*, vol. 187, no. 1, pp. 424–433, 2011.

[93] D. W. Beasley, M. C. Whiteman, S. Zhang, C. Y.-H. Huang, B. S. Schneider, D. R. Smith, G. D. Gromowski, S. Higgs, R. M. Kinney, and A. D. Barrett, "Envelope protein glycosylation status influences mouse neuroinvasion phenotype of genetic lineage 1 west nile virus strains," *Journal of virology*, vol. 79, no. 13, pp. 8339–8347, 2005.

[94] L. B. Young, E. B. Melian, Y. X. Setoh, P. R. Young, and A. A. Khromykh, "Last 20 aa of the west nile virus ns1 protein are responsible for its retention in cells and the formation of unique heat-stable dimers," *Journal of General Virology*, vol. 96, no. 5, pp. 1042–1054, 2015.

[95] L. B. Young, E. B. Melian, and A. A. Khromykh, "Ns1 colocalizes with ns1 and can substitute for ns1 in west nile virus replication," *Journal of virology*, vol. 87, no. 16, pp. 9384–9390, 2013.

[96] K. A. Trychta, S. Bäck, M. J. Henderson, and B. K. Harvey, "Kdel receptors are differentially regulated to maintain the er proteome under calcium deficiency," *Cell reports*, vol. 25, no. 7, pp. 1829–1840, 2018.

[97] K. W. K. Chan, S. Watanabe, J. Y. Jin, J. Pompon, D. Teng, S. Alonso, D. Vijaykrishna, S. B. Halstead, J. K. Marzinek, P. J. Bond *et al.*, "A t164s mutation in the dengue virus ns1 protein is associated with greater disease severity in mice," *Science Translational Medicine*, vol. 11, no. 498, p. eaat7726, 2019.

[98] P. Avirutnan, N. Punyadee, S. Noisakran, C. Komoltri, S. Thiemmeca, K. Auethavornanan, A. Jairungsri, R. Kanlaya, N. Tangthawornchaikul, C. Puttikhunt *et al.*, "Vascular leakage in severe dengue virus infections: a potential role for the nonstructural viral protein ns1 and complement," *The Journal of infectious diseases*, vol. 193, no. 8, pp. 1078–1088, 2006.

[99] M. J. Pryor and P. J. Wright, "Glycosylation mutants of dengue virus ns1 protein," *Journal of General Virology*, vol. 75, no. 5, pp. 1183–1187, 1994.

[100] S. Noisakran, T. Dechtawewat, P. Avirutnan, T. Kinoshita, U. Siripanyaphinyo, C. Puttikhunt, W. Kasinrerk, P. Malasit, and N. Sittisombut, "Association of dengue virus ns1 protein with lipid rafts," *Journal of General Virology*, vol. 89, no. 10, pp. 2492–2500, 2008.

[101] P. Desprès, M. Girard, and M. Bouloy, "Characterization of yellow fever virus proteins e and ns1 expressed in vero and spodoptera frugiperda cells," *Journal of general virology*, vol. 72, no. 6, pp. 1331–1342, 1991.

[102] Y. Taguchi and H. M. Schätzl, "Small-scale triton x-114 extraction of hydrophobic proteins," *Bio-protocol*, vol. 4, no. 11, 2014.

[103] S. Noisakran, T. Dechtawewat, P. Rinkaewkan, C. Puttikhunt, A. Kanjanahaluethai, W. Kasinrerk, N. Sittisombut, and P. Malasit, "Characterization of dengue virus ns1 stably expressed in 293t cell lines," *Journal of virological methods*, vol. 142, no. 1-2, pp. 67–80, 2007.

[104] H. Leblois and P. Young, "Maturation of the dengue-2 virus ns1 protein in insect cells: effects of downstream ns2a sequences on baculovirus-expressed gene constructs," *Journal of general virology*, vol. 76, no. 4, pp. 979–984, 1995.

[105] W. Furnon, P. Fender, M.-P. Confort, S. Desloire, S. Nangola, K. Kitidee, C. Leroux, M. Ratinier, F. Arnaud, S. Lecollinet *et al.*, "Remodeling of the actin network associated with the non-structural protein 1 (ns1) of west nile virus and formation of ns1-containing tunneling nanotubes," *Viruses*, vol. 11, no. 10, p. 901, 2019.

[106] C. Wang, H. Puerta-Guardo, S. B. Biering, D. R. Glasner, E. B. Tran, M. Patana, T. A. Gomberg, C. Malvar, N. T. Lo, D. A. Espinosa *et al.*, "Endocytosis of flavivirus ns1 is required for ns1-mediated endothelial hyperpermeability and is abolished by a single n-glycosylation site mutation," *PLoS pathogens*, vol. 15, no. 7, p. e1007938, 2019.

[107] E. Fuglebakk and N. Reuter, "A model for hydrophobic protrusions on peripheral membrane proteins," *PLoS computational biology*, vol. 14, no. 7, p. e1006325, 2018.

[108] Y. Ci, Z.-Y. Liu, N.-N. Zhang, Y. Niu, Y. Yang, C. Xu, W. Yang, C.-F. Qin, and L. Shi, "Zika ns1–induced er remodeling is essential for viral replicationzika ns1 remodels er for viral replication," *The Journal of Cell Biology*, vol. 219, no. 2, 2020.

[109] R. Perera, C. Riley, G. Isaac, A. S. Hopf-Jannasch, R. J. Moore, K. W. Weitz, L. Pasa-Tolic, T. O. Metz, J. Adamec, and R. J. Kuhn, "Dengue virus infection perturbs lipid homeostasis in infected mosquito cells," *PLoS pathogens*, vol. 8, no. 3, p. e1002584, 2012.

[110] L. Cui, Y. H. Lee, Y. Kumar, F. Xu, K. Lu, E. E. Ooi, S. R. Tannenbaum, and C. N. Ong, "Serum metabolome and lipidome changes in adult patients with primary dengue infection," *PLoS neglected tropical diseases*, vol. 7, no. 8, p. e2373, 2013.

[111] M. A. Martín-Acebes, T. Merino-Ramos, A.-B. Blázquez, J. Casas, E. Escribano-Romero, F. Sobrino, and J.-C. Saiz, "The composition of west nile virus lipid envelope unveils a role of sphingolipid metabolism in flavivirus biogenesis," *Journal of virology*, vol. 88, no. 20, pp. 12 041–12 054, 2014.

[112] M. A. Martin-Acebes, A. Vazquez-Calvo, and J.-C. Saiz, "Lipids and flaviviruses, present and future perspectives for the control of dengue, zika, and west nile viruses," *Progress in lipid research*, vol. 64, pp. 123–137, 2016.

[113] T. E. Aktepe, H. Pham, and J. M. Mackenzie, "Differential utilisation of ceramide during replication of the flaviviruses west nile and dengue virus," *Virology*, vol. 484, pp. 241–250, 2015.

[114] E. G. Bligh and W. J. Dyer, "A rapid method of total lipid extraction and purification," *Canadian journal of biochemistry and physiology*, vol. 37, no. 8, pp. 911–917, 1959.

[115] H. C. Leier, W. B. Messer, and F. G. Tafesse, "Lipids and pathogenic flaviviruses: An intimate union," *PLoS pathogens*, vol. 14, no. 5, 2018.

[116] A. Kontush, M. Lhomme, and M. J. Chapman, "Unraveling the complexities of the hdl lipidome," *Journal of lipid research*, vol. 54, no. 11, pp. 2950–2963, 2013.

[117] M. Noori, M. Darabi, A. Rahimipour, M. Rahbani, N. A. Abadi, M. Darabi, and K. Ghatrehsamani, "Fatty acid composition of hdl phospholipids and coronary artery disease," *Journal of clinical lipidology*, vol. 3, no. 1, pp. 39–44, 2009.

[118] S. T. Chiesa and M. Charakida, "High-density lipoprotein function and dysfunction in health and disease," *Cardiovascular drugs and therapy*, vol. 33, no. 2, pp. 207–219, 2019.

[119] T. Speer, L. Rohrer, P. Blyszczuk, R. Shroff, K. Kuschnerus, N. Kränkel, G. Kania, S. Zewinger, A. Akhmedov, Y. Shi *et al.*, "Abnormal high-density lipoprotein induces endothelial dysfunction via activation of toll-like receptor-2," *Immunity*, vol. 38, no. 4, pp. 754–768, 2013.

[120] R. Dawaliby, C. Trubbia, C. Delporte, C. Noyon, J.-M. Ruysschaert, P. Van Antwerpen, and C. Govaerts, "Phosphatidylethanolamine is a key regulator of membrane fluidity in eukaryotic cells," *Journal of Biological Chemistry*, vol. 291, no. 7, pp. 3658–3667, 2016.

[121] D. A. Muller, M. J. Landsberg, C. Bletchly, R. Rothnagel, L. Waddington, B. Hankamer, and P. R. Young, "Structure of the dengue virus glycoprotein non-structural protein 1 by electron microscopy and single-particle analysis," *Journal of General Virology*, vol. 93, no. 4, pp. 771–779, 2012.

[122] J. M. Lee, A. J. Crooks, and J. R. Stephenson, "The synthesis and maturation of a non-structural extracellular antigen from tick-borne encephalitis virus and its relationship to the intracellular ns1 protein," *Journal of general virology*, vol. 70, no. 2, pp. 335–343, 1989.

[123] P. W. Mason, "Maturation of japanese encephalitis virus glycoproteins produced by infected mammalian and mosquito cells," *Virology*, vol. 169, no. 2, pp. 354–364, 1989.

[124] V. D. Krishna, M. Rangappa, and V. Satchidanandam, "Virus-specific cytolytic antibodies to nonstructural protein 1 of japanese encephalitis virus effect reduction of virus output from infected cells," *Journal of virology*, vol. 83, no. 10, pp. 4766–4777, 2009.

[125] D. Watterson, B. Kobe, and P. R. Young, "Residues in domain iii of the dengue virus envelope glycoprotein involved in cell-surface glycosaminoglycan binding," *Journal of General Virology*, vol. 93, no. 1, pp. 72–82, 2012.

VITA

VITA

Thu M. Cao was born on October 16^{th}, 1986 in Vietnam. She obtained a Bachelor of Sciences degree at University of Sciences at Ho Chi Minh city in 2008. Her undergraduate research was to study an oncogene E7 of Human papilloma virus in order to develop a diagnosis assay for the infection. The research gave her excitement for laboratory work and meaning of the research for the society. Therefore, she proceeded to Master degree at Minnesota State University, working in the laboratory of Dr. Timothy Secott. During this time, she investigated components from conditioned medium to resuscitate dormant form of *Mycobacterium avium* subspecies *paratuberculosis*. In 2013, she joined Purdue University in Biological Sciences Department for Ph.D and later worked in the laboratory of Dr. Richard J. Kuhn. Her work focused on flaviviruses, including West Nile and Dengue virus, in order to understand roles of a non-structural protein (NS1) in the flavivirus life cycle. Thu plans to continue scientific research and has been seeking for postdoctoral position in academia.